An investigation into inviscid theory applied to manoeuvring bodies in fluid

Ali Hatam

School of Computing, Science & Engineering

Informatics Research Institute (IRIS)

University of Salford, Salford, UK

Submitted in Partial Fulfillment of the Requirements of the Degree of Doctor of Philosophy, August 2005

Contents

Abstract

This thesis focuses on the appropriateness of the inviscid potential flow model for determining the manoeuvring characteristics of a body moving through fluid. This model is widespread in many key applications for ships, submarines, aircraft, rockets, missiles, as well as for the swimming of marine animals and the flying of birds. Despite the widespread use, there are important anomalies in the theory, in particular relating to the lift induced by shed vorticity. These anomalies have been identified in the recent publication by Chadwick which states that the lift has been calculated incorrectly, and apparent agreement in wing theory is fortuitous due to "two wrongs" in the theory giving the right answer.

In this thesis, the inviscid flow is further investigated, and the work of Chadwick is extended and developed further.

In the first two chapters, careful description of the basic fluid concepts and then derivation of the fluid equations is given. In chapter four, the lift and drag on a wing are considered. The lift evaluation comes out to be half that expected and this is in agreement and essentially repeats the analysis in Chadwick's recent paper [1]. However, the analysis is extended to evaluate the drag, and surprisingly the drag is determined to be infinite.

In chapter five, further investigation into the lift on a thin wing is undertaken, and it is seen that there is uncalculated jump in the lift at the trailing edge. This is calculated from the pressure integral across the trailing edge.

Finally, in chapter six, inviscid flow slender body theory is investigated. A complete near field expansion is given for a singularity distribution of sources over an infinite line by using the Fourier transform method. In this thesis, this result is extended for the finite line by using the integral splitting technique. By taking the ends to infinity, the result for the infinite line is recovered and the two methods shown to be equivalent for this specific case. The method presented here relies upon allowing a singular wake to exist behind the body. This introduces non-uniqueness in the matching and the implications of this are discussed.

Appropriate references to other researchers are given in individual introductions for each chapter.

Acknowledgement

I would like to thank my supervisor Dr Edmund Chadwick, for his many suggestions, guidance, constant support and kindly supervision during this research and specially for his help through the early years of chaos and confusion. I also would like to thank Dr Kevin Sandiford and Dr Aleksey Pichugin which kindly helped me in computer programming. Finally, I would like to thank Dr Steven Nixon, Mr Mohammad Abuhamad and Dr Danila Prikaschikove for their kind friendship.

Chapter 1

Introduction

The inviscid flow equations with the thin wing theory and also the slender body theory have been used especially for solving manoeuvring problems in fluids. Key applications for ships, submarines, aircraft, rockets, missiles, as well as for the swimming of marine animals and the flying of birds, make use of these asymptotic theories. (A thin body is defined such that the body thickness is small compared to the body length. Examples of such bodies are wings and sheets. A slender body is defined such that the body distance measure in the cross-sectional plane to the axial direction of the body is small compared to the body length. Examples of such bodies are ships and submarines.)

Wing theory

Wing theory began with the work of Lanchester [2] [3] and Prandtl [4] who assume a trailing vortex sheet emanates from the trailing edge of the wing such that the Kutta condition is satisfied. The vortex sheet is then approximated by a distribution of horseshoe vortices. This is the fundamental description for most numerical Euler codes used to determine aircraft lift. By summing the contribution from all horseshoe vortices, the total lift on the wing is then obtained. However, both Goldstein [5] and Batchelor [6] [7] have expressed concerns over this model.

Batchelor [6] considers steady laminar flow with closed streamlines at large Reynolds number, and incorporates a viscous component in order to satisfy the boundary conditions of the problem. In another paper [7], on axial flow in trailing line vortices, he again argues that the viscous component determines the leading order solution near the vortex line, and uses the Oseen linearisation to determine this. In this way, the fluid velocity at the centre of the vortex line and the kinetic energy of the system are finite, which is not the case in a purely inviscid model. Batchelor introduces the concept of the vortex core, outside of which is approximately inviscid flow and inside which viscosity becomes important. Similarly, Chadwick [1] retains the viscous component, although small, to develop a model using the Oseen equations for uniform flow past a wing. The consequences of retaining the viscous component are discussed later in this introduction.

Goldstein [5] p131-134 also has concerns about the viscosity being initially set to zero, as this can lead to two different flows (p.133): "If we consider a motion started from rest in a viscous fluid, it is known that $\lim_{t\to\infty}\lim_{\mu\to 0}$ and $\lim_{\mu\to 0}\lim_{t\to\infty}$ are different. Because of the action of viscosity in diffusing the vorticity, diffused vorticity cannot occur in the former, although vortex sheets may; but regions of diffused vorticity may occur in the second limit." Here, μ is defined as the dynamical coefficient of viscosity, and t as time. He then goes on to give two examples of flows where, by using the different limits, different solutions are obtained. These are the flow between sliding flat plates, and uniform flow past a finite length flat plate. Chadwick [1] considers a more realistic example by considering small disturbance flow past a wing. Considering inviscid flow, this leads to linearized aerofoil/wing theory [8], and corresponds to Goldstein's first limit. However in [1] the viscous terms are retained and a solution corresponding to Goldstein second limit, in which vorticity diffuses, is obtained, see figure 1.1.

The most important difference noted by Chadwick between the two different limiting cases is in the calculation of the lift force on the body. The lift Oseenlet is induced from a velocity potential flow field and a viscous velocity flow field. Each of these flow fields induce equal lift force on the body. This is puzzling since there is no viscous velocity flow field in the inviscid formulation, and this contribution appears to be lost. In the thesis, we investigate this difference further by extending the work of Chadwick [1] in inviscid theory by considering on additional lateral flow velocity term. The outcome of this extension shall be to show that, once again, the lift is half that expected but also that the drag is infinite.

As in the Lanchester-Prandtl approach, we need consider only one infinitesimal horseshoe

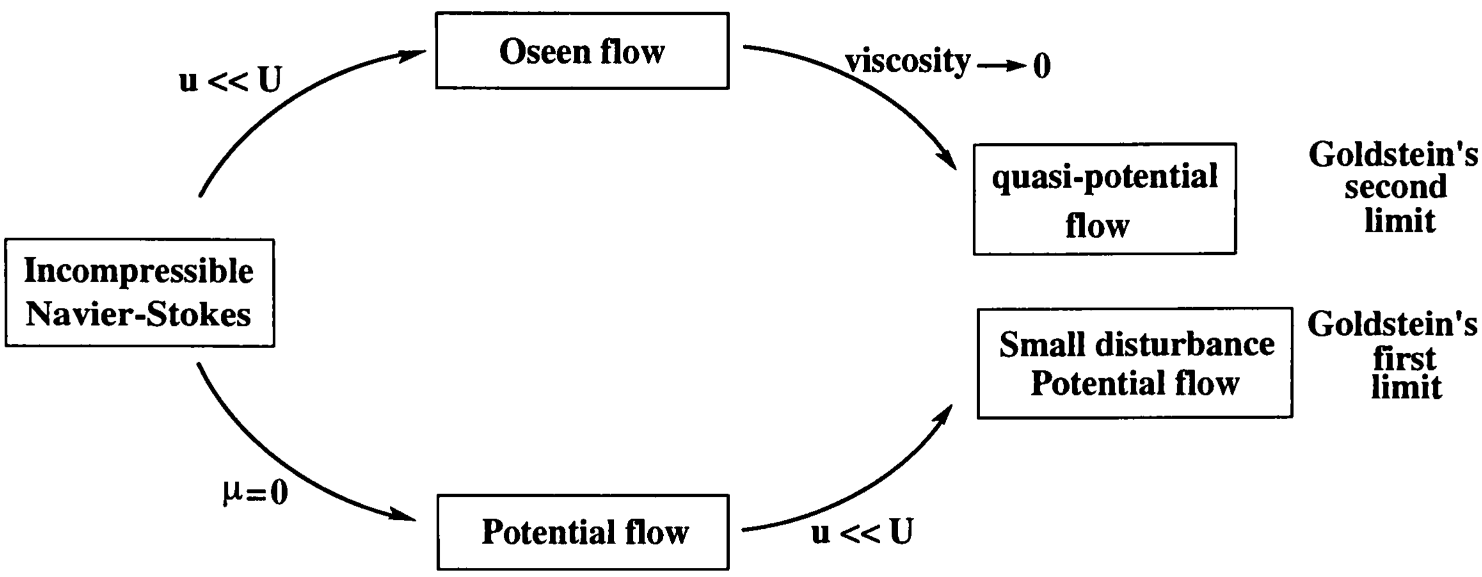

Figure 1.1: Two limiting procedures for small disturbance flow past a wing.

vortex, as the lift can be represented by a linear summation of the force contributions from each horseshoe vortex in the model. An investigation into how the lift is calculated, using the inviscid flow model, from the pressure distribution over the wing surface is then undertaken. It is shown that the puzzling difference in the lift calculation is due to a calculation, always omitted in the standard approach, of a lift jump at the wing's trailing edge.

Slender body theory

Slender body theory began with the work of Munk [9], and was extended for the slender wing case by Jones [10]. In slender body theory, the fluid motion is approximated near to the body by a two-dimensional flow in the transverse plane to the body's length axis. This asymptotic approximation is applied by assuming that the fluid velocity changes in the axial direction are lower in magnitude than the fluid velocity changes in the cross-section plane. The first order approximation then relates a distribution of three dimensional sources to the two dimensional source strength in the transverse plane.

Subsequent important developments include: Lighthill's theory for the motion of slender fish [11], Ursell's application to free surface linear water wave problems [12]; and Nielsen's development for missile dynamics [13].

More recently, slender body theory has been applied to Stokes flow [14] and Oseen flow [15]. There are a wide variety of slender body or strip theory methods in use, but perhaps the two most common are the integral splitting technique and the transform analysis approach. For a general review of slender body theory development and methods, see Tuck [16].

The integral splitting technique splits the integrals into parts, over integrals near to the fluid point and over integrals far from the fluid point. Appropriate expansions can then be applied to the integrals, and in this way the variables in the transverse plane separated from the axial variable. However, the analysis requires involved integration by parts that means only a few terms in the near field expansion have ever been found using this method.

If instead a distribution of source potentials over an infinite length is considered, then use can be made of transform analysis such as Fourier or Laplace transforms [8].

In this way, the complete expansions can be obtained in transform space. Taking the inverse transform yields a complete expansion to all orders, assuming an infinitely differentiable strength function [16]. However, the integration is now restricted to the infinite rather than finite line.

In this thesis, we give the complete expansion over a finite line. The integral splitting technique is used but applied to the generator potential rather than the source potential. The advantage of starting with the generator potential is that separation into the transverse plane and streamwise variables is immediate and does not require involved integration by parts, or application of restrictive end conditions. In this way, an expansion to all orders shall be obtained but over a finite length body rather than the infinite length of the transform methods. The advantage is that now a slender body approximation representing a finite length body can now be given to any degree of accuracy, depending upon the smoothness of the strength function.

In the first two chapters, careful description of the basic fluid concepts and then derivation of the fluid equations is given. In chapter four, the lift and drag on a wing are considered. The lift evaluation comes out to be half that expected and this is in agreement and essentially repeats the analysis in [1]. However, the analysis is extended to evaluate the drag, and the drag is determined to be infinite.

In chapter five, further investigation into the lift on a thin wing is undertaken, and it is seen that there is a jump in the calculated lift force at trailing edge of the wing which is not obtained from the standard potential theory. This jump in the lift arises from the pressure integral across the trailing edge.

Finally, in chapter six, inviscid flow slender body theory is investigated. Tuck [16] gives a complete near field expansion for a singularity distribution of sources over an infinite line by using the Fourier transform method. In this thesis, this result is extended for the finite line by using the integral splitting technique. By taking the ends to infinity, the result for the infinite line is recovered and the two methods shown to be equivalent for this specific case. The method presented here relies upon allowing a singular wake to exist behind the body. This introduces non-uniqueness in the matching and the implications of this are discussed.

Chapter 2

Some basic concepts

In this section some definitions and briefly explanation about some concepts that may be used in this thesis, has been presented.

Two fundamental laws which are applied to any fluid are [17]:

1. The conservation of mass.
2. Newton's second law of motion.

2.1 Fluid as a continuum

All fluids are composed of molecules in constant motion. However, in most engineering applications we are interested in the average or macroscopic effects of many molecules. It is these macroscopic effects that we ordinarily perceive and measure. We thus treat a fluid as an infinitely divisible substance, a *continuum*, and do not concern ourselves with the behavior of individual molecules.

As a consequence of the continuum assumption, each fluid property is assumed to have a definite value at every point in space. Thus fluid properties such as density, temperature, velocity and so on, are considered to be continuous functions of position and time.

2.2 Timelines, pathlines, streaklines and streamlines

Here we are defining some basic concepts such as Timelines, pathlines, streaklines and streamlines.

Timelines: If a number of adjacent fluid particles in a flow field are marked at a given instant, they form a line in the fluid at that instant; this line is called a *timeline.*

Pathline: A *pathline* is the path or trajectory traced out by a moving fluid particle. To make a pathline visible, we might identify a fluid particle at a given instant, for example by the use of dye, and then take a long exposure photograph of its subsequent motion. the line traced out by the particle is a pathline.

Streaklines: We might choose to focus our attention on a fixed location in space and identify, again by the use of dye, all fluid particles passing through this point. After a short period of time we would have a number of identifiable fluid particles in the flow, all of which had, at some time, passed through one fixed location in space. The line joining these fluid particles is defined as a *streakline.*

Streamlines: *Streamlines* are lines drawn in the flow at every point in the flow field so that at a given instant they are tangent to the direction of flow at every point in the flow field. Since the streamlines are tangent to the velocity vector at every point in the flow field, there can be no flow across a streamline.

2.3 Body forces, surface forces, stress

We also here defining some basic concepts such as Body forces, surface forces and stresses.

Body forces Those forces which act on all elements of volume of a continuum are known as *body forces* (like gravity and inertia forces).

Surface forces Those forces which act on a surface element, whether it is a portion of the bounding surface of the continuum or perhaps an arbitrary internal surface, are known as *surface forces*. Contact forces between bodies are a type of surface force.

Stress The force that compresses a body or expands a body (in other words the force which deform a body)is called *stress*.

2.4 Incompressible and compressible fluid

In general, a liquid is an incompressible fluid, and gas a compressible fluid. Nevertheless, even in the case of a liquid it becomes necessary to take compressibility into account whenever the liquid is highly pressurised, such as oil in a hydraulic machine. Similarly, even in the case of a gas, the compressibility may be disregarded whenever the change in pressure is small.

2.5 Compressibility and viscosity

Fluids are divided into liquids and gases. A liquid is hard to compress and as in the ancient saying "Water takes the shape of the vessel containing it", it changes its shape according to the shape of its container with an upper free surface. Gas on the other hand is easy to compress, and fully expands to fill its container. There is thus no free surface. Consequently, an important characteristic of a fluid from the viewpoint of fluid mechanics is its compressibility. Another characteristic is its viscosity. Whereas a solid shows its elasticity in tension, compression or shearing stress, a fluid does so only for compression. In other words, a fluid increases its pressure against compression, trying to retain its original volume. This characteristic is called compressibility. Furthermore, a fluid shows resistance whenever two layers slide over each other. This characteristic is called viscosity. In general, liquids are called incompressible fluids and gases compressible fluids. Nevertheless, for liquids, compressibility must be taken into account whenever they are highly pressurised, and for gases compressibility may be disregarded whenever the change in pressure is small. Although a fluid is an aggregate of molecules in constant motion, the mean free path of these molecules is 0.06pm even for air of normal temperature and pressure, so a fluid is treated as a continuous isotropic substance. Meanwhile, a non-existent, assumed fluid without either viscosity or compressibility is called an ideal fluid or perfect fluid. A fluid with compressibility but without viscosity is occasionally discriminated and called a perfect fluid, too. Furthermore, a gas subject to Boyles-Charles law is called a perfect or ideal gas.

2.6 Viscosity and strain

Fluids offer resistance to a shearing force. *Viscosity* is a property of a fluid that determines the amount of this resistance. Viscosities of liquids vary inversely with temperature, while viscosities of gases vary directly with temperature.

Here we briefly show the rule governing the viscosity function in fluid formulas [18]. Observations show that, while the fluid clearly has a finite velocity v at any finite distance from the boundary, the velocity is zero at a stationary boundary. Thus the velocity increases with increasing distance from the boundary. These facts are summarised by the *velocity profile* which indicates relative motion between any two adjacent layers. Two such layers are shown having an infinitesimal thickness dy, the lower layer moving with velocity v, the upper with velocity $v + dv$.

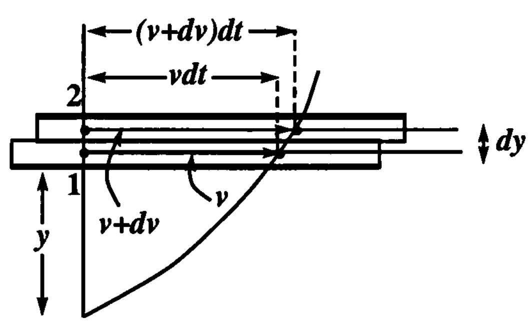

Figure 2.1: Laminar motion and strain

In figure 2.1 (taken from [18]), two particles 1 and 2, starting on the same vertical line, move different distances $d_1 = vdt$ and $d_2 = (v + dv)dt$ in an infinitesimal time dt. Thus, the fluid is distorted or sheared as t increases. In general for isotropic solids behaving elastically the stress due to shear is proportional to the strain (i.e., relative displacement);

$$\text{Strain} = \frac{d_2 - d_1}{dy} = \frac{dv\,dt}{dy} = \frac{dv}{dy}dt.$$

However, a fluid flows under the slightest stress. In fact, in fluid flow problems, the stress is related to the *rate of strain* rather than to the total strain; in this case

$$\text{Rate of strain} = \frac{(dv/dy)dt}{dt} = \frac{dv}{dy}.$$

The friction or shearing force that must exist between fluid layers can be expressed as a *shearing* or *frictional stress* per unit of contact area and is designated by τ. For laminar (nonturbulent) motion (in which viscosity plays a predominant role) τ is observed to be proportional to the rate of strain, that is, to the velocity gradient, dv/dy, with a constant of proportionality, μ defined as the *coefficient of viscosity.*

$$\tau = \mu\frac{dv}{dy}. \tag{2.6.1}$$

This is also called the *dynamic viscosity* (absolute viscosity or viscosity) of the fluid.

Rearranging (2.6.1) such that

$$\mu = \frac{\tau}{\frac{dv}{dy}}, \tag{2.6.2}$$

gives a typical unit of viscosity which is

$$\frac{N/m^2}{(m/s)/m} = \frac{N.s}{m^2}, \tag{2.6.3}$$

in the International System units. The *kinematic viscosity*, ν, is defined as

$$\nu = \frac{\mu}{\rho}, \tag{2.6.4}$$

where ρ is mass density, and it has the unit $\frac{(N.s)/m^2}{kg/m^3} = \frac{m^2}{s}$ since $N = \frac{kg.m}{s^2}$.

The dynamic viscosity of water and air are 1.75×10^{-3} and 1.72×10^{-5} $N.s/m^2$ at 0° C respectively, while the kinematic viscosity of water and air are 1.75×10^{-6} and 1.33×10^{-5} m^2/s respectively. Both viscosities vary with temperature.

Reynolds number

Reynolds conducted many experiments using glass tubes of 7, 9, 15 and 27 mm diameter and water temperatures from 4 to 44° C. He discovered that a laminar flow turns to a turbulent flow when the value of the non-dimensional quantity $\rho vd/\mu$ reaches a certain amount whatever the values of the average velocity v, glass tube diameter d, water density ρ and water viscosity μ. Later, to commemorate Reynolds achievement,

$$Re = \frac{\rho vd}{\mu},$$

was called the *Reynolds number.* In fact Reynolds number Re, expresses the ratio of inertial to viscous forces, so if a flow is characterized by a certain length l, velocity v and density ρ, the Reynolds number is

$$Re = \frac{vl}{\nu},$$

where $\nu = \frac{\mu}{\rho}$ is the kinematic viscosity (2.6.4).

Newtonian and non-Newtonian fluids

The nonappearance of pressure in equation (2.6.1) shows that τ and μ are independent of pressure, however viscosity usually increases very slightly with the pressure, but the change is negligible. This is Newton's suggestion, which led to (2.6.1), and the equation is called Newton's law of viscosity. Fluids that follow this law and for which μ has a constant value are known as *Newtonian* or *incompressible* fluids. Fluid, which do not follow this law are known as $non - Newtonian$.

2.7 Steady flow

A flow for which all velocities and properties at a given location are independent of time is called *steady.*

2.8 Vorticity, irrotational flow and circulation

As it is shown in figure 2.2, an elementary rectangle of fluid $ABCD$ with sides dx and dy, which is located at O at time t moves to O' while deforming itself to $A'B'C'D'$ time

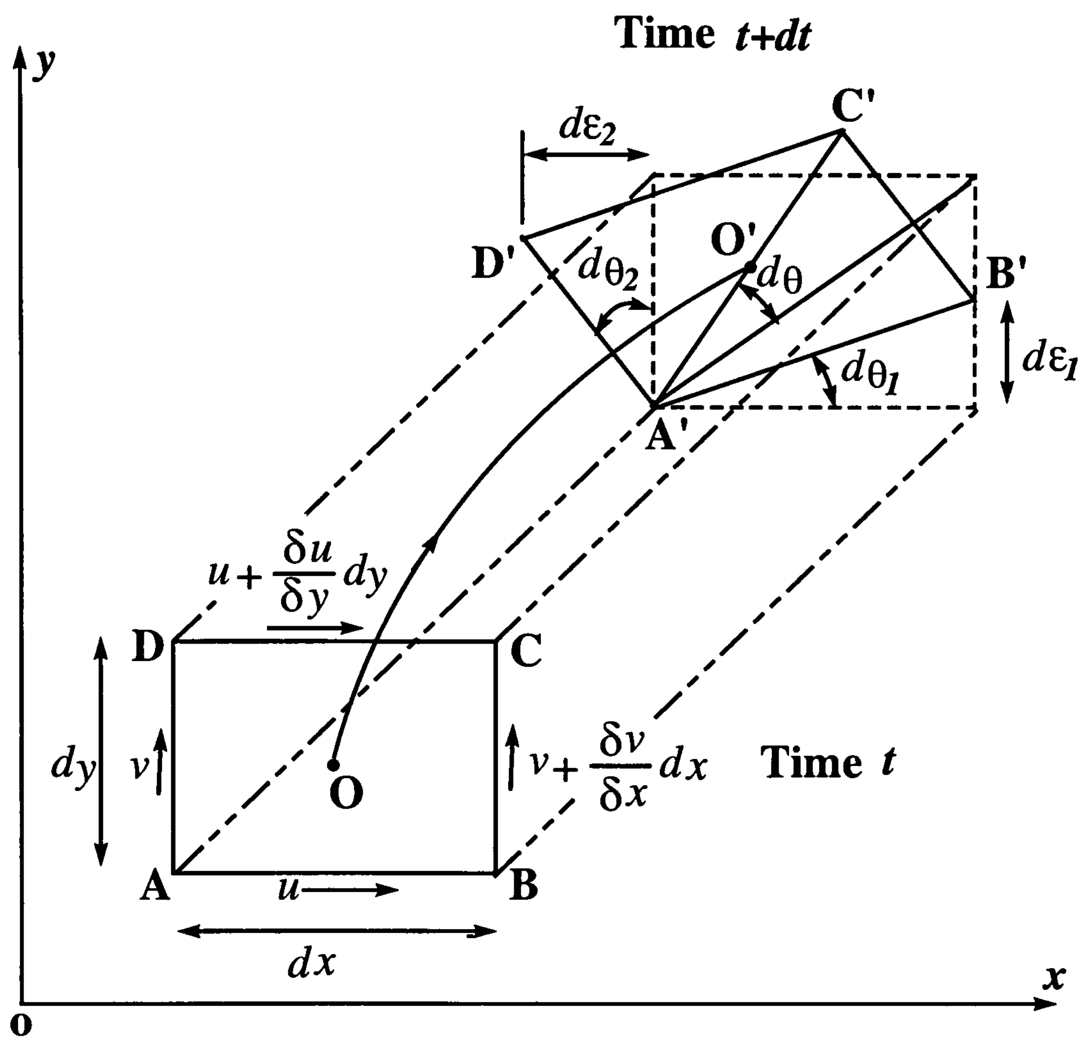

Figure 2.2: Deformation of elementary rectangle of fluid

dt later. AB in the x direction moves to $A'B'$ while rotating by $d\varepsilon_1$, and AD in the y direction rotates by $d\varepsilon_2$. Thus

$$d\varepsilon_1 = \frac{\partial v}{\partial x}dxdt, \quad d\varepsilon_2 = -\frac{\partial u}{\partial y}dydt.$$

Let the angular velocities of AB and AD be ω_1 and ω_2 respectively:

$$\omega_1 = \frac{d\theta_1}{dt}, \quad \omega_2 = \frac{d\theta_2}{dt},$$

since $d\theta_1 = \frac{d\varepsilon_1}{dx}$, $d\theta_2 = \frac{d\varepsilon_2}{dy}$, so $\omega_1 = \frac{\partial v}{\partial x}$, $\omega_2 = -\frac{\partial u}{\partial y}$, and hence for centre O, the average angular velocity ω is

$$\omega_z = \frac{1}{2}(\omega_1 + \omega_2) = \frac{1}{2}(\frac{\partial v}{\partial x} - \frac{\partial u}{\partial y}).$$

The term in the brackets is called the *vorticity* for the z axis. Hurricanes, eddying water currents and tornadoes are familiar examples of natural vortices. The case where the vorticity is zero, namely the case where the fluid movement obeys

$$\frac{\partial v}{\partial x} - \frac{\partial u}{\partial y} = 0,$$

is called *irrotational* flow [19].

In general, for fluid velocity $\mathbf{v}$ the vector $\xi = \nabla \times \mathbf{v}$ is called the rotation of $\mathbf{v}$, and therefore $\omega_x = \xi \cdot \hat{\mathbf{x}}$, $\omega_y = \xi \cdot \hat{\mathbf{y}}$ and $\omega_z = \xi \cdot \hat{\mathbf{z}}$.

The *circulation* C around the loop is defined as the line integral of the tangential component of the velocity $\mathbf{v}$ around the closed loop L,

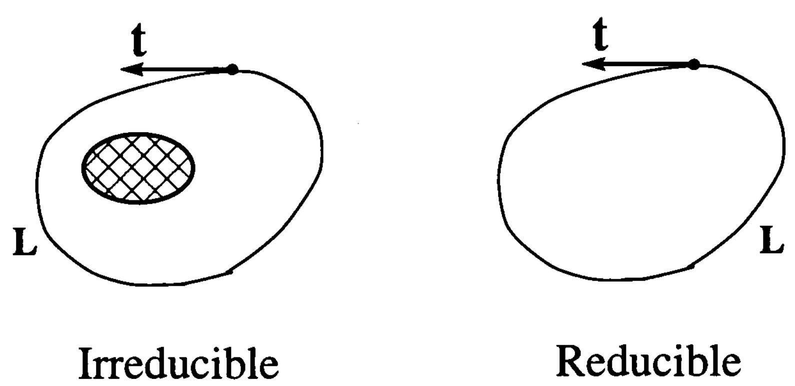

Figure 2.3: Reducible and irreducible loops in a two-dimensional flow. The shaded area represents flow boundary.

$$C = \oint_L \mathbf{v} \cdot \mathbf{t} dl,$$

where the unit tangent vector $\mathbf{t}$ points in the counterclockwise direction along L. If the loop is reducible, that is, if it can be shrunk to a point without crossing flow boundaries or singular points, we may use Stokes's circulation theorem to express the circulation around the loop as the areal integral of the strength of the vorticity over the area D enclosed by the loop L,

$$C = \int_D \omega_z dxdy.$$

In other word the circulation is equal to the product of vorticity by area. By Stokes' theorem, whenever there is no vorticity inside a closed loop, then the circulation around it is zero. The Stokes circulation theorem is used in fluid dynamics to study the flow inside the impeller of pumps and blowers as well as the flow around an aircraft wing [20].

Chapter 3

Derivation of the fluid flow equations

Potential flow is a key model considered in most fluid texts. Batchelor [21] discussed the inadequacies of the potential flow model when we ignore the boundary layer. Batchelor illustrates the fact that at a large Reynolds number the flow will be irrotational but he also details the necessity of including the effects of the thin, viscous boundary layer (and of the need to understand more about viscous fluid and boundary layer separation). It is shown to be a much more accurate potential flow model to include the effects of the viscous boundary layer (particularly in relation to the inclusion of vorticity in the wake of the body). A result of the potential flow approximation is the introduction of the velocity potential, ϕ. We define the velocity vector $\mathbf{u} = \nabla\phi$. We will give some properties of the velocity potential and derive Bernoulli's equation. This equation is also known as the pressure equation because it can be used to find an expression for the pressure term. To do this the Navier-Stokes equations must be derived which build on the concepts discussed in chapter 2.

3.1 History

Sir Isaac Newton (1642-1727) was the first to establish the relationship between force, momentum and acceleration (his famous *"principa"*). Following his work Daniel Bernoulli (1700-1782) [22] used the concept of internal pressure with confidence and clarity in the study of moving fluids to achieve his most famous equation relating the pressure and the velocity.

Leonhard Euler (1707-1783) found some inconsistencies in Newton's models and developed it into a more suitable form, and tied this with Jean le Ronald D' Alembert's (1717-1783) experimental results. To do this, he introduced the concept of linear momentum that the total force on a body is equal to the rate of change of total momentum of the body, with the clear understanding that the term "body" might be applied to each of every part of a continuous medium such as a fluid or elastic solid. He combined this with the concept of internal pressure to give the equations of motion of an inviscid fluid.

Augustin Louis Cauchy(1789-1857) introduced the concept of a stress tensor and combined this with Euler's laws of mechanics to give the general framework for the motion of any continuous medium. He derived Cauchy's law of motion from Newton's second law of motion.

Sir George Gabriel Stokes(1819-1903) extended Newton's original hypothesis and added the appropriate physical properties of a Newtonian viscous fluid to give the Navier-Stokes equations of motion. Oseen (1927) [23] used a linear approximation to the Navier-Stokes equations which are called Ossen's equations.

3.2 Stresses

3.2.1 Cauchy's stress principle

Consider a material continuum occupying the region R of space, and subjected to surface forces f_i and body forces b_i. As a result of forces being transmitted from one portion of the continuum to another, the material within an arbitrary volume V enclosed by the surface S interacts with the materials outside the volume. Let $\hat{\mathbf{n}}$ be the outward normal at point $P \in \Delta S \subseteq S$ (in this thesis we have denoted the vectors by bold face letters and unit vectors by hat bold face.), let Δf_i be the resultant forces exerted across ΔS upon the material within V by the material outside of V. The *Cauchy stress principle* asserts that $\Delta f_i/\Delta S$ tends to a definite limit df_i/dS as ΔS approach to zero at point P, while at the same time the moment of Δf_i about the point P vanishes in the limiting process. The resulting vector df_i/dS is called *stress vector* $t_i^{(\hat{\mathbf{n}})}$ (If the moment at P were not to vanish in the limiting process, a *couple – stress vector*, would also be defined at the point; one branch of the theory of elasticity considers such couple stress.). Mathematically the stress vector is defined by

$$t_i^{(\hat{\mathbf{n}})} = \lim_{\Delta S \to 0} \frac{\Delta f_i}{\Delta S} = \frac{df_i}{ds} \quad \text{or} \quad \mathbf{t}^{(\hat{\mathbf{n}})} = \lim_{\Delta S \to 0} \frac{\Delta \mathbf{f}}{\Delta S} = \frac{d\mathbf{f}}{ds}. \tag{3.2.1}$$

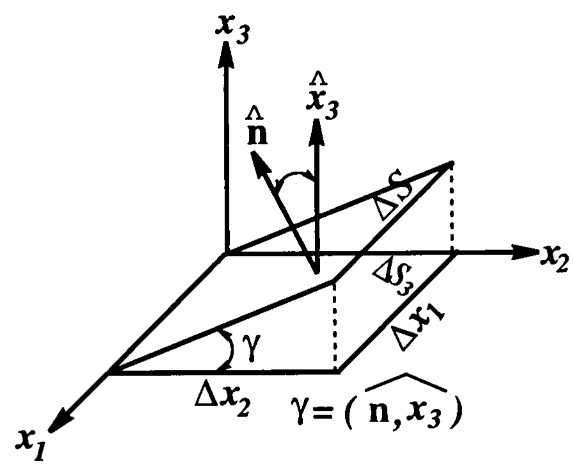

Figure 3.1: $\mathbf{\Delta s_3}$ is the projection of $\mathbf{\Delta s}$ on plane perpendicular to x_3

From figure 3.1 we obtain

$$\Delta s = \frac{\Delta x_2}{\cos(\widehat{\mathbf{n}, \mathbf{x}_3})} \times \Delta x_1 = \frac{\Delta s_3}{n_3}, \tag{3.2.2}$$

where Δs_j is the projection of Δs on plane perpendicular to x_j axis (see figure 3.1).

Eq. (3.2.2) is also valid in the limit so,

$$\frac{ds_j}{ds} = n_j, \tag{3.2.3}$$

Now from (3.2.1) and (3.2.3) we have:

$$t_i^{(\hat{\mathbf{n}})} = \frac{df_i}{ds} = \frac{df_i}{ds_1}\frac{ds_1}{ds} + \frac{df_i}{ds_2}\frac{ds_2}{ds} + \frac{df_i}{\partial s_3}\frac{ds_3}{ds} = \frac{df_i}{ds_j} n_j, \tag{3.2.4}$$

where the repeated suffix implies a summation over j. Eq. (3.2.4) asserts that the notation $t_i^{(\hat{\mathbf{n}})}$ (or $\mathbf{t}^{(\hat{\mathbf{n}})}$) is used to emphasize the fact that the stress vector at a given point P in the continuum depends explicitly upon the particular surface element ΔS chosen there, as represented by the unit normal n_i (or $\hat{\mathbf{n}}$).

For some differently oriented surface element, having a different unit normal, the associated stress vector at P will also be different. The stress vector arising from the action across ΔS at P of the material within V upon the material outside is the vector $-t_i^{(\hat{\mathbf{n}})}$. Thus by Newton's law of action and reaction,

$$-t_i^{(\hat{\mathbf{n}})} = t_i^{(-\hat{\mathbf{n}})} \quad \text{or} \quad -\mathbf{t}^{(\hat{\mathbf{n}})} = \mathbf{t}^{(-\hat{\mathbf{n}})}.$$

The *stress vector* is very often referred to as the *traction vector.*

3.2.2 Stress tensor

The totality of all possible pairs of such vectors $t_i^{(\hat{\mathbf{n}})}$ and n_i at P defines the *state of stress* at that point. Fortunately it is not necessary to specify every pair of stress and normal vectors to completely describe the state of stress at a given point. This may be accomplished by giving the stress vector on each of three mutually perpendicular planes at P. Coordinate transformation equations then serve to relate the stress vector on any plane at the point to the three planes updated to the coordinate system.

We set

$$\mathbf{t}^{(\hat{\mathbf{n}})} = t_1^{(\hat{\mathbf{n}})}\hat{\mathbf{x}}_1 + t_2^{(\hat{\mathbf{n}})}\hat{\mathbf{x}}_2 + t_3^{(\hat{\mathbf{n}})}\hat{\mathbf{x}}_3 = t_i^{(\hat{\mathbf{n}})}\hat{\mathbf{x}}_i, \tag{3.2.5}$$

then each of the three coordinate-plane stress vectors may be written as

$$\mathbf{t}^{(\hat{\mathbf{x}}_j)} = t_1^{(\hat{\mathbf{x}}_j)}\hat{\mathbf{x}}_1 + t_2^{(\hat{\mathbf{x}}_j)}\hat{\mathbf{x}}_2 + t_3^{(\hat{\mathbf{x}}_j)}\hat{\mathbf{x}}_3 = t_i^{(\hat{\mathbf{x}}_j)}\hat{\mathbf{x}}_i, \quad j = 1, 2, 3. \tag{3.2.6}$$

By replacing $\hat{\mathbf{n}} = \hat{\mathbf{x}}_j$ in (3.2.4) we will have

$$t_i^{(\hat{\mathbf{x}}_j)} = \frac{df_i}{ds_j}.$$

The nine stress vector components

$$t_i^{(\hat{\mathbf{x}}_j)} = \tau_{ji}.$$

in (3.2.6) are the components of a second-order Cartesian tensor known as the *stress tensor*.

We now follow (3.2.5)

$$
\begin{aligned}
\mathbf{t}^{(\hat{\mathbf{n}})} &= (t_1{}^{(\hat{\mathbf{n}})}, t_2{}^{(\hat{\mathbf{n}})}, t_3{}^{(\hat{\mathbf{n}})}) = (\frac{df_1}{ds}, \frac{df_2}{ds}, \frac{df_3}{ds}) \\
&= (\frac{df_1}{ds_1}n_1 + \frac{df_1}{ds_2}n_2 + \frac{df_1}{ds_3}n_3\ ,\ \frac{df_2}{ds_1}n_1 + \frac{df_2}{ds_2}n_2 + \frac{df_2}{ds_3}n_3\ ,\ \frac{df_3}{ds_1}n_1 + \frac{df_3}{ds_2}n_2 + \frac{df_3}{ds_3}n_3) \\
&= (\tau_{11}n_1 + \tau_{21}n_2 + \tau_{31}n_3\ ,\ \tau_{12}n_1 + \tau_{22}n_2 + \tau_{32}n_3\ ,\ \tau_{13}n_1 + \tau_{23}n_2 + \tau_{33}n_3) \\
&= (\tau_{1j}n_1 + \tau_{2j}n_2 + \tau_{3j}n_3)\hat{\mathbf{x}}_j,
\end{aligned}
\tag{3.2.7}
$$

or

$$
\mathbf{t}^{(\hat{\mathbf{n}})} = \begin{bmatrix} t_1^{(\hat{\mathbf{n}})} \\ t_2^{(\hat{\mathbf{n}})} \\ t_3^{(\hat{\mathbf{n}})} \end{bmatrix} = (\begin{bmatrix} n_1 & n_2 & n_3 \end{bmatrix} \begin{bmatrix} \tau_{11} & \tau_{12} & \tau_{13} \\ \tau_{21} & \tau_{22} & \tau_{23} \\ \tau_{31} & \tau_{32} & \tau_{33} \end{bmatrix})^T = (\hat{\mathbf{n}}\Sigma)^T. \tag{3.2.8}
$$

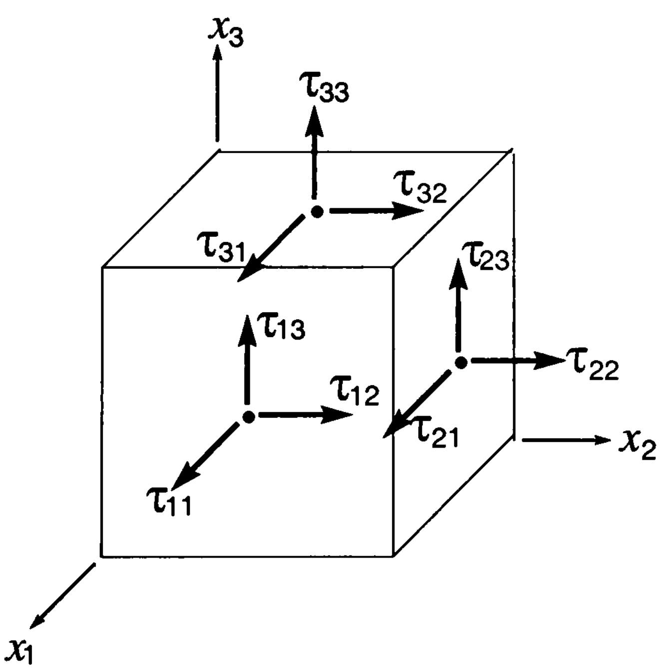

Figure 3.2: Normal stress and shear stresses acting on an element of fluid.

3.2.3 Normal and shear stresses

Pictorially, the stress tensor components may be displayed with reference to the coordinates plane as shown in figure 3.2. The components perpendicular to the planes (τ_{11} , τ_{22} , τ_{33}) are called *normal stress.* Those acting in (tangent to) the planes (τ_{12} , τ_{13} , τ_{21} , τ_{23} , τ_{31} , τ_{32}) are called *shear stresses.* A stress component is *positive* when it acts in the positive direction of the coordinate axes, and on a plane whose outer normal points in one of the positive coordinate directions. The component τ_{ij} acts in the direction of the jth coordinate axis and on the plane whose outward normal is parallel to the ith coordinate axis. The stress components shown in figure 3.2 are all positive.

3.2.4 The stress tensor-stress vector relationship

The relation between the stress tensor τ_{ij} at point P and the stress vector $t_i^{(\hat{n})}$ on a plane of arbitrary orientation at that point may be established through the force equilibrium or momentum balance of a small tetrahedron of the continuum, having its vertex at P (figure 3.3).

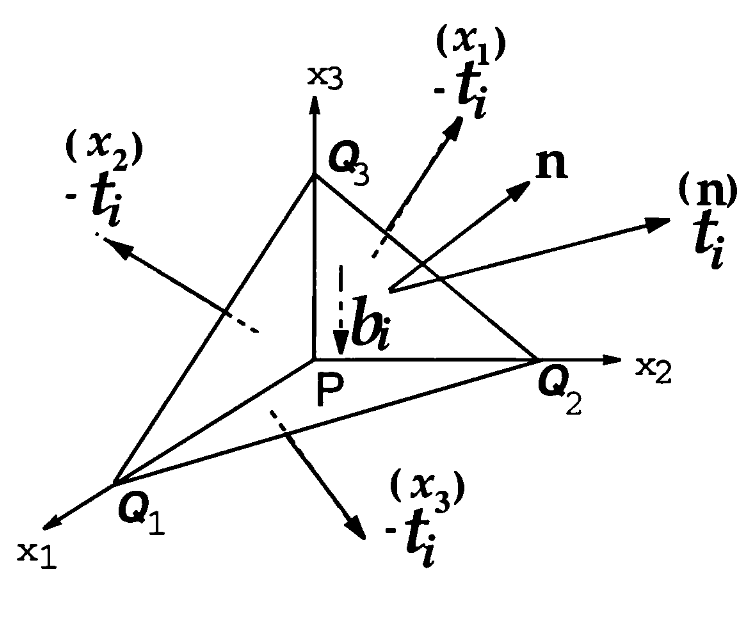

Figure 3.3: Stress components on an arbitrary surface

The base of the tetrahedron is taken perpendicular to n_i and the three faces are taken perpendicular to the coordinate planes as shown by figure 3.3. According to (3.2.3) designating the area of the base $Q_1Q_2Q_3$ as ds, the areas of the faces are the projected areas $dS_1 = dSn_1$ for face Q_3PQ_2, $dS_2 = dSn_2$ for face Q_3PQ_1, $dS_3 = dSn_3$ for face

Q_1PQ_2 or as we showed in (3.2.3) $dS_i = dSn_i$.

The average traction vector $-t_i^{(\hat{\mathbf{x}}_j)}$ on the faces and $t_i^{(\hat{\mathbf{n}})}$ on the base, together with the average body force (including inertial forces, if present), acting on the tetrahedron are shown in the figure 3.3. Equilibrium requires that

$$t_i^{(\hat{\mathbf{n}})} dS - t_i^{(\hat{\mathbf{x}}_1)} dS_1 - t_i^{(\hat{\mathbf{x}}_2)} dS_2 - t_i^{(\hat{\mathbf{x}}_3)} dS_3 + \rho b_i dV = 0. \tag{3.2.9}$$

If now the linear dimensions of the tetrahedron are reduced in a constant ratio, the body forces , being an order higher in the small dimensions tend to zero more rapidly than the surface forces. At the same time the average stress vectors approach the specific values appropriate to the designated direction at P. Therefore by this limiting process and the substitution (3.2.3), equation (3.2.9) reduces to

$$t_i^{(\hat{\mathbf{n}})} dS = t_i^{(\hat{\mathbf{x}}_1)} dS_1 + t_i^{(\hat{\mathbf{x}}_2)} dS_2 + t_i^{(\hat{\mathbf{x}}_3)} dS_3 = t_i^{(\hat{\mathbf{x}}_j)} n_j dS \ . \tag{3.2.10}$$

Cancelling the common factor dS and using the identity $t_i^{(\hat{\mathbf{x}}_j)} = \tau_{ji}$, (3.2.10) is equivalent to

$$t_i^{(\hat{\mathbf{n}})} = n_j \tau_{ji}, \tag{3.2.11}$$

which is same result we already mathematically found in (3.2.8).

3.2.5 Stress tensor symmetry

Proof 1

Equilibrium of any arbitrary volume V of a continuum subject to a system of surface forces $t_i^{(\hat{\mathbf{n}})}$ and body forces b_i (including inertia forces if present) requires that the resultant force and moment acting on the volume be zero [24]. Summation of surface and body forces results in the integral relation,

$$\int_S t_i^{(\hat{\mathbf{n}})} dS + \int_V \rho b_i dV = 0,$$

or

$$\int_S t^{(\hat{\mathbf{n}})} dS + \int_V \rho \mathbf{b} dV = 0.$$

Replacing $t_i^{(\hat{\mathbf{n}})}$ here by $\tau_{ij} n_j$ and applying the divergence theorem we get

$$\int_V (\tau_{ij,j} + \rho b_i) dV = 0 \quad \text{or} \quad \int_V (\nabla \cdot \Sigma + \rho \mathbf{b}) dV = 0.$$

Since the volume V is arbitrary then

$$\tau_{ij,j} + \rho b_i = 0 \quad \text{or} \quad \nabla \cdot \Sigma + \rho \mathbf{b} = 0. \tag{3.2.12}$$

which are called the *equilibrium equations.*

In the absence of distributed moments or couple-stress, the equilibrium of moments about the origin requires that

$$\int_S \epsilon_{ijk} x_j t_k^{(\hat{\mathbf{n}})} dS + \int_V \epsilon_{ijk} x_j \rho b_k dV = 0,$$

(where ϵ_{ijk} shows the sign of triple inner product ijk of three basis vectors i, j and k.)

or

$$\int_S \mathbf{x} \times t^{(\hat{\mathbf{n}})} dS + \int_V \mathbf{x} \times \rho \mathbf{b} dV = 0, \tag{3.2.13}$$

in which x_i is the position vector of the elements of surface and volume. Again, making the substitution $t_i^{(\hat{\mathbf{n}})} = \tau_{ij} n_j$, applying divergence theorem and using the expressed in (3.2.12), the integrals of (3.2.13) are combined and reduced to

$$\int_V \epsilon_{ijk} \tau_{jk} dV = 0 \quad \text{or} \quad \int_V \Sigma_v dV = 0,$$

which for the arbitrary volume V requires

$$\epsilon_{ijk} \tau_{jk} = 0 \quad \text{or} \quad \Sigma_v = 0,$$

which means

$$\tau_{jk} = \tau_{kj},$$

which says the *stress tensor is symmetric.* In view of $\tau_{ij} = \tau_{ji}$, the equilibrium equations (3.2.12) are often written

$$\frac{\partial \tau_{ij}}{\partial x_j} + \rho b_i = 0.$$

Proof 2

Let us concentrate our attention on the shear stresses that contribute to a torque about an axis through the centre of the element and parallel to the z-axis [25]. The torque produced by these forces about the centre of gravity of the element can be directly computed as

$$T = \tau_{xy} dxdzdy - \tau_{yx} dydzdx.$$

Since (the moment of inertia in respect to the previously specified axis of rotation is

$$\begin{aligned} I &= \sum_i \delta m_i r^2 \approx \int_{\delta v} \rho r^2 dv = \rho \int_{-\frac{dz}{2}}^{\frac{dz}{2}} \int_{-\frac{dx}{2}}^{\frac{dx}{2}} \int_{-\frac{dy}{2}}^{\frac{dy}{2}} (s^2 + t^2) ds dt du \\ &= \rho \frac{dxdydz}{12} (dx^2 + dy^2) (\text{ or } = \frac{M}{12} (dx^2 + dy^2)). \end{aligned}$$

Applying Newton's law, the torque may be equated to the product of angular acceleration, $\ddot{\omega}$, and moment of inertia, both to be taken in respect to the same axis of rotation the z-axis). We then obtain

$$(\tau_{xy} - \tau_{yx}) dxdydz = \rho \frac{dxdydz}{12} (dx^2 + dy^2) \ddot{\omega}_z,$$

or

$$(\tau_{xy} - \tau_{yx}) = \frac{\rho}{12} (dx^2 + dy^2) \ddot{\omega}_z. \tag{3.2.14}$$

Recalling now that dx and dy are infinitesimal, it must be concluded from (3.2.14) that the acceleration of any infinitesimal element would tend to infinity as dx and dy approach to zero (which is not possible) unless

$$\tau_{xy} = \tau_{yx}. \tag{3.2.15}$$

Hence by inference $\tau_{ij} = \tau_{ji}$.

3.3 The continuity equation

Applying two main concepts [25]:

- the conversation of mass principle which merely states that mass cannot be created (or destroyed)
- neglecting all effects of special relativity and Einstein's famous mass-energy equation

to an infinitesimal volume within the flow, where variation in density and velocity has taken place, will lead us to a differential equation which is usually called the *continuity equation*. Following there are three ways to derive this equation.

1. Infinitesimal volume

Several approaches for deriving it shall be investigated. To derive this equation we now apply the principle of conversation of mass to a small volume of space through which a flow takes place. This volume is an imaginary volume *fixed* in position and offering no resistance of any kind to the flow. It may be imagined, for example, as a thin wire cage. For convenience we shall adopt a Cartesian coordinate system (x, y, z), but for the sake of simplicity we shall treat only a two-dimensional flow as shown in figure 3.4 in which there is a component of flow along the z-axis. Sections normal to the z-axis, therefore, have an identical flow pattern, so that it is sufficient to consider a unit width in the z-direction. The fluid velocity in the x-direction will be designated by u, and that in the y-direction by v, while the density will be indicated by ρ. Both the velocity components and density are functions of position and time. The principle of conversation of mass requires that the net outflow of mass from the volume be equal to the decrease of mass within the volume. This is readily calculated with reference to figure 3.4. The flow of mass per unit time and area through a surface is the product of the velocity normal to the surface and the density. Thus the x-component of the mass flux per unit area at the center of the volume is ρu. This flux, however, changes from point to point, as indicated in figure 3.4. The net outflow of mass per unit time therefore, is

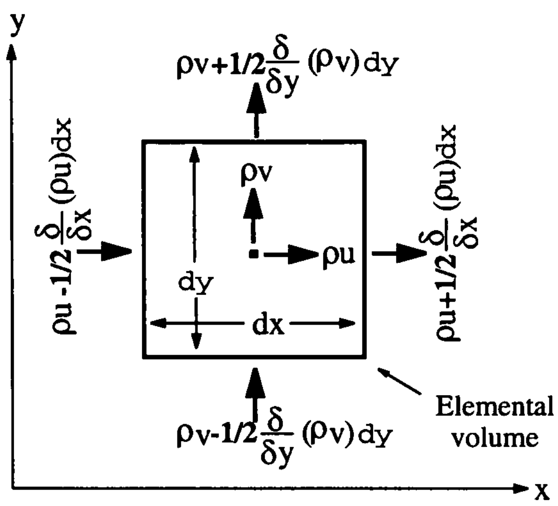

Figure 3.4: Velocities and densities for mass flow balance through a fixed volume element in two dimensions.

$$\{\rho u + \tfrac{1}{2}\tfrac{\partial}{\partial x}(\rho u)dx\}dy + \{\rho v + \tfrac{1}{2}\tfrac{\partial}{\partial y}(\rho v)dy\}dx - \{\rho u - \tfrac{1}{2}\tfrac{\partial}{\partial x}(\rho u)dx\}dy$$
$$-\{\rho v - \tfrac{1}{2}\tfrac{\partial}{\partial y}(\rho v)dy\}dx,$$

and this must equal the rate of mass decrease within the element

$$-\frac{\partial \rho}{\partial t}dxdy.$$

Upon simplification this becomes $\frac{\partial \rho}{\partial t} + \frac{\partial}{\partial x}(\rho u) + \frac{\partial}{\partial y}(\rho v) = 0$. Generalised to 3-dimension this is

$$\frac{\partial \rho}{\partial t} + \frac{\partial}{\partial x}(\rho u) + \frac{\partial}{\partial y}(\rho v) + \frac{\partial}{\partial z}(\rho w) = 0. \tag{3.3.1}$$

Equation (3.3.1) is called the *continuity equation.* If the density is constant (i.e. the fluid is incompressible), the continuity equation becomes

$$\frac{\partial u}{\partial x} + \frac{\partial v}{\partial y} + \frac{\partial w}{\partial z} = 0. \tag{3.3.2}$$

This equation is valid whether the velocity is time dependent or not.

2. Mass outflow

The mass outflow per unit time through the surface of the volume is

$$\int_S \rho\mathbf{u}\cdot\hat{\mathbf{n}}dS,$$

and this must be equal to the rate of decrease of mass contained within the fixed volume

$$-\int_V \frac{\partial\rho}{\partial t}dv.$$

Applying Gauss's theorem yields

$$\int_V \left(\frac{\partial\rho}{\partial t} + \boldsymbol{\nabla}\cdot(\rho\mathbf{u})\right)dv = 0. \tag{3.3.3}$$

(3.3.3) must hold for all arbitrary volumes and therefore

$$\frac{\partial\rho}{\partial t} + \boldsymbol{\nabla}\cdot(\rho\mathbf{u}) = 0, \tag{3.3.4}$$

will be the general case of equation of continuity. From (3.3.4) we will have

$$\frac{\partial\rho}{\partial t} + (\boldsymbol{\nabla}\rho)\cdot\mathbf{u} + \rho(\boldsymbol{\nabla}\cdot\mathbf{u}) = 0 \ \text{ or } \ \frac{1}{\rho}\frac{D\rho}{Dt} + \boldsymbol{\nabla}\cdot\mathbf{u} = 0, \tag{3.3.5}$$

where,

$$\frac{D}{Dt} = \frac{\partial}{\partial t} + \mathbf{u}\cdot\boldsymbol{\nabla}. \tag{3.3.6}$$

3. Conversation of mass

Applying conservation of mass

$$M = \int_{V(t)} \rho(\mathbf{x},t)dv = \int_{V(t+\Delta t)} \rho(\mathbf{x},t+\Delta t)dv,$$

which implies that,

$$\int_{V(t+\Delta t)} \rho(\mathbf{x},t+\Delta t)dv - \int_{V(t)} \rho(\mathbf{x},t)dv = 0,$$

and since $V(t+\Delta t) = V(t) + S(t)\mathbf{u}\cdot\mathbf{n}\Delta t$ therefore,

$$\int_{V(t)} \rho(\mathbf{x}, t+\Delta t)dv + \int_{S(t)} \rho(\mathbf{x}, t+\Delta t)\mathbf{u}\cdot\mathbf{n}\Delta t ds - \int_{V(t)} \rho(\mathbf{x}, t)dv = 0.$$

Applying Gauss's theorem yields,

$$\int_{V(t)} \frac{\partial \rho}{\partial t}\Delta t dv + \int_{V(t)} \boldsymbol{\nabla}\cdot(\rho\mathbf{u})\Delta t dv = 0,$$

since $V(t)$ is arbitrary volume element, therefore,

$$\frac{\partial \rho}{\partial t} + \boldsymbol{\nabla}\cdot(\rho\mathbf{u}) = 0.$$

3.4 Equation of motion

A Newtonian fluid is assumed to have continuous density and thus the motion to obey continuum mechanics. We consider an element of fluid of volume δV, density ρ and velocity $\underline{u}^{\dagger}$. A force $\underline{f}$ is exerted on the fluid element. Thus, from Newton's equations of motion, the force equals the rate of change of momentum:

$$f_i = \frac{D}{Dt}(\rho\delta V u_i^{\dagger}). \tag{3.4.1}$$

We now consider a region of fluid enclosed by the surface S. According to definition (3.2.1) the force on the fluid, $\mathbf{f}$, is such that

$$f_i = \int_S t_i^{(\hat{\mathbf{n}})} ds, \tag{3.4.2}$$

replacing $t_i^{(\hat{\mathbf{n}})}$ from (3.2.11) and applying divergence theorem implies that

$$f_i = \int_S \tau_{ij} n_j ds = \int_V \frac{\partial \tau_{ij}}{\partial x_j} dV. \tag{3.4.3}$$

Hence $f_i = \delta V \frac{\partial \tau_{ij}}{\partial x_j}$ and equating with (3.4.1), so the "*equation of motion*" becomes

$$\frac{D(\rho u_i^{\dagger})}{Dt} = \frac{\partial \tau_{ij}}{\partial x_j}. \tag{3.4.4}$$

3.5 The constitutive relations for the fluid

Applying stresses on the surface of the fluid element makes the fluid element distort. According to the differential of a function we express the change in velocity $\delta u_i^\dagger$ for a displacement δx_i as we are expanding $\delta u_1^\dagger$

$$\begin{aligned}\delta u_1^\dagger &= \frac{\partial u_1^\dagger}{\partial x_1}\delta x_1 + \frac{\partial u_1^\dagger}{\partial x_2}\delta x_2 + \frac{\partial u_1^\dagger}{\partial x_3}\delta x_3 \\ &= \frac{\partial u_1^\dagger}{\partial x_1}\delta x_1 + \frac{1}{2}\{(\frac{\partial u_1^\dagger}{\partial x_2} + \frac{\partial u_2^\dagger}{\partial x_1})\delta x_2 + (\frac{\partial u_3^\dagger}{\partial x_1} + \frac{\partial u_1^\dagger}{\partial x_3})\delta x_3\} \\ &+ \frac{1}{2}\{(\frac{\partial u_1^\dagger}{\partial x_3} - \frac{\partial u_3^\dagger}{\partial x_1})\delta x_3 - (\frac{\partial u_2^\dagger}{\partial x_1} - \frac{\partial u_1^\dagger}{\partial x_2})\delta x_2\}.\end{aligned} \tag{3.5.1}$$

We also expected a relation between the stress tensor field τ_{ij} and the "rate of *strain tensor field*" $e_{ij} = \frac{\partial u_i^\dagger}{\partial x_j} + \frac{\partial u_j^\dagger}{\partial x_i}$. We define $\boldsymbol{\omega} = (\omega_1, \omega_2, \omega_3) = \boldsymbol{\nabla} \times \mathbf{u}^\dagger$, by following (3.5.1) then we'll have

$$\delta u_1^\dagger = (1/2)(e_{11}\delta x_1 + e_{12}\delta x_2 + e_{13}\delta x_3) + (1/2)(\omega_2\delta x_3 - \omega_3\delta x_2),$$

$$\delta u_2^\dagger = (1/2)(e_{21}\delta x_1 + e_{22}\delta x_2 + e_{23}\delta x_3) + (1/2)(\omega_3\delta x_1 - \omega_1\delta x_3),$$

$$\delta u_3^\dagger = (1/2)(e_{31}\delta x_1 + e_{32}\delta x_2 + e_{33}\delta x_3) + (1/2)(\omega_1\delta x_2 - \omega_2\delta x_1).$$

or

$$\begin{bmatrix}\delta u_1^\dagger \\ \delta u_2^\dagger \\ \delta u_3^\dagger\end{bmatrix} = \frac{1}{2}(\begin{bmatrix}e_{11} & e_{12} & e_{13} \\ e_{21} & e_{22} & e_{23} \\ e_{31} & e_{32} & e_{33}\end{bmatrix} + \begin{bmatrix}0 & -\omega_3 & \omega_2 \\ \omega_3 & 0 & -\omega_1 \\ -\omega_2 & \omega_1 & 0\end{bmatrix})\begin{bmatrix}\delta x_1 \\ \delta x_2 \\ \delta x_3\end{bmatrix}.$$

The terms in e_{ij} give the distortion of the fluid element, whereas the velocity change due to the terms in ω_i is $(1/2)(\boldsymbol{\omega} \times \boldsymbol{\delta}\mathbf{r})$ which represents a rotation of the fluid element where $\boldsymbol{\delta}\mathbf{r} = (\delta x_1, \delta x_2, \delta x_3)$. The tensor components e_{ij} give the different rate of strains of the fluid element.

The simplest relation between the stress tensor field τ_{ij} and the rate of strain tensor field e_{ij} is linear:

$$\tau_{ij} = A_{ij} + B_{ij,mp}e_{mp}. \tag{3.5.2}$$

In deriving the Navier-Stokes equations we assume the relation takes the above linear form. Since the Navier-Stokes equations give accurate fluid flow descriptions, the above linear relation must describe the fluid flow. We assume the fluid is isotropic. As a consequence of the fluid having no directional properties the tensors A_{ij} and $B_{ij,mp}$ are isotropic. Therefore

A_{ij} and $B_{ij,mp}$ are isotropic. Therefore

$$A_{ij} = -p\delta_{ij},$$

$$B_{ij,mp} = \lambda\delta_{ij}\delta_{mp} + (\mu/2)(\delta_{im}\delta_{jp} + \delta_{ip}\delta_{jm}) + \nu(\delta_{im}\delta_{jp} - \delta_{ip}\delta_{jm}).$$

Substituting these relations into equation (2.8) gives:

$$\tau_{ij} = -p\delta_{ij} + \lambda\delta_{ij}e_{mm} + \mu e_{ij}.$$

If the fluid is incompressible, we expect the rate of increase of a fluid element e_{mm} to be zero. This means that the dilatation of the rate of strain tensor is zero.

Hence we obtain the constitutive relation

$$\tau_{ij} = -p\delta_{ij} + \mu e_{ij}, \tag{3.5.3}$$

where p is defined as $p = -(1/2)\tau_{kk}$ and may be called the "*pressure of the fluid*".

We now substitute the constitutive relation into the equation of motion for a fluid element in order to obtain Navier-Stokes equations.

3.6 The Navier-Stokes equations

We now consider the equation of motion of the fluid is given by equation (3.4.4) as

$$\frac{D(\rho u_i^\dagger)}{Dt} = \frac{\partial \tau_{ij}}{\partial x_j},$$

and the constitutive relations for the fluid is given by equation (3.5.3) as

$$\tau_{ij} = -p\delta_{ij} + \mu(\frac{\partial u_i^\dagger}{\partial x_j} + \frac{\partial u_j^\dagger}{\partial x_i}). \tag{3.6.1}$$

Thus differentiating both sides (3.6.1) gives

$$\frac{D(\rho u_i^\dagger)}{Dt} = -\frac{\partial p}{\partial x_i} + \mu(\nabla^2 u_i^\dagger + \frac{\partial^2 u_j^\dagger}{\partial x_i \partial x_j}). \tag{3.6.2}$$

Since we are dealing with an incompressible fluid then,

$$\nabla . u^\dagger = \frac{\partial u_j^\dagger}{\partial x_j} = 0. \tag{3.6.3}$$

If the flow is steady, then $\frac{\partial u_i^\dagger}{\partial t} = 0$ and therefore $\frac{D}{Dt} = u_i^\dagger \frac{\partial}{\partial x_i}$. So from (3.6.2) we obtain the Navier-Stokes equations for steady incompressible flow:

$$\rho u_j^\dagger \frac{\partial u_i^\dagger}{\partial x_j} = -\frac{\partial p}{\partial x_i} + \mu \nabla^2 u_i^\dagger. \tag{3.6.4}$$

3.7 Oseen equations

Oseen's approximation to the fluid flow is that the velocity perturbation **u** to the uniform stream U is small compared to the stream velocity U.

We let the uniform stream U be parallel to the x_1 axis. Thus the velocity $\mathbf{u}^\dagger$ is given by

$$(u_1^\dagger, u_2^\dagger, u_3^\dagger) = (U + u_1, u_2, u_3),$$

where the Oseen approximation is $|u_i| \ll U$.

Considering the Navier-Stokes equation, the term $u_j^\dagger \frac{\partial}{\partial x_j}$ is

$$(U + u_1)\frac{\partial}{\partial x_1} + u_2 \frac{\partial}{\partial x_2} + u_3 \frac{\partial}{\partial x_3} = U(\frac{\partial}{\partial x_1} + \frac{u_1 \partial}{U \partial x_1} + \frac{u_2 \partial}{U \partial x_2} + \frac{u_3 \partial}{U \partial x_3}).$$

Applying Oseen's approximation that $\frac{|u_i|}{U} \ll 1$, we obtain

$$u_j^\dagger \frac{\partial}{\partial x_j} = U \frac{\partial}{\partial x_1}. \tag{3.7.1}$$

Applying (3.7.1) on (3.6.4) yields

$$U\frac{\partial \mathbf{u}}{\partial x_1} = -(1/\rho)\boldsymbol{\nabla}\mathbf{p} + \nu\nabla^2\mathbf{u}. \tag{3.7.2}$$

Taking the divergence of (3.7.2),

$$U\frac{\partial}{\partial x_1}\{\frac{\partial u_1}{\partial x_1} + \frac{\partial u_2}{\partial x_2} + \frac{\partial u_3}{\partial x_3}\} = -(1/\rho)\nabla^2 p + \nu\{\nabla^2[\frac{\partial u_1}{\partial x_1} + \frac{\partial u_2}{\partial x_2} + \frac{\partial u_3}{\partial x_3}]\}. \tag{3.7.3}$$

Since the flow is incompressible, applying (3.6.3) on (3.7.3) yields $\nabla^2 p = 0$.

The equations

$$\begin{cases} U\frac{\partial \mathbf{u}}{\partial x_1} = -(1/\rho)\boldsymbol{\nabla}\mathbf{p} + \nu\nabla^2\mathbf{u}, \\ \nabla^2 p = 0, \end{cases} \tag{3.7.4}$$

are the Oseen's equations for steady flow.

3.8 Bernoulli equation

For high Reynolds numbers assume that the viscosity can be set to zero. The steady Navier-Stokes equations then reduce to

$$u_j\frac{\partial u_i}{\partial x_j} = -\frac{1}{\rho}\frac{\partial P}{\partial x_i}.$$

From this, we can derive the Bernoulli equation for two different cases (see figures 3.5 and 3.6).

$$P + \frac{1}{2}\rho u_j u_j = \text{const.}$$

Case 1 is valid everywhere for irrotational flow. Case 2 is valid along a streamline. First consider the two cases for time independent flow, and then for time dependent flow.

Time independent flow

Case 1. For irrotational (potential)flow

1. 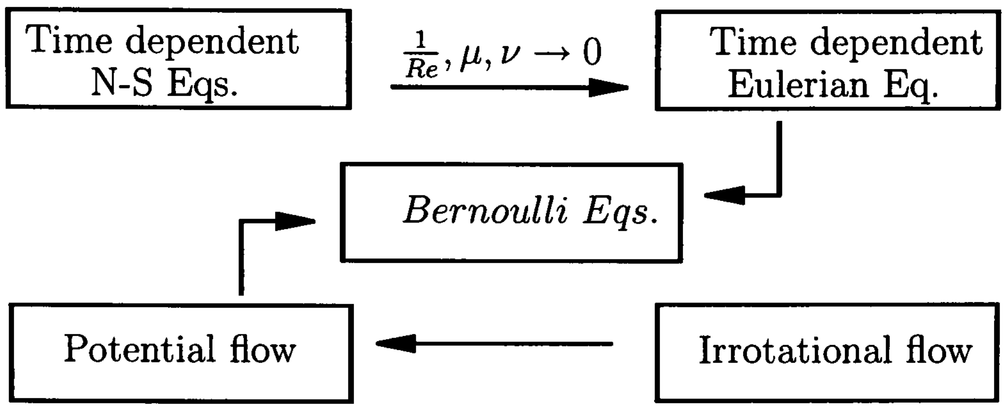

Figure 3.5: Derivation of Bernoulli Eq. Case 1

2. 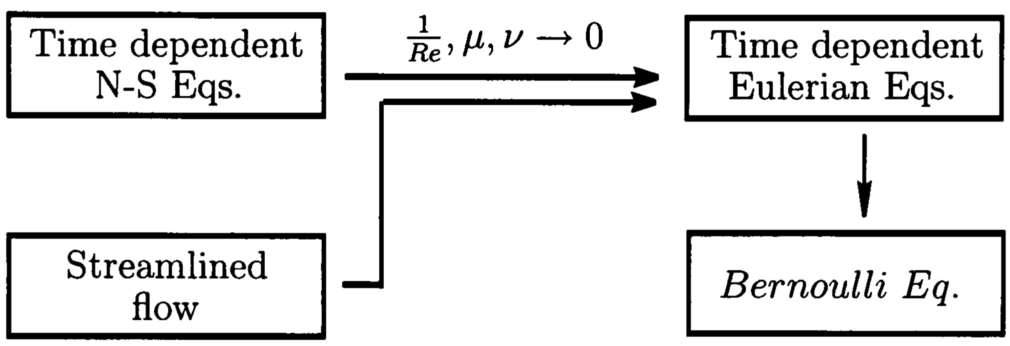

Figure 3.6: Derivation of Bernoulli Eq. Case 2

There exist φ such that $\varphi = \int_{\text{streamlined}} \mathbf{u} \cdot \mathbf{dr}$ for irrotational flow such that the rotational part is zero $\boldsymbol{\nabla} \times \mathbf{u} = \mathbf{0}$,

so, $u_i = \frac{\partial \varphi}{\partial x_i}$ and

$$\frac{\partial u_i}{\partial x_j} = \frac{\partial^2 \varphi}{\partial x_j \partial x_i} = \frac{\partial^2 \varphi}{\partial x_i \partial x_j} = \frac{\partial u_j}{\partial x_i},$$

$$u_j \frac{\partial u_j}{\partial x_i} = \frac{1}{2}\frac{\partial}{\partial x_i}(u_j u_j) = -\frac{1}{\rho}\frac{\partial P}{\partial x_i},$$

$$\frac{\partial}{\partial x_i}(\frac{1}{2}\rho u_j u_j + P) = 0,$$

$$P + \frac{1}{2}\rho V^2 = \text{const.} \tag{3.8.1}$$

where $V^2 = u_j u_j$. Equation (3.8.1) is the simplest form of the Bernoulli equation, named in honor of Daniel Bernoulli (1700-1782) [25].

Case 2. For streamlined flow

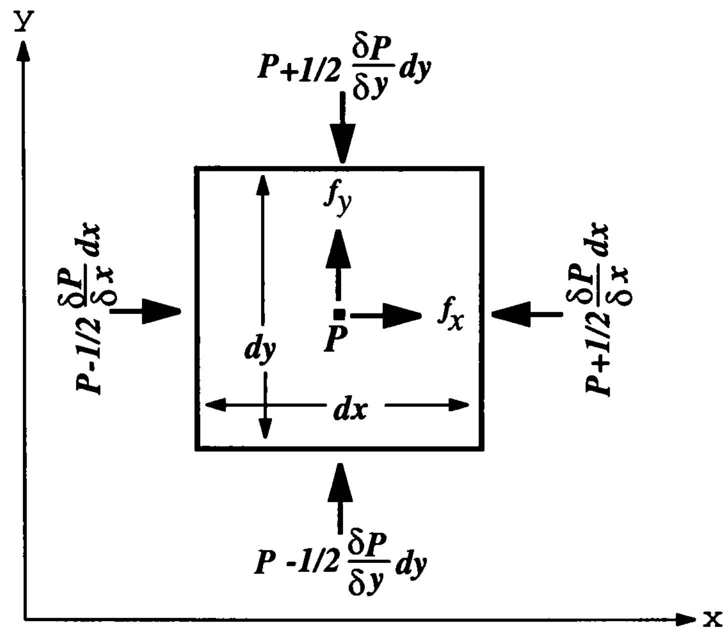

Figure 3.7: Forces on a fluid element in the absence of friction.

From Newton's law the force acting on a given mass is equal to the product of this mass times its acceleration. So we may write $F_x = ma_x$, where F_x is the force in the positive x-direction acting on the particle of mass m and a_x is acceleration in the x-direction. Since $ma_x = \rho dxdy\frac{Du}{Dt}$ and in absence of friction the forces acting on fluid element are pressure P and body force $\mathbf{f}$, so as it is pictorially shown in two-dimension figure 3.7, we may have $F_x = -\frac{\partial P}{\partial x}dxdy + \rho f_x dxdy$, and therefore $\frac{Du}{Dt} = -\frac{1}{\rho}\frac{\partial P}{\partial x} + f_x$. Similarly we will have the Eulerian equations

$$\frac{Du}{Dt} = -\frac{1}{\rho}\frac{\partial P}{\partial x} + f_x, \quad \frac{Dv}{Dt} = -\frac{1}{\rho}\frac{\partial P}{\partial y} + f_y, \quad \frac{Dw}{Dt} = -\frac{1}{\rho}\frac{\partial P}{\partial z} + f_z. \tag{3.8.2}$$

Let us consider the steady 2-D flow of an incompressible, inviscid fluid in the absence of body forces; The Eulerian equations (3.8.2) for this case are

$$u\frac{\partial u}{\partial x} + v\frac{\partial u}{\partial y} = -\frac{1}{\rho}\frac{\partial P}{\partial x}, \quad u\frac{\partial v}{\partial x} + v\frac{\partial v}{\partial y} = -\frac{1}{\rho}\frac{\partial P}{\partial y}.$$

This set of equations is readily integrated along a streamline. Multiplying first equation by dx and second one by dy and eliminating v in the first and u in the second equation and applying $\frac{dy}{dx} = (\frac{dy}{dt})/(\frac{dx}{dt}) = \frac{v}{u}$, we shall have

$$u\frac{\partial u}{\partial x}dx + u\frac{\partial u}{\partial y}dy = -\frac{1}{\rho}\frac{\partial P}{\partial x}dx, \quad v\frac{\partial v}{\partial x}dx + v\frac{\partial v}{\partial y}dy = -\frac{1}{\rho}\frac{\partial P}{\partial y}dy.$$

Adding both sides to each other implies

$$\frac{1}{2}d(u^2+v^2)=\frac{1}{2}\frac{\partial}{\partial x}(u^2+v^2)dx+\frac{1}{2}\frac{\partial}{\partial y}(u^2+v^2)dy=-\frac{1}{\rho}dP,$$

since ρ is constant then,

$$d(\frac{V^2}{2}+\frac{P}{\rho})=0, \quad (3.8.3)$$

or

$$\frac{1}{2}\rho V^2+P=\text{const.} \quad (3.8.4)$$

where $V^2=u^2+v^2$.

We now in equation (3.8.2) suppose the body force $\mathbf{f}$ is a *conservative force*, so there exist a function U such that $\nabla U=\mathbf{f}$. When such a force is included in the equation of motion, the Bernoulli equation will be

$$d(\frac{V^2}{2}+\frac{P}{\rho}-U)=0, \quad (3.8.5)$$

or for two points along the same streamline in a steady, inviscid and incompressible flow we have:

$$\frac{V_1{}^2}{2}+\frac{P_1}{\rho}-U_1=\frac{V_2{}^2}{2}+\frac{P_2}{\rho}-U_2. \quad (3.8.6)$$

Time dependent flow

So far we have considered steady flow and have omitted the nonsteady term, but this term may be included in equation (3.8.5). We must then add the terms $\frac{\partial u}{\partial t}dx$, $\frac{\partial v}{\partial t}dy$ for x and y-directions to the equation leading to (3.8.3).

since ds is an element of the streamline and

$$\frac{\partial V}{\partial t}ds=\frac{\partial V}{\partial t}\frac{ds}{dt}dt=\frac{u\frac{\partial u}{\partial t}+v\frac{\partial v}{\partial t}}{V}\frac{ds}{dt}dt=(u\frac{\partial u}{\partial t}+v\frac{\partial v}{\partial t})dt=\frac{\partial u}{\partial t}dx+\frac{\partial v}{\partial t}dy,$$

then we obtain

$$d(\int_s\frac{\partial V}{\partial t}ds+\frac{V^2}{2}+\frac{P}{\rho}-U)=0, \quad (3.8.7)$$

in which the integration of the nonsteady term is carried out along a given streamline at a given instant of time starting from an arbitrary reference point. Equation (3.8.7) shows that

$$\int_l \frac{\partial V}{\partial t} ds + \frac{V^2}{2} + \frac{P}{\rho} - U = \text{const. (integration along the streamline)} \tag{3.8.8}$$

In (3.8.8) the constant sometimes called the Bernoulli constant and denoted by B or because of the integration has been carried out along a special path at a given instant of time, so the Bernoulli constant should be a function of t as $B(t)$. Integrating between two points of the streamline leads to the expression

$$\int_{p_1}^{p_2} \frac{\partial V}{\partial t} ds + \frac{{V_2}^2}{2} + \frac{P_2}{\rho} - U_2 = \frac{{V_1}^2}{2} + \frac{P_1}{\rho} - U_1. \tag{3.8.9}$$

Equation (3.8.9) is applicable to two points on a given streamline in a nonsteady flow of an incompressible fluid in the presence of conservation forces.

The force potential most usually considered is that due to gravity. Let us take the y-axis to be positive when pointing upward and normal to the surface of the earth. The force per unit mass due to gravity is therefore directed downward and is of magnitude g. Thus $f_x = 0$, $f_y = -g$ and hence $U = -gy$. Substituting in Eq.(3.8.9), we obtain the equation that takes into account effect of the gravitational potential:

$$\int_{p_1}^{p_2} \frac{\partial V}{\partial t} ds + \frac{{V_2}^2}{2} + \frac{P_2}{\rho} - gy_2 = \frac{{V_1}^2}{2} + \frac{P_1}{\rho} - gy_1. \tag{3.8.10}$$

Chapter 4

Some inconsistencies in the aerodynamic potential flow theory

4.1 Introduction

There are predominantly high Reynolds number [26] flows and so the coefficient of the viscous term in the Navier-Stokes equation is small. The potential flow model is then obtained by assuming that this term is negligible. Flow models are then obtained satisfying Bernoulli's equation [27, 22]. (Also, Lamb [27] provides equations for the flow in terms of the kinetic energy of the fluid and added mass of the body.)

In aerodynamics, Prandtl [28] found that the boundary layer of fluid close to the body significantly alters the dynamics of the flow even though it has negligible thickness; the boundary layer separates, and using the theorems of Kutta [29] and Joukowski [30] it is generally assumed that separation occurs at the trailing edge at which point the Kutta condition holds.

The resulting trailing wake is modelled by a vortex distribution [2] and classically this is further modelled by a finite number of horseshoe vortices.

Let us assume the classical textbook representation of the flow past a wing, by a distribution of horseshoe vortices emanating into the fluid at the trailing edge. In particular, we follow the description given by Lighthill (§11, [31]). A discrete number of horseshoe vortices are used to represent the trailing vortex sheet. We therefore expect that as the number of horseshoe vortices used to model the flow increases, the better the discrete approximation to the vortex sheet. Chadwick [1] therefore considers this limiting process and obtains an integral distribution of what he calls lifting elements which exactly represents the vortex sheet.

In this chapter, we determine the forces [27]

$$\mathbf{F} = -\int_{S_B} P\hat{\mathbf{n}}ds, \tag{4.1.1}$$

on a lifting element and substitute pressure P from Bernoulli equation (3.8.1) and find anomalies both in the lift and drag that help us understand Goldstein' concerns about inviscid flow theory [5]. (By lift and drag it is meant the forces perpendicular to the axis of the body and tangential to the axis of the body respectively. So this is different from the standard definitions of lift and drag which are related to the axis of the uniform flow direction.)

4.2 Potential flow

The equations of motion for potential flow necessary for subsequent analysis are now derived.

4.2.1 Statement of problem

We start with the time independent incompressible Navier-Stokes equations [27] p. 577 (or Eq. (3.6.4)) with the viscosity set to zero, and also continuity equation for incompressible flow

$$\rho u_j^\dagger \frac{\partial u_i^\dagger}{\partial x_j} = -\frac{\partial p^\dagger}{\partial x_i}, \quad \frac{\partial u_j^\dagger}{\partial x_j} = 0. \tag{4.2.1}$$

$u_j^\dagger$ and $p^\dagger$ are the velocity and pressure respectively in suffix notation for the cartesian co-ordinate system (x_1, x_2, x_3). ρ is the fluid density and is assumed to be constant.

Assume the slip body boundary condition, then

$$u_j^\dagger n_j = 0, \tag{4.2.2}$$

on the body surface S_B, where n_i is the outward pointing normal.

Finally, we assume that away from the vortex wake region, the velocity can be represented by a potential velocity $\phi^\dagger$ such that $u_i^\dagger = \frac{\partial \phi^\dagger}{\partial x_i}$. Then,

$$p^\dagger + \frac{1}{2}\rho \frac{\partial \phi^\dagger}{\partial x_i}\frac{\partial \phi^\dagger}{\partial x_i} = p_0, \quad \frac{\partial^2 \phi^\dagger}{\partial x_j \partial x_j} = 0, \tag{4.2.3}$$

where p_0 is a constant. These equation given in (4.2.3) are the Bernoulli equation and Laplace equation respectively. We assume that the pressure tends to zero in the far field $p^\dagger \to 0$, and the velocity tends to a uniform stream predominately in the x_1 direction $\frac{\partial \phi^\dagger}{\partial x_i} \to U\delta_{i1} + V\delta_{i2}$ as $R = \sqrt{x_1^2 + x_2^2 + x_3^2} \to \infty$; The velocities are such that $U \gg V$, and δ_{ij} is delta Kronecker. So $p_0 = (1/2)\rho(U^2 + V^2)$.

Boundary conditions

Consider uniform flow $(U, V, 0)$ at infinity past a fixed closed body of surface S_B such that the "slip boundary condition"

$$\mathbf{u}^\dagger.\hat{\mathbf{n}} = \nabla\phi^\dagger.\hat{\mathbf{n}} = \frac{\partial \phi^\dagger}{\partial \hat{\mathbf{n}}} = u_j^\dagger n_j = 0, \tag{4.2.4}$$

holds where $\hat{\mathbf{n}} = (n_1, n_2, n_3)$ is the outward pointing normal to the body surface S_B and $\mathbf{u}^\dagger = \nabla\phi^\dagger$ is the fluid velocity (figure 4.1).

Letting $\mathbf{u}$ be the perturbation velocity for the uniform stream velocity $(U, V, 0)$, then $\mathbf{u}^\dagger = \nabla\phi^\dagger = U\hat{\mathbf{x}}_1 + V\hat{\mathbf{x}}_2 + \mathbf{u}$. This then becomes

$$\phi^\dagger = Ux_1 + Vx_2 + \varphi, \tag{4.2.5}$$

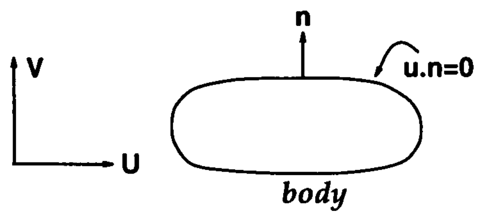

Figure 4.1: $(U, V, 0)$ Uniform potential velocity of the fluid.

where $\mathbf{u} = \nabla\varphi$. Denoting $\mathbf{u}^\dagger = (u_1^\dagger, u_2^\dagger, u_3^\dagger)$, implies $u_i^\dagger = (\delta_{i1}U + \delta_{i2}V + \frac{\partial\varphi}{\partial x_i})$.

It is clear that $\phi^\dagger \rightarrow Ux_1 + Vx_2$ as $R \rightarrow \infty$, and therefore $\mathbf{u}^\dagger = (U, V, 0)$ at infinity.

Limiting element

Consider an aerodynamic streamlined body such as a wing in high Reynolds number flow.

We now consider modelling the flow by the standard textbook approach, for example following Lighthill (§11,[31]) as a distribution of horseshoe vortices. This is represented pictorially by the figure 4.2.1 taken from (Fig 86, §11.3, [31]), where the circulation γ of each horseshoe vortex and we consider the steady state such that the time $t \rightarrow \infty$.

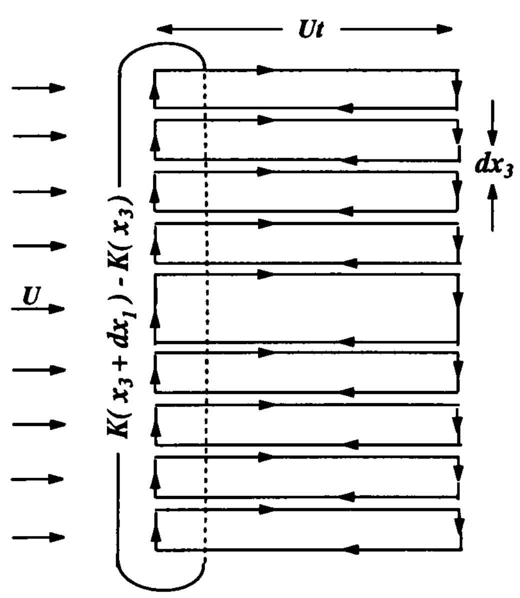

Figure 4.2: Pictorial representation of a wing by a finite distribution of horseshoe vortices taken from Lighthill ([31], §11.3 figure 86).

Consider the method of Chadwick [15], the limiting representation as the number of horseshoe vortices increases and hence their span decreases.

For example, consider the horseshoe vortex given by three vortex lines from $(\infty, 0, s)$ to $(0, 0, s)$, from $(0, 0, s)$ to $(0, 0, 0)$ and from $(0, 0, 0)$ to $(\infty, 0, 0)$ shown in figure 4.3.

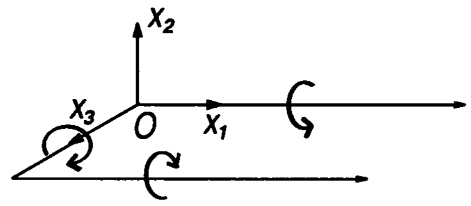

Figure 4.3: Horseshoe Vortex.

The velocity of the horseshoe vortex is given by [1] as

$$\begin{aligned} u_i =& \frac{-\gamma}{4\pi}\int_0^\infty \delta_{k1}\epsilon_{ijk}\frac{\partial}{\partial x_j}(\frac{1}{\{(x_1-\xi)^2+x_2^2+(x_3-s)^2\}^{\frac{1}{2}}})d\xi \\ &+ \frac{\gamma}{4\pi}\int_0^\infty \delta_{k1}\epsilon_{ijk}\frac{\partial}{\partial x_j}(\frac{1}{\{(x_1-\xi)^2+x_2^2+x_3^2\}^{\frac{1}{2}}})d\xi \\ &- \frac{\gamma}{4\pi}\int_0^s \delta_{k3}\epsilon_{ijk}\frac{\partial}{\partial x_j}(\frac{1}{\{x_1^2+x_2^2+(x_3-\xi)^2\}^{\frac{1}{2}}})d\xi, \end{aligned} \tag{4.2.6}$$

where s is the span and γ is the circulation.

Evaluating each velocity components in turn as $s \to 0$,

$$\begin{aligned} u_1 =& -\frac{\gamma}{4\pi}\int_0^s \frac{\partial}{\partial x_2}(\frac{1}{\{x_1^2+x_2^2+(x_3-\xi)^2\}^{\frac{1}{2}}})d\xi \\ \approx& -\frac{\gamma s}{4\pi}\frac{\partial}{\partial x_2}(\frac{1}{R}) \\ =& \frac{\gamma s}{4\pi}\frac{\partial}{\partial x_1}\{\frac{\partial}{\partial x_2}\ln(R-x_1)\}. \end{aligned} \tag{4.2.7}$$

Similarly,

$$
\begin{aligned}
u_2 = &-\frac{\gamma}{4\pi}\int_0^\infty \frac{\partial}{\partial x_3}\Big(\frac{1}{\{(x_1-\xi)^2+x_2^2+(x_3-s)^2\}^{\frac{1}{2}}}\Big)d\xi \\
&+\frac{\gamma}{4\pi}\int_0^\infty \frac{\partial}{\partial x_3}\Big(\frac{1}{\{(x_1-\xi)^2+x_2^2+x_3^2\}^{\frac{1}{2}}}\Big)d\xi \\
&+\frac{\gamma}{4\pi}\int_0^s \frac{\partial}{\partial x_1}\Big(\frac{1}{\{x_1^2+x_2^2+(x_3-\xi)^2\}^{\frac{1}{2}}}\Big)d\xi \\
&\approx \frac{\gamma}{4\pi}\int_0^\infty \frac{\partial^2}{\partial x_3^2}\Big(\frac{1}{\{(x_1-\xi)^2+x_2^2+x_3^2\}^{\frac{1}{2}}}\Big)d\xi + \frac{\gamma s}{4\pi}\frac{\partial}{\partial x_1}\Big(\frac{1}{R}\Big) \\
&= -\frac{\gamma s}{4\pi}\frac{\partial^2}{\partial x_3^2}\ln(R-x_1) - \frac{\gamma s}{4\pi}\frac{\partial^2}{\partial x_1^2}\ln(R-x_1) \\
&= \frac{\gamma s}{4\pi}\frac{\partial}{\partial x_2}\Big\{\frac{\partial}{\partial x_2}\ln(R-x_1)\Big\},
\end{aligned}
\tag{4.2.8}
$$

and where we have used the integral identity given in Appendix 4.5:

$$
\frac{\partial}{\partial x_j}\ln(R-x_1) = -\int_0^\infty \frac{\partial}{\partial x_j}\Big(\frac{1}{\{(x_1-\xi)^2+x_2^2+x_3^2\}^{\frac{1}{2}}}\Big)d\xi. \tag{4.2.9}
$$

Finally, the third velocity component is

$$
\begin{aligned}
u_3 = &\frac{\gamma}{4\pi}\int_0^\infty \frac{\partial}{\partial x_2}\Big(\frac{1}{\{(x_1-\xi)^2+x_2^2+(x_3-s)^2\}^{\frac{1}{2}}}\Big)d\xi \\
&-\frac{\gamma}{4\pi}\int_0^\infty \frac{\partial}{\partial x_2}\Big(\frac{1}{\{(x_1-\xi)^2+x_2^2+x_3^2\}^{\frac{1}{2}}}\Big)d\xi \\
&\approx -\frac{\gamma s}{4\pi}\int_0^\infty \frac{\partial^2}{\partial x_2 \partial x_3}\Big(\frac{1}{\{(x_1-\xi)^2+x_2^2+x_3^2\}^{\frac{1}{2}}}\Big)d\xi \\
&= \frac{\gamma s}{4\pi}\frac{\partial}{\partial x_3}\Big\{\frac{\partial}{\partial x_2}\ln(R-x_1)\Big\},
\end{aligned}
\tag{4.2.10}
$$

again, the integral identity given in Appendix 4.5 was used.

Thus the potential of the " lifting element", the limiting vortex of the horseshoe vortex, is

$$
\varphi = \frac{1}{4\pi\rho U}\frac{\partial}{\partial x_2}\ln(R-x_1). \tag{4.2.11}
$$

This is the potential part of the lift Oseenlet [32, 23] for Oseen flow.

4.2.2 Force integral for the limiting element

The force is represented by a surface integral of the normal pressure over the body surface [27] such that

$$\mathbf{F} = -\int_{S_B} P\hat{\mathbf{n}}ds. \tag{4.2.12}$$

Let $\mathbf{F} = (F_1, F_2, F_3)$, now we replace P from the Bernoulli equation (4.2.3) and applying divergence theorem to omit the constant term p_0, to deduce

$$F_i = -\int_{S_B} Pn_i ds = \frac{1}{2}\rho\int_{S_B} (u_j^\dagger u_j^\dagger)n_i ds, \tag{4.2.13}$$

where F_i is the force on the body due to the fluid, ds is an element of the surface, then for closed surface S_B containing volume V divergence theorem for appropriate case gives

$$\int_{S_B} (u_j^\dagger u_j^\dagger)n_i ds = \int_V \frac{\partial}{\partial x_i}(u_j^\dagger u_j^\dagger)dv,$$

and since Laplace's equation in (4.2.3) holds, so

$$\begin{aligned} \frac{\partial}{\partial x_i}(u_j^\dagger u_j^\dagger) &= \frac{\partial}{\partial x_i}(\frac{\partial\phi^\dagger}{\partial x_j}\frac{\partial\phi^\dagger}{\partial x_j}) = 2\frac{\partial^2\phi^\dagger}{\partial x_i\partial x_j}\frac{\partial\phi^\dagger}{\partial x_j} = 2(\frac{\partial^2\phi^\dagger}{\partial x_j\partial x_i}\frac{\partial\phi^\dagger}{\partial x_j} + \frac{\partial\phi^\dagger}{\partial x_i}\frac{\partial^2\phi^\dagger}{\partial x_j\partial x_j}) \\ &= 2\frac{\partial}{\partial x_j}(\frac{\partial\phi^\dagger}{\partial x_i}\frac{\partial\phi^\dagger}{\partial x_j}), \end{aligned} \tag{4.2.14}$$

this leads us to use slip boundary condition (4.2.4) and rewrite F_i in the following form

$$F_i = \frac{1}{2}\rho\int_{S_B} \{(u_j^\dagger u_j^\dagger)n_i - 2(u_i^\dagger u_j^\dagger n_j)\}ds. \tag{4.2.15}$$

Let us determine the force F_i in (4.2.15) by substituting in the fluid velocity $\mathbf{u}$ given by the potential (4.2.11). Consider the problem described in the figure 4.4 which consists of a lifting element located at the origin.

In this figure $\hat{\mathbf{n}}_B = -\hat{\mathbf{n}}$, $\hat{\mathbf{n}}_R$ shows outward pointing normal to general surface S_R enclosing the body and $\hat{\mathbf{n}}_C$ the outward pointing normal to ϵ-radius cylinder S_C ($\epsilon < R$) along the

x-axis and finally V is the volume between the general surface S_R and the body and surface S_C. The divergence theorem for an appropriate vector field $\mathbf{g}$ is given by

$$\int_{S_B} \mathbf{g}.\hat{\mathbf{n}}_B ds + \int_{S_C} \mathbf{g}.\hat{\mathbf{n}}_C ds + \int_{S_R} \mathbf{g}.\hat{\mathbf{n}}_R ds = \int_V (\text{div } \mathbf{g}) dv.$$

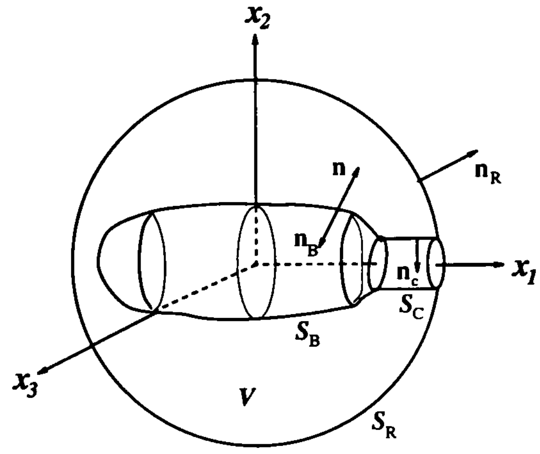

Figure 4.4: Singularity about x-axis

So,

$$\begin{aligned} F_i = \frac{1}{2}\rho \int_{S_B} \{u_j^\dagger u_j^\dagger n_i - 2u_i^\dagger u_j^\dagger n_j\} ds = \\ -\frac{1}{2}\rho \int_{S_B} \{u_j^\dagger u_j^\dagger (n_i)_B - 2u_i^\dagger u_j^\dagger (n_j)_B\} ds = \\ -\frac{1}{2}\rho \{ \int_V \{ \frac{\partial}{\partial x_i} (\frac{\partial \phi^\dagger}{\partial x_j} \frac{\partial \phi^\dagger}{\partial x_j}) - 2\frac{\partial}{\partial x_j} (\frac{\partial \phi^\dagger}{\partial x_i} \frac{\partial \phi^\dagger}{\partial x_j}) \} dv \\ - \int_{S_R} \{u_j^\dagger u_j^\dagger (n_i)_{S_R} - 2u_i^\dagger u_j^\dagger (n_j)_{S_R}\} ds \\ - \int_{S_C} \{u_j^\dagger u_j^\dagger (n_i)_{S_C} - 2u_i^\dagger u_j^\dagger (n_j)_{S_C}\} ds \}, \end{aligned}$$

but from (4.2.14) we have $\frac{\partial}{\partial x_i} (\frac{\partial \phi^\dagger}{\partial x_j} \frac{\partial \phi^\dagger}{\partial x_j}) - 2\frac{\partial}{\partial x_j} (\frac{\partial \phi^\dagger}{\partial x_i} \frac{\partial \phi^\dagger}{\partial x_j}) = 0$, therefore

$$\begin{aligned} F_i = &\frac{1}{2}\rho (\int_{S_R} \{u_j^\dagger u_j^\dagger (n_i)_{S_R} - 2u_i^\dagger u_j^\dagger (n_j)_{S_R}\} ds \\ &+ \int_{S_C} \{u_j^\dagger u_j^\dagger (n_i)_{S_C} - 2u_i^\dagger u_j^\dagger (n_j)_{S_C}\} ds). \end{aligned} \tag{4.2.16}$$

For the sake of simplicity we denote the common integrand by

$$\textbf{Integrand}(F_i) = \{u_j^\dagger u_j^\dagger n_i - 2u_i^\dagger u_j^\dagger n_j\},$$

and therefore,

$$F_i = \frac{1}{2}\rho(\int_{S_R} \textbf{Integrand}(F_i)_{S_R} ds + \int_{S_C} \textbf{Integrand}(F_i)_{S_C} ds). \tag{4.2.17}$$

Since

$\{u_j^\dagger u_j^\dagger n_i - 2u_i^\dagger u_j^\dagger n_j\} =$

$\{(U^2+V^2+2U\frac{\partial\varphi}{\partial x_1}+2V\frac{\partial\varphi}{\partial x_2}+\nabla\varphi.\nabla\varphi)n_i \; -2(\delta_{i1}U+\delta_{i2}V+\frac{\partial\varphi}{\partial x_i})(\delta_{j1}U+\delta_{j2}V+\frac{\partial\varphi}{\partial x_j})n_j\} =$
$\{(U^2+V^2+2U\frac{\partial\varphi}{\partial x_1}+2V\frac{\partial\varphi}{\partial x_2}+\nabla\varphi.\nabla\varphi)n_i \; -2[(\delta_{i1}U^2+\delta_{i2}UV+U\frac{\partial\varphi}{\partial x_i})n_1+(\delta_{i2}V^2+\delta_{i1}UV+$
$V\frac{\partial\varphi}{\partial x_i})n_2 \; +(\delta_{i1}U\frac{\partial\varphi}{\partial x_j}+\delta_{i2}V\frac{\partial\varphi}{\partial x_j}+\frac{\partial\varphi}{\partial x_i}\frac{\partial\varphi}{\partial x_j})n_j]\},$

we have:

$\textbf{Integrand}(\mathbf{F}_1) =$

$(-U^2+V^2-2U\frac{\partial\varphi}{\partial x_1}+2V\frac{\partial\varphi}{\partial x_2}-(\frac{\partial\varphi}{\partial x_1})^2+(\frac{\partial\varphi}{\partial x_2})^2+(\frac{\partial\varphi}{\partial x_3})^2)n_1 \; -2(UV+U\frac{\partial\varphi}{\partial x_2}+V\frac{\partial\varphi}{\partial x}+\frac{\partial\varphi}{\partial x_1}\frac{\partial\varphi}{\partial x_2})n_2-$
$2(U\frac{\partial\varphi}{\partial z}+\frac{\partial\varphi}{\partial x_1}\frac{\partial\varphi}{\partial x_3})n_3;$

$\textbf{Integrand}(\mathbf{F}_2) =$

$-2(UV+V\frac{\partial\varphi}{\partial x_1}+U\frac{\partial\varphi}{\partial x_2}+\frac{\partial\varphi}{\partial x_1}\frac{\partial\varphi}{\partial x_2})n_1 \; +(U^2-V^2+2U\frac{\partial\varphi}{\partial x_1}-2V\frac{\partial\varphi}{\partial x_2}+(\frac{\partial\varphi}{\partial x_1})^2-(\frac{\partial\varphi}{\partial x_2})^2+(\frac{\partial\varphi}{\partial x_3})^2)n_2$
$-2(V\frac{\partial\varphi}{\partial x_3}+\frac{\partial\varphi}{\partial x_2}\frac{\partial\varphi}{\partial x_3})n_3;$

$\textbf{Integrand}(\mathbf{F}_3) =$

$-2(U\frac{\partial\varphi}{\partial x_3}+\frac{\partial\varphi}{\partial x_1}\frac{\partial\varphi}{\partial x_3})n_1-2(V\frac{\partial\varphi}{\partial x_3}+\frac{\partial\varphi}{\partial x_2}\frac{\partial\varphi}{\partial x_3})n_2 \; +(U^2+V^2+2U\frac{\partial\varphi}{\partial x_1}+2V\frac{\partial\varphi}{\partial x_2}+(\frac{\partial\varphi}{\partial x_1})^2+(\frac{\partial\varphi}{\partial x_2})^2-$
$(\frac{\partial\varphi}{\partial x_3})^2)n_3.$

4.3 Force calculation

4.3.1 Representation

In this section we compute the force (4.2.17) for the problem. Because φ is singular along $x_1 \geq 0,\ x_2 = 0,\ x_3 = 0$, we consider the surface consisting of the cylinder S_C and punctured sphere S_R (figure 4.4) given by

$$S_C : \begin{cases} {x_2}^2 + {x_3}^2 = \epsilon^2, \\ a \le x_1 \le \sqrt{R^2 - \epsilon^2}, \end{cases} \qquad \begin{cases} x_2 = \epsilon\cos\phi,\ x_3 = \epsilon\sin\phi,\ 0 \le \phi \le 2\pi, \\ \mathbf{n}_C = -(0, \cos\phi, \sin\phi),\ ds = \epsilon d\phi dx_1. \end{cases}$$

$$S_R : \begin{cases} {x_1}^2 + {x_2}^2 + {x_3}^2 = R^2, \\ -R \le x_1 \le \sqrt{R^2 - \epsilon^2}, \\ \mathbf{n}_R = \frac{1}{R}(x_1, x_2, x_3), \end{cases} \qquad \begin{cases} x_1 = R\cos\theta,\ x_2 = R\sin\theta\cos\phi,\ x_3 = R\sin\theta\sin\phi, \\ 0 \le \phi \le 2\pi,\ \ \arccos(\frac{\sqrt{R^2-\epsilon^2}}{R}) \le \theta \le \pi, \\ ds = R^2 \sin\theta d\theta d\phi. \end{cases}$$

The **Integrand**($\mathbf{F}_i$) is then given as follows.

Force components on S_R :

Integrand$(\mathbf{F}_1)_{S_R}$ =

$$\begin{aligned} &(-U^2 + V^2 - 2U\frac{\partial\varphi}{\partial x_1} + 2V\frac{\partial\varphi}{\partial x_2} - (\frac{\partial\varphi}{\partial x_1})^2 + (\frac{\partial\varphi}{\partial x_2})^2 + (\frac{\partial\varphi}{\partial x_3})^2)(\frac{x_1}{R}) \\ &- 2(UV + U\frac{\partial\varphi}{\partial x_2} + V\frac{\partial\varphi}{\partial x_1} + \frac{\partial\varphi}{\partial x_1}\frac{\partial\varphi}{\partial x_2})(\frac{x_2}{R}) - 2(U\frac{\partial\varphi}{\partial x_3} + \frac{\partial\varphi}{\partial x_1}\frac{\partial\varphi}{\partial x_3})(\frac{x_3}{R}), \end{aligned} \tag{4.3.1}$$

Integrand$(\mathbf{F}_2)_{S_R}$ =

$$\begin{aligned} &- 2(UV + V\frac{\partial\varphi}{\partial x_1} + U\frac{\partial\varphi}{\partial x_2} + \frac{\partial\varphi}{\partial x_1}\frac{\partial\varphi}{\partial x_2})(\frac{x_1}{R}) \\ &+ (U^2 - V^2 + 2U\frac{\partial\varphi}{\partial x_1} - 2V\frac{\partial\varphi}{\partial x_2} + (\frac{\partial\varphi}{\partial x_1})^2 - (\frac{\partial\varphi}{\partial x_2})^2 + (\frac{\partial\varphi}{\partial x_3})^2)(\frac{x_2}{R}) \\ &- 2(V\frac{\partial\varphi}{\partial x_3} + \frac{\partial\varphi}{\partial x_2}\frac{\partial\varphi}{\partial x_3})(\frac{x_3}{R}), \end{aligned} \tag{4.3.2}$$

Integrand$(\mathbf{F}_3)_{S_R}$ =

$$\begin{aligned} &- 2(U\frac{\partial\varphi}{\partial x_3} + \frac{\partial\varphi}{\partial x_1}\frac{\partial\varphi}{\partial x_3})(\frac{x_1}{R}) - 2(V\frac{\partial\varphi}{\partial x_3} + \frac{\partial\varphi}{\partial x_2}\frac{\partial\varphi}{\partial x_3})(\frac{x_2}{R}) \\ &+ (U^2 + V^2 + 2U\frac{\partial\varphi}{\partial x_1} + 2V\frac{\partial\varphi}{\partial x_2} + (\frac{\partial\varphi}{\partial x_1})^2 + (\frac{\partial\varphi}{\partial x_2})^2 - (\frac{\partial\varphi}{\partial x_3})^2)(\frac{x_3}{R}). \end{aligned} \tag{4.3.3}$$

Force components on S_C :

Integrand$(\mathbf{F}_1)_{S_C}$ =

$$-2(UV+U\frac{\partial\varphi}{\partial x_2}+V\frac{\partial\varphi}{\partial x_1}+\frac{\partial\varphi}{\partial x_1}\frac{\partial\varphi}{\partial x_2})(-\frac{x_2}{\epsilon})-2(U\frac{\partial\varphi}{\partial x_3}+\frac{\partial\varphi}{\partial x_1}\frac{\partial\varphi}{\partial x_3})(-\frac{x_3}{\epsilon}), \tag{4.3.4}$$

Integrand$(\mathbf{F}_2)_{S_C}$ =

$$\begin{aligned}&(U^2-V^2+2U\frac{\partial\varphi}{\partial x_1}-2V\frac{\partial\varphi}{\partial x_2}+(\frac{\partial\varphi}{\partial x_1})^2-(\frac{\partial\varphi}{\partial x_2})^2+(\frac{\partial\varphi}{\partial x_3})^2)(-\frac{x_2}{\epsilon})\\&-2(V\frac{\partial\varphi}{\partial x_3}+\frac{\partial\varphi}{\partial x_2}\frac{\partial\varphi}{\partial x_3})(-\frac{x_3}{\epsilon}),\end{aligned} \tag{4.3.5}$$

Integrand$(\mathbf{F}_3)_{S_C}$ =

$$\begin{aligned}&-2(V\frac{\partial\varphi}{\partial x_3}+\frac{\partial\varphi}{\partial x_2}\frac{\partial\varphi}{\partial x_3})(-\frac{x_2}{\epsilon})+\\&(U^2+V^2+2U\frac{\partial\varphi}{\partial x_1}+2V\frac{\partial\varphi}{\partial x_2}+(\frac{\partial\varphi}{\partial x_1})^2+(\frac{\partial\varphi}{\partial x_2})^2-(\frac{\partial\varphi}{\partial x_3})^2)(-\frac{x_3}{\epsilon}).\end{aligned} \tag{4.3.6}$$

4.3.2 Useful properties simplifying the analysis

We employ two useful properties, symmetry of integrand and harmonics of function, to simply the analysis which are described below. We then use these properties in our determination of the forces on the body.

Symmetry

Since the surface S_R is symmetric with respect to the x_1x_3 and x_1x_2 planes, then $\int_{S_R} g ds = 0$ if g is an antisymmetric function in terms of x_2 or x_3. It is easy to verify that if f is a symmetric (even) function in terms of x_1, then its derivative with respect to x_1 will be an antisymmetric (odd) function in terms of x_1 (and vice versa). Accordingly $\frac{\partial}{\partial x_2}\ln(\sqrt{{x_1}^2+{x_2}^2+{x_3}^2}-x_1)$ would be an antisymmetric function in terms of x_2 because $\ln(\sqrt{{x_1}^2+{x_2}^2+{x_3}^2}-x_1)$ is a symmetric function in terms of x_2. We summarize these results for φ from (4.2.11) in the table 1.

Symmetry	$\frac{\partial\varphi}{\partial x_1}$	$\frac{\partial\varphi}{\partial x_2}$	$\frac{\partial\varphi}{\partial x_3}$
in terms of x_1	even	none	none
in terms of x_2	odd	even	odd
in terms of x_3	even	even	odd

Table 4.1: Symmetry properties of partial differentials of φ

Harmonics

We shall prove a theorem about some harmonic functions.

Theorem 4.3.1. *In any region of* $\mathbb{R}^3$ *excluding the non-negative x-axis,*

$$\nabla^2 \ln(R - x_1) = 0, \text{ where } R = \sqrt{{x_1}^2 + {x_2}^2 + {x_3}^2}.$$

Proof. A simple computation shows

$\frac{\partial}{\partial x_1} \ln(R - x_1) = -\frac{1}{R}, \frac{\partial^2}{\partial {x_1}^2} \ln(R - x_1) = \frac{x_1}{R^3}.$

$\frac{\partial}{\partial x_2} \ln(R - x_1) = \frac{x_2}{R(R-x_1)}, \frac{\partial^2}{\partial {x_2}^2} \ln(R - x_1) = \frac{R^3 - R^2 x_1 - x_2(2x_2 R - x_1 x_2)}{R^3(R-x_1)^2}.$

$\frac{\partial}{\partial x_3} \ln(R - x_1) = \frac{x_3}{R(R-x_1)}, \frac{\partial^2}{\partial {x_3}^2} \ln(R - x_1) = \frac{R^3 - R^2 x_1 - x_3(2x_3 R - x_1 x_3)}{R^3(R-x_1)^2}.$

So,

$$(\frac{\partial^2}{\partial {x_1}^2} + \frac{\partial^2}{\partial {x_2}^2} + \frac{\partial^2}{\partial {x_3}^2}) \ln(R - x_1) = 0. \tag{4.3.7}$$

□

Corollary 4.3.2. *Since* $\ln(R-x_1)$ *is harmonic then so are* $\frac{\partial}{\partial x_1} \ln(R-x_1)$ *and* $\frac{\partial}{\partial x_2} \ln(R-x_1)$ *in the same region, so,*

$$\nabla^2 \frac{\partial}{\partial x_1} \ln(R - x_1) = 0 \ , \quad \nabla^2 \frac{\partial}{\partial x_2} \ln(R - x_1) = 0. \tag{4.3.8}$$

4.3.3 Drag force

We calculate the contribution to the drag from the lifting element.

Evaluation over sphere

First consider the contribution over the sphere surface S_R. The integrand is given by (4.3.1).

$\mathbf{Integrand}(F_1)_{S_R} =$

$(-U^2+V^2-2U\frac{\partial\varphi}{\partial x_1}+2V\frac{\partial\varphi}{\partial x_2}-(\frac{\partial\varphi}{\partial x_1})^2+(\frac{\partial\varphi}{\partial x_2})^2+(\frac{\partial\varphi}{\partial x_3})^2)(\frac{x_1}{R})$

$-2(UV+U\frac{\partial\varphi}{\partial x_2}+V\frac{\partial\varphi}{\partial x_1}+\frac{\partial\varphi}{\partial x_1}\frac{\partial\varphi}{\partial x_2})(\frac{x_2}{R})-2(U\frac{\partial\varphi}{\partial x_3}+\frac{\partial\varphi}{\partial x_1}\frac{\partial\varphi}{\partial x_3})(\frac{x_3}{R}).$

We calculate each term in turn. Some of these evaluations are determined using Maple software [33].

1. $\int_{S_R}\{(-2U\frac{\partial\varphi}{\partial x_1})\frac{x_1}{R}+((-2UV)+(-2U\frac{\partial\varphi}{\partial x_2}))\frac{x_2}{R}+(-2U\frac{\partial\varphi}{\partial x_3})\frac{x_3}{R}\}ds=0$ because of anti-symmetry of the integrand in terms of x_2.

2. $\int_{S_R}(-U^2+V^2)\frac{x_1}{R}ds=(U^2-V^2)\pi\epsilon^2.$

3. $\int_{S_R}(-(\frac{\partial\varphi}{\partial x_1})^2)\frac{x_1}{R}ds=-\frac{1}{64R^6\pi\rho^2U^2}\epsilon^4.$

4. $\int_{S_R}(2V\frac{\partial\varphi}{\partial x_2})\frac{x_1}{R}ds=\frac{V}{2\pi\rho U}\int_{S_R}(\frac{\partial^2}{\partial x_2{}^2}(\ln(R-x_1)))\frac{x_1}{R}ds$
$=\frac{V}{2\pi\rho U}(\frac{1}{2}\int_{S_R}\{((\frac{\partial^2}{\partial x_2{}^2}+\frac{\partial^2}{\partial x_3{}^2})\ln(R-x_1))\frac{x_1}{R}\}ds).$
From (4.3.7) we have $(\frac{\partial^2}{\partial x_2{}^2}+\frac{\partial^2}{\partial x_3{}^2})\ln(R-x_1)=-\frac{\partial^2}{\partial x_1{}^2}\ln(R-x_1)=\frac{x_1}{R^3}$, so,
$\int_{S_R}(2V\frac{\partial\varphi}{\partial x_2})\frac{x_1}{R}ds=-\frac{V}{4\pi\rho U}\int_{S_R}\frac{x_1{}^2}{R^4}ds$
$=-\frac{V}{4\pi\rho U}(\frac{1}{3}\int_{S_R}\frac{x_1{}^2+x_2{}^2+x_3{}^2}{R^4}ds)=-\frac{V}{3\rho U}$. Similarly,

5. $\int_{S_R}(-2V\frac{\partial\varphi}{\partial x_1})\frac{x_2}{R}ds=-\frac{2V}{3\rho U}.$

6. $\int_{S_R}((\frac{\partial\varphi}{\partial x_2})^2)n_1ds=\frac{1}{16\epsilon^2\pi\rho^2U^2}+\frac{1}{16\epsilon^2R\pi\rho^2U^2}\sqrt{R^2-\epsilon^2}-\frac{3}{32R^2\pi\rho^2U^2}$
$-\frac{1}{16R^3\pi\rho^2U^2}\sqrt{R^2-\epsilon^2}+\frac{1}{128}\frac{\epsilon^2}{R^4\pi\rho^2U^2}+\frac{3}{256}\frac{\epsilon^4}{R^6\pi\rho^2U^2}.$

7. $\int_{S_R}((\frac{\partial\varphi}{\partial x_3})^2)\mathbf{n}_1ds=\frac{1}{16\epsilon^2\pi\rho^2U^2}+\frac{1}{16R\epsilon^2\pi\rho^2U^2}\sqrt{R^2-\epsilon^2}-\frac{3}{32R^2\pi\rho^2U^2}$
$-\frac{1}{16R^3\pi\rho^2U^2}\sqrt{R^2-\epsilon^2}+\frac{3}{128R^4}\frac{\epsilon^2}{\pi\rho^2U^2}+\frac{1}{256R^6}\frac{\epsilon^4}{\pi\rho^2U^2}.$

8. $-\mathbf{2}\int_{S_R}(\frac{\partial\varphi}{\partial x_1}\frac{\partial\varphi}{\partial x_2})\mathbf{n}_2ds=\frac{1}{128}\frac{8R^4-4R^2\epsilon^2-3\epsilon^4+8\sqrt{R^2-\epsilon^2}R^3}{R^6U^2\rho^2\pi}=$
$\frac{1}{16R^2\pi\rho^2U^2}-\frac{1}{32R^4U^2\rho^2\pi}\epsilon^2-\frac{3}{128R^6U^2\rho^2\pi}\epsilon^4+\frac{1}{16R^3U^2\rho^2\pi}\sqrt{R^2-\epsilon^2}.$

9. $-\mathbf{2}\int_{S_R}(\frac{\partial\varphi}{\partial x_1}\frac{\partial\varphi}{\partial x_3})\mathbf{n}_3ds=\frac{1}{16R^2U^2\rho^2\pi}-\frac{1}{32R^4U^2\rho^2\pi}\epsilon^2-\frac{1}{128R^6U^2\rho^2\pi}\epsilon^4$
$+\frac{1}{16R^3U^2\rho^2\pi}\sqrt{R^2-\epsilon^2}.$

Evaluation over cylinder

We now calculate the contribution to the drag from the lifting element over the cylindrical surface S_C. The integrand is given by (4.3.4).

Integrand$(\mathbf{F}_1)_{S_C}$

$$= -2(UV + U\tfrac{\partial\varphi}{\partial x_2} + V\tfrac{\partial\varphi}{\partial x_1} + \tfrac{\partial\varphi}{\partial x_1}\tfrac{\partial\varphi}{\partial x_2})(-\tfrac{x_2}{\epsilon}) - 2(U\tfrac{\partial\varphi}{\partial x_3} + \tfrac{\partial\varphi}{\partial x_1}\tfrac{\partial\varphi}{\partial x_3})(-\tfrac{x_3}{\epsilon}).$$

We calculate each term in turn. Some of these evaluations are determined using Maple software [33].

1. $\int_{S_C}\{(-2UV)(-\frac{x_2}{\epsilon}) + (-2U\frac{\partial\varphi}{\partial x_2})(-\frac{x_2}{\epsilon}) + (-2U\frac{\partial\varphi}{\partial x_3})(-\frac{x_3}{\epsilon})\}ds = 0$ because of antisymmetry of integrand in terms of x_2.

2. $\int_{S_C}(-2V\frac{\partial\varphi}{\partial x_1})(-\frac{x_2}{\epsilon})ds = \frac{1}{2}\frac{V}{\rho UR}\sqrt{R^2-\epsilon^2} - \frac{1}{2}\frac{V}{\rho U\sqrt{a^2+\epsilon^2}}a$

3. $\int_{S_C}(-2\frac{\partial\varphi}{\partial x_1}\frac{\partial\varphi}{\partial x_2})(-\frac{x_2}{\epsilon})ds =$
$$\frac{3}{128U^2\rho^2\pi}\frac{\epsilon^6}{R^4(a^2+\epsilon^2)^2} - \frac{1}{32U^2\rho^2\pi}\frac{\epsilon^4}{(a^2+\epsilon^2)^2R^3}\sqrt{R^2-\epsilon^2}$$
$$+\frac{3}{64U^2\rho^2\pi}\frac{\epsilon^4}{R^4(a^2+\epsilon^2)^2}a^2 - \frac{1}{16U^2\rho^2\pi}\frac{\epsilon^2}{(a^2+\epsilon^2)^2R^3}\sqrt{R^2-\epsilon^2}a^2$$
$$-\frac{1}{16U^2\rho^2\pi}\frac{\epsilon^2}{(a^2+\epsilon^2)^2R}\sqrt{R^2-\epsilon^2} - \frac{15}{128U^2\rho^2\pi}\frac{\epsilon^2}{(a^2+\epsilon^2)^2} + \frac{3}{128U^2\rho^2\pi}\frac{\epsilon^2}{R^4(a^2+\epsilon^2)^2}a^4$$
$$+\frac{3}{32U^2\rho^2\pi}\frac{\epsilon^2}{(a^2+\epsilon^2)^{\frac{5}{2}}}a - \frac{1}{32U^2\rho^2\pi(a^2+\epsilon^2)^2R^3}\sqrt{R^2-\epsilon^2}a^4 + \frac{5}{32U^2\rho^2\pi(a^2+\epsilon^2)^{\frac{5}{2}}}a^3$$
$$-\frac{1}{8U^2\rho^2\pi(a^2+\epsilon^2)^2R}\sqrt{R^2-\epsilon^2}a^2 - \frac{1}{16U^2\rho^2\pi\epsilon^2(a^2+\epsilon^2)^2R}\sqrt{R^2-\epsilon^2}a^4$$
$$+\frac{1}{16U^2\rho^2\pi\epsilon^2(a^2+\epsilon^2)^{\frac{5}{2}}}a^5 - \frac{1}{8U^2\rho^2\pi\epsilon^2R(a^2+\epsilon^2)}\sqrt{R^2-\epsilon^2}a^2$$
$$-\frac{1}{8U^2\rho^2\pi R(a^2+\epsilon^2)}\sqrt{R^2-\epsilon^2} + \frac{1}{32U^2\rho^2\pi R^3(a^2+\epsilon^2)}\sqrt{R^2-\epsilon^2}a^2$$
$$+\frac{1}{32U^2\rho^2\pi}\frac{\epsilon^2}{R^3(a^2+\epsilon^2)}\sqrt{R^2-\epsilon^2} + \frac{1}{8U^2\rho^2\pi\epsilon^2}\frac{a^3}{(a^2+\epsilon^2)^{\frac{3}{2}}} + \frac{3}{32U^2\rho^2\pi(a^2+\epsilon^2)^{\frac{3}{2}}}a$$
$$+\frac{3}{32U^2\rho^2\pi R^2(a^2+\epsilon^2)^5}a^4 + \frac{3}{16U^2\rho^2\pi}\frac{\epsilon^2}{R^2(a^2+\epsilon^2)^2}a^2$$
$$+\frac{3}{32U^2\rho^2\pi}\frac{\epsilon^4}{R^2(a^2+\epsilon^2)^2} - \frac{3}{32U^2\rho^2\pi(a^2+\epsilon^2)^2}a^2.$$

4. $\int_{S_C}(-2\frac{\partial\varphi}{\partial x_1}\frac{\partial\varphi}{\partial x_3})(-\frac{x_3}{\epsilon})ds =$
$$\frac{1}{128\pi\rho^2U^2}\frac{\epsilon^2}{R^4(a^2+\epsilon^2)^2}a^4 + \frac{1}{64\pi\rho^2U^2}\frac{\epsilon^4}{R^4(a^2+\epsilon^2)^2}a^2$$
$$+\frac{1}{128\pi\rho^2U^2}\frac{\epsilon^6}{R^4(a^2+\epsilon^2)^2} + \frac{1}{32\pi\rho^2U^2R^2(a^2+\epsilon^2)^2}a^4 +$$
$$\frac{1}{16\pi\rho^2U^2}\frac{\epsilon^2}{R^2(a^2+\epsilon^2)^2}a^2 + \frac{1}{32\pi\rho^2U^2}\frac{\epsilon^4}{R^2(a^2+\epsilon^2)^2} - \frac{5}{128\pi\rho^2U^2}\frac{\epsilon^2}{(a^2+\epsilon^2)^2}$$

$$-\frac{1}{32\pi\rho^2U^2(a^2+\epsilon^2)^2}a^2 - \frac{1}{16\pi\rho^2U^2\epsilon^2R(a^2+\epsilon^2)}\sqrt{R^2-\epsilon^2}a^2$$
$$-\frac{1}{16\pi\rho^2U^2R(a^2+\epsilon^2)}\sqrt{R^2-\epsilon^2} + \frac{1}{16\pi\rho^2U^2\epsilon^2}\frac{a^3}{(a^2+\epsilon^2)^{\frac{3}{2}}} + \frac{1}{16\pi\rho^2U^2}\frac{a}{(a^2+\epsilon^2)^{\frac{3}{2}}}.$$

Result

Combining all the results together, we get

$$\mathbf{F}_1 = \lim_{\epsilon\to 0}\{\tfrac{1}{2}\rho(\textstyle\int_{S_R}\mathbf{Integrand}(F_1)_{S_R} + \int_{S_C}\mathbf{Integrand}(F_1)_{S_C}ds)\}$$
$$= -\frac{1}{2}\frac{V}{U} + \frac{1}{32\rho\pi U^2R^2} - \frac{1}{16a^2\rho\pi U^2} +$$

$$\lim_{\epsilon\to 0}\{\frac{1}{32}\frac{\begin{array}{c}2\sqrt{a^2+\epsilon^2}R\epsilon^4 + 2\sqrt{R^2-\epsilon^2}\sqrt{a^2+\epsilon^2}\epsilon^4 + 3\epsilon^2a^3R \\ +\sqrt{R^2-\epsilon^2}\sqrt{a^2+\epsilon^2}a^2\epsilon^2 + 4\sqrt{a^2+\epsilon^2}Ra^2\epsilon^2 \\ +4a^5R - 2\sqrt{R^2-\epsilon^2}a^4\sqrt{a^2+\epsilon^2} + 2\sqrt{a^2+\epsilon^2}Ra^4\end{array}}{R(a^2+\epsilon^2)^{\frac{5}{2}}\rho\epsilon^2\pi U^2}\}$$

and since

$$-2\sqrt{R^2-\epsilon^2}a^4\sqrt{a^2+\epsilon^2} + 2\sqrt{a^2+\epsilon^2}Ra^4 = 2a^4\sqrt{a^2+\epsilon^2}(R-\sqrt{R^2-\epsilon^2}) > 0,$$

then $\mathbf{F}_1$ is of order $O(\frac{1}{\epsilon^2})$ and therefore tends to $+\infty$ as $\epsilon \to 0$. Hence the drag force is infinite. The implication of this is discussed later in §4.4.

4.3.4 Lift force

In a similar way as for the drag force we calculate the contribution to the lift from the lifting element. First consider the contribution over the sphere surface S_R. The integrand is given by (4.3.2).

Evaluation over sphere

Integrand$(F_2)_{S_R} =$

$-2(UV + V\frac{\partial\varphi}{\partial x_1} + U\frac{\partial\varphi}{\partial x_2} + \frac{\partial\varphi}{\partial x_1}\frac{\partial\varphi}{\partial x_2})(\frac{x_1}{R})$

$+ (U^2 - V^2 + 2U\frac{\partial\varphi}{\partial x_1} - 2V\frac{\partial\varphi}{\partial x_2} + (\frac{\partial\varphi}{\partial x_1})^2 - (\frac{\partial\varphi}{\partial x_2})^2 + (\frac{\partial\varphi}{\partial x_3})^2)(\frac{x_2}{R})$

$-2(V\frac{\partial\varphi}{\partial x_3} + \frac{\partial\varphi}{\partial x_2}\frac{\partial\varphi}{\partial x_3})(\frac{x_3}{R}),$

We calculate each term in turn. Some of these evaluations are determined using Maple software [33].

1. $\int_{S_R}\{-2(\frac{\partial\varphi}{\partial x_1}\frac{\partial\varphi}{\partial x_2})(\frac{x_1}{R})+ (U^2 - V^2 + 2U\frac{\partial\varphi}{\partial x_1} - 2V\frac{\partial\varphi}{\partial x_2} + (\frac{\partial\varphi}{\partial x_1})^2 - (\frac{\partial\varphi}{\partial x_2})^2 + (\frac{\partial\varphi}{\partial x_3})^2)(\frac{x_2}{R})$
$-2(V\frac{\partial\varphi}{\partial x_3} + \frac{\partial\varphi}{\partial x_2}\frac{\partial\varphi}{\partial x_3})(\frac{x_3}{R})\}ds = 0$ because of antisymmetry of integrand in terms of x_2.
2. $\int_{S_R}(-2UV)\frac{x_1}{R}ds = \int_{S_R}(-2UV)(\cos\theta)(R^2\sin\theta)d\phi d\theta =$
$\int_{\arccos(\frac{\sqrt{R^2-\epsilon^2}}{R})}^{\pi}(\int_0^{2\pi}(-2UV)(\cos\theta)(R^2\sin\theta)d\phi)d\theta = 2\epsilon^2UV\pi.$
3. $\int_{S_R}(-2V\frac{\partial\varphi}{\partial x_1})\frac{x_1}{R}ds =$
$\int_{\arccos(\frac{\sqrt{R^2-\epsilon^2}}{R})}^{\pi}(\int_0^{2\pi}(-2V(\frac{1}{4\pi\rho UR^2}\sin\theta\cos\phi))(\cos\theta)(R^2\sin\theta)d\phi)d\theta = 0.$

   Similar to item 4 in §4.3.3 we have:

4. $\int_{S_R}(-2U\frac{\partial\varphi}{\partial x_2})\frac{x_1}{R}ds = \frac{1}{3\rho}.$
5. $\int_{S_R}(2U\frac{\partial\varphi}{\partial x_1})\frac{x_2}{R}ds = \frac{2}{3\rho}.$

Evaluation over cylinder

We now calculate the contribution to the lift from the lifting element over the cylindrical surface S_C. The integrand is given by (4.3.5).

Integrand$(\mathbf{F}_2)_{S_C}$

$= (U^2 - V^2 + 2U\frac{\partial\varphi}{\partial x_1} - 2V\frac{\partial\varphi}{\partial x_2} + (\frac{\partial\varphi}{\partial x_1})^2 - (\frac{\partial\varphi}{\partial x_2})^2 + (\frac{\partial\varphi}{\partial x_3})^2)(-\frac{x_2}{\epsilon})$

$-2(V\frac{\partial\varphi}{\partial x_3} + \frac{\partial\varphi}{\partial x_2}\frac{\partial\varphi}{\partial x_3})(-\frac{x_3}{\epsilon})$.

Calculating each term in turn,

$\int_{S_C}\{(U^2 - V^2 - 2V\frac{\partial\varphi}{\partial x_2} + (\frac{\partial\varphi}{\partial x_1})^2 - (\frac{\partial\varphi}{\partial x_2})^2 + (\frac{\partial\varphi}{\partial x_3})^2)(-\frac{x_2}{\epsilon})$

$-2(V\frac{\partial\varphi}{\partial x_3} + \frac{\partial\varphi}{\partial x_2}\frac{\partial\varphi}{\partial x_3})(-\frac{x_3}{\epsilon})\}ds = 0$ because of antisymmetry of integrand in terms of y.

$\int_{S_C}(2U\frac{\partial\varphi}{\partial x_1})(-\frac{x_2}{\epsilon})ds = -\frac{1}{2\rho}\frac{\left(\sqrt{R^2-\epsilon^2}\sqrt{a^2+\epsilon^2}-aR\right)}{R\sqrt{a^2+\epsilon^2}}$, using Maple [33]

Result

Combining all the results together, we get

$\mathbf{F}_2 = \lim_{\epsilon\to 0}\{\frac{1}{2}\rho(\int_{S_R}\textbf{Integrand}(F_2)_{S_R} + \int_{S_C}\textbf{Integrand}(F_2)_{S_C}ds)\}$

$= \lim_{\epsilon\to 0}\{\frac{1}{2}\rho(2\epsilon^2 UV\pi + \frac{2}{3\rho} + \frac{1}{3\rho} - \frac{1}{2\rho}\frac{\left(\sqrt{R^2-\epsilon^2}\sqrt{a^2+\epsilon^2}-aR\right)}{R\sqrt{a^2+\epsilon^2}})\} = \frac{1}{2}$.

From the standard potential model we would expect the lift force for this particular potential velocity to be equal to 1. The implication of this disparity is discussed later in §4.4.

4.3.5 Side force

In this case since the whole integrand given in (4.3.3) over S_R and the integrand given in (4.3.6) over S_C are antisymmetric in terms of z. (Of course, if the cylinder intersects the body at an angle, then there will be an additional contribution for which we cannot use the symmetry properties. However, it can be shown this contribution is negligible (see Appendix 4.6). The remaining contribution is then,

$\mathbf{F}_3 = \{\frac{1}{2}\rho(\int_{S_R}\textbf{Integrand}(F_2)_{S_R} + \int_{S_C}\textbf{Integrand}(F_2)_{S_C}ds)\} = 0$.

4.4 Chapter 4 Discussion

We have considered the force contributions on a body due to the lifting element potential $\varphi = \frac{1}{4\pi\rho U}\frac{\partial}{\partial x_2}\ln(R - x_1)$ and have found that the side force is zero, lift force is a half and drag force is infinite.

This has implications for aerodynamic potential wing theory, as the classical approach [2] models this by a vortex sheet and which we represent by a distribution of lifting element potentials. (This is because the limiting value of the horseshoe vortex potential as its span tends to zero is the lifting element potential.)

These results mean that the lift force on the wing would be half that expected from the classical approach. In [1], Chadwick argues that this is because the wrong limiting value for the lift of a horseshoe vortex has been used in the standard approach. (Essentially, the 2-D result $L = \rho U\gamma s$ has been wrongly assumed.)

Furthermore, in this chapter we have also found that the drag force on the wing is infinite.

This result may not be surprising to us as the kinetic energy associated with the flow is also infinite (see Appendix 4.7). This further means that we cannot use Lamb's equations of motion for potential flow as he represents them in terms of the kinetic energy. (However, Lamb assumes that the potential is regular and not singular everywhere in the fluid.)

Therefore we cast doubt on the validity of the aerodynamic potential flow model.

To model this problem appropriately, we must also include the viscous wake velocity even though the Reynolds number is large [1]. We suggest that one way of doing this is by using the Oseen equations [34, 15].

4.5 Chapter 4 Appendix: Relation between 2-D potential and 3-D

We show that

$$\frac{\partial}{\partial x_j}\ln(R-x_1) = -\int_0^\infty \frac{\partial}{\partial x_j}\frac{d\xi}{\{(x_1-\xi)^2+x_2^2+x_3^2\}^{\frac{1}{2}}}. \tag{4.5.1}$$

In practice we have:

For $j=1$:

$$LHS(4.5.1) = -\frac{1}{R}, \tag{4.5.2}$$

and

$$RHS(4.5.1) = \int_0^\infty \frac{x_1-\xi}{\{(x_1-\xi)^2+x_2^2+x_3^2\}}d\xi = [\frac{1}{\{(x_1-\xi)^2+x_2^2+x_3^2\}^{\frac{1}{2}}}]_0^\infty = -\frac{1}{R}. \tag{4.5.3}$$

For $j \neq 1$:

$$LHS(4.5.1) = \frac{x_j}{R(R-x_1)} = \frac{x_j(R+x_1)}{R(x_2^2+x_3^2)}, \tag{4.5.4}$$

and

$$\begin{aligned} RHS(4.5.1) =& \int_0^\infty \frac{x_j}{\{(x_1-\xi)^2+x_2^2+x_3^2\}^{\frac{3}{2}}}d\xi \\ =& \frac{x_j}{x_2^2+x_3^2}[\frac{\xi-x_1}{\{(x_1-\xi)^2+x_2^2+x_3^2\}^{\frac{1}{2}}}]_0^\infty = \frac{x_j(R+x_1)}{R(x_2^2+x_3^2)}. \end{aligned} \tag{4.5.5}$$

But alternatively by denoting $x_2^2+x_3^2=r^2$, we have

$$\begin{aligned} \ln(R-x_1) =& \ln(-x_1+\sqrt{x_1^2+r^2}) \\ =& \ln r + \ln(-\frac{x_1}{r}+\sqrt{(\frac{x_1}{r})^2+1}) = \ln r - \sinh^{-1}(\frac{x_1}{r}). \end{aligned} \tag{4.5.6}$$

Also

$$\int_0^X \frac{d\xi}{\{(x_1-\xi)^2+x_2^2+x_3^2\}^{\frac{1}{2}}} = \int_0^X \frac{d\xi}{\{(x_1-\xi)^2+r^2\}^{\frac{1}{2}}}$$
$$= \int_{-\frac{x_1}{r}}^{\frac{X-x_1}{r}} \frac{d\zeta}{\sqrt{\zeta^2+1}} = \sinh^{-1}(\frac{X-x_1}{r}) + \sinh^{-1}(\frac{x_1}{r}) \tag{4.5.7}$$
$$= \ln(\frac{X-x_1}{r} + \sqrt{(\frac{X-x_1}{r})^2+1}) + \sinh^{-1}(\frac{x_1}{r}),$$

and therefore for large X,

$$\int_0^X \frac{d\xi}{\{(x_1-\xi)^2+x_2^2+x_3^2\}^{\frac{1}{2}}} \approx \ln\frac{2X}{r} + \sinh^{-1}(\frac{x_1}{r}),$$

so

$$-\int_0^X \frac{d\xi}{\{(x_1-\xi)^2+x_2^2+x_3^2\}^{\frac{1}{2}}} + \ln 2X \approx \ln r - \sinh^{-1}(\frac{x_1}{r}). \tag{4.5.8}$$

Combining (4.5.6) and (4.5.8) gives

$$\ln(R-x_1) = \lim_{X\to\infty}(-\int_0^X \frac{d\xi}{\{(x_1-\xi)^2+x_2^2+x_3^2\}^{\frac{1}{2}}} + \ln 2X). \tag{4.5.9}$$

Now differentiating both sides of (4.5.9) with respect to x_j yields (4.5.1).

4.6 Chapter 4 Appendix: F_3 computation

When computing the force F_3, we considered an intersection of the cylinder and the body which was symmetric about the x-axis (see §4.3.5). If the intersection of the cylinder and the body is not symmetric, we show below that we get the same result as for the symmetric intersection. We define the additional surface to be included because the intersection is not symmetric as the surface $(S_C)^\circ$ and show the contribution to the force F_3 over the surface is negligible. We suppose the surface $(S_C)^\circ$ follows the parametric representations in §4.3.1 for $0 \leq \phi \leq 2\pi$, $\alpha \leq x \leq \beta$. The integral is broken up into the following two parts

1. $\int_{(S_C)^\circ}(U^2+V^2)\frac{x_3}{R}ds = (U^2+V^2)\int_{(S_C)^\circ}(\sin\phi)ds = \int_0^{2\pi}(\int_\alpha^\beta \epsilon\sin\phi dx)d\phi = 0,$

2. The integrand of

   $\int_{(S_C)^\circ}(-2V\frac{\partial\varphi}{\partial x_3})(-\frac{x_2}{\epsilon})ds = \int_0^{2\pi}(\int_\alpha^\beta(-2V\frac{\partial\varphi}{\partial x_3})(-\frac{x_2}{\epsilon})ds$ is

$$-\frac{1}{2}V(\frac{x_1\epsilon^3(\cos^2\phi\sin\phi)-2\sqrt{\epsilon^2+x_1{}^2}\epsilon^3(\cos^2\phi\sin\phi)}{\pi\rho U\left(\sqrt{\epsilon^2+x_1{}^2}-x_1\right)^2(\epsilon^2+x_1{}^2)^{\frac{3}{2}}}) =$$

$$\frac{1}{2}V\epsilon^3(\cos^2\phi\sin\phi)\frac{x_1-2\sqrt{\epsilon^2+x^2}}{\pi\rho U\left(\sqrt{\epsilon^2+x_1{}^2}-x_1\right)^2(\epsilon^2+x_1{}^2)^{\frac{3}{2}}} =$$

$$\frac{(x_1-2\sqrt{\epsilon^2+x_1{}^2})(V\left(\cos^2\phi\sin\phi\right))}{2\pi\rho Ux_1{}^2(\epsilon^2+x_1{}^2)^{\frac{3}{2}}}\frac{\epsilon^3}{(\sqrt{1+\frac{\epsilon^2}{x_1{}^2}}-1)^2},$$

and since

$$\sqrt{1+\frac{\epsilon^2}{x_1{}^2}}-1 = \frac{1}{2}\frac{\epsilon^2}{x_1{}^2}-\frac{1}{2!2^2}(\frac{\epsilon^2}{x_1{}^2})^2+\frac{1\times 3}{3!2^3}(\frac{\epsilon^2}{x_1{}^2})^3-\ldots = O(\epsilon^2),$$

then

$$\frac{(x_1-2\sqrt{\epsilon^2+x_1{}^2})(V\left(\cos^2\phi\sin\phi\right))}{2\pi\rho Ux_1{}^2(\epsilon^2+x_1{}^2)^{\frac{3}{2}}}\frac{\epsilon^3}{(\sqrt{1+\frac{\epsilon^2}{x_1{}^2}}-1)^2}.$$

The integrand is then

$$\int_\alpha^\beta(-\frac{1}{2}V\frac{x_1\epsilon^3(\cos^2\phi\sin\phi)-2\sqrt{\epsilon^2+x_1{}^2}\epsilon^3(\cos^2\phi\sin\phi)}{\pi\rho U\left(\sqrt{\epsilon^2+x_1{}^2}-x_1\right)^2(\epsilon^2+x_1{}^2)^{\frac{3}{2}}})dx_1 = (-\frac{1}{2}V\cos^2\phi\sin\phi)$$

$$\frac{-2\sqrt{\epsilon^2+\beta^2}\sqrt{\epsilon^2+\alpha^2}\beta+2\sqrt{\epsilon^2+\beta^2}\sqrt{\epsilon^2+\alpha^2}\alpha-2\sqrt{\epsilon^2+\alpha^2}\beta^2-\sqrt{\epsilon^2+\alpha^2}\epsilon^2+2\sqrt{\epsilon^2+\beta^2}\alpha^2+\sqrt{\epsilon^2+\beta^2}\epsilon^2}{\sqrt{\epsilon^2+\beta^2}\pi\rho U\epsilon\sqrt{\epsilon^2+\alpha^2}}.$$

So

$$\int_{(S_C)^\circ}(-2V\frac{\partial\varphi}{\partial x_3})(-\frac{x_2}{\epsilon})ds =$$

$$\int_0^{2\pi}(\int_\alpha^\beta(-\frac{1}{2}V\frac{x\epsilon^3(\cos^2\phi\sin\phi)-2\sqrt{\epsilon^2+x_1{}^2}\epsilon^3(\cos^2\phi\sin\phi)}{\pi\rho U\left(\sqrt{\epsilon^2+x_1{}^2}-x\right)^2(\epsilon^2+x_1{}^2)^{\frac{3}{2}}})dx_1)d\phi = 0.$$

4.7 Chapter 4 Appendix: Kinetic energy computation

Theorem 4.7.1. *Green's Theorem*

Let $\mathbf{u} = (u_1, u_2, u_3)$ *and hence* $div\mathbf{u} = \frac{\partial u_1}{\partial x_1} + \frac{\partial u_2}{\partial x_2} + \frac{\partial u_3}{\partial x_3}$,

$$\int_S \mathbf{u}.\hat{\mathbf{n}} ds = -\int_V div\mathbf{u} dv, \tag{4.7.1}$$

u_1, u_2, u_3 *any three functions which are finite and differentiable at all points of a connected region completely bounded by one or more closed surface* S, *[27].*

Kinetic energy

If φ is the velocity-potential of an irrotational motion of a fluid then $\nabla^2\varphi = 0$, so substituting $\mathbf{u} = \varphi\nabla\varphi$ into (4.7.1) implies

$$\int_{\mathbf{S}} \varphi\frac{\partial\varphi}{\partial\hat{\mathbf{n}}} ds = -\int_V (\nabla\varphi \cdot \nabla\varphi + \varphi\nabla^2\varphi) dx_1 dx_2 dx_3 = -\int_V (\nabla\varphi \cdot \nabla\varphi) dx_1 dx_2 dx_3. \tag{4.7.2}$$

If $K.E$ denotes the total kinetic energy of the incompressible fluid and ρ shows the density of it, then [27]

$$K.E = \frac{1}{2}\rho\int_V (\nabla\varphi \cdot \nabla\varphi) dx_1 dx_2 dx_3 = -\frac{1}{2}\rho\int_{\mathbf{S}} \varphi\frac{\partial\varphi}{\partial\hat{\mathbf{n}}} ds.$$

We now present the computation of the kinetic energy

$$K.E = \frac{1}{2}\rho\int_V \boldsymbol{\nabla}\varphi.\boldsymbol{\nabla}\varphi dv, \tag{4.7.3}$$

for the potential flow $\varphi(x_1, x_2, x_3) = \frac{1}{4\pi\rho U}\frac{\partial}{\partial x_2}\ln(\sqrt{x_1{}^2 + x_2{}^2 + x_3{}^2} - x_1)$ where V is:

1. a cylinder of volume V_C with radius ϵ along the x_1-axis where, $0 < a \leq x_1 \leq b$,

2. a sphere of volume V_S of radius R, with center lying on the x_1-axis at point $(c, 0, 0)$ where, $c > 2R$, (figure 4.5).

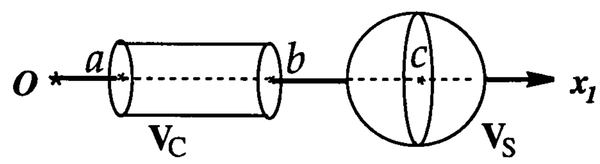

Figure 4.5: Cylinder V_C and Sphere V_S

Let $M > 1$ be any real number, we show that $K.E > M$ and since M is arbitrary so $K.E \to +\infty$. We follow with the fact $\nabla\varphi.\nabla\varphi \geq (\frac{\partial\varphi}{\partial x_1})^2 = (\frac{1}{4\pi\rho U}\frac{x_2}{R^3})^2$.

i. Computing $K.E$ on V_C

$$\text{Volume } V_C : \begin{cases} {x_2}^2 + {x_3}^2 \leq \epsilon^2, \ 0 \prec a \leq x_1 \leq b, \\ x_2 = r\cos\phi, \ x_3 = r\sin\phi, \ 0 \leq \phi \leq 2\pi, \ 0 \leq r \leq \epsilon. \end{cases}$$

We take $0 < \delta < \sqrt{\frac{A\epsilon^2}{A+M\epsilon^2}}$ where $A = \frac{(b-a)}{64\pi\rho U^2}$, then $\frac{(b-a)}{32\pi\rho^2U^2}\frac{-\delta^2+\epsilon^2}{\epsilon^2\delta^2} > \frac{2M}{\rho}$. Then

$$K.E|_{V_C} = \frac{\rho}{2}\int_{V_C}\nabla\varphi.\nabla\varphi dv \geq \frac{\rho}{2}\int_{V_C}(\frac{\partial\varphi}{\partial x_1})^2 dv = \frac{\rho}{2}\int_0^\epsilon\int_a^b\int_0^{2\pi}(\frac{\partial\varphi}{\partial x_1})^2 r d\phi dx dr \geq$$
$$\frac{\rho}{2}\int_\delta^\epsilon\int_a^b\int_0^{2\pi}(\frac{\partial\varphi}{\partial x_1})^2 r d\phi dx dr =$$
$$\frac{\rho}{2}\int_\delta^\epsilon(\int_a^b(\int_0^{2\pi}(\frac{\cos^2\phi}{16\pi^2\rho^2U^2r^4})d\phi)dx)rdr = \frac{\rho}{2}(\frac{(b-a)}{32\pi\rho^2U^2}\frac{-\delta^2+\epsilon^2}{\epsilon^2\delta^2}) > M,$$

therefore $K.E|_{V_C} \to +\infty$.

ii. Computing $K.E$ on V_S

$$\text{Volume } V_S : \begin{cases} (x_1 - c)^2 + {x_2}^2 + {x_3}^2 \leq R^2, \\ x_1 = c + h\cos\theta, \quad x_2 = h\sin\theta\cos\phi, \quad x_3 = h\sin\theta\sin\phi, \\ 0 \leq \theta \leq \pi, \ 0 \leq \phi \leq 2\pi, \ 0 \leq h \leq R. \end{cases}$$

We take $0 < \delta < \frac{AR}{A+RM}$ where $A = \frac{1}{24\pi\rho U^2}$, then $\frac{1}{12\pi\rho^2U^2}\frac{R-\delta}{R\delta} > \frac{2M}{\rho}$. This implies

$$
\begin{aligned}
K.E|_{V_S} =& \frac{\rho}{2}\int_{V_S} \nabla\varphi.\nabla\varphi dv \geq \frac{\rho}{2}\int_{V_S} (\frac{\partial\varphi}{\partial x_1})^2 dv = \\
& \frac{\rho}{2}\int_0^R \int_0^\pi \int_0^{2\pi} (\frac{\partial\varphi}{\partial x_1})^2 h^2 \sin\theta d\phi d\theta dh \geq \\
& \frac{\rho}{2}\int_\delta^R \int_0^\pi \int_0^{2\pi} (\frac{\partial\varphi}{\partial x_1})^2 h^2 \sin\theta d\phi d\theta dh = \\
& \frac{\rho}{2}\int_\delta^R (\int_0^\pi (\int_0^{2\pi} (\frac{\sin^2\theta\cos^2\phi}{16\pi^2\rho^2U^2h^4}) d\phi) \sin\theta d\theta) h^2 dh = \\
& \frac{\rho}{2}(\frac{1}{12\pi\rho^2U^2}\frac{R-\delta}{R\delta}) > M,
\end{aligned}
$$

therefore $K.E|_{V_S} \longrightarrow +\infty$.

We now compute the kinetic energy due to φ on the volume V in figure 4.4. The kinetic energy for this volume is much bigger than kinetic energy exerted on volume V_{R-r} shown in figure 4.6, because of the positive integrand in (4.7.3). In figure 4.6, V_{R-r} is the volume inside the sphere S_R and outside the sphere S_r which completely surrounds the body and this volume excludes the cylinder S_C, in other words $S_B \subset V_{R-r} \subset V$. We suppose the sphere S_r has radius r and the volume V_{R-r} is included in the domain $\alpha \leq \theta \leq 2\pi$ in spherical coordinates according to parameterization in (§4.3.1) for S_R, where $\alpha \geq \arccos(\frac{\sqrt{R^2-\epsilon^2}}{R})$.

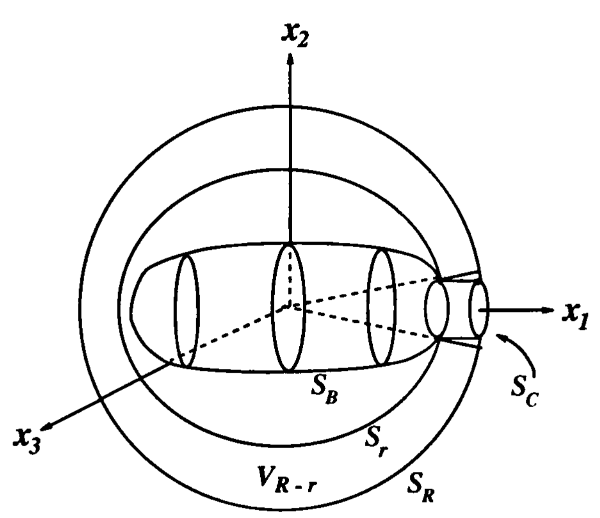

Figure 4.6: Volume V_{R-r}

So,

$$
\begin{aligned}
&K.E|_V \geq K.E|_{V_{R-r}} = \frac{\rho}{2}\int_{V_{R-r}} \nabla\varphi.\nabla\varphi dv \\
&\geq \frac{\rho}{2}\int_{V_{R-r}} (\frac{\partial\varphi}{\partial x_2})^2 dv = \frac{\rho}{2}\int_r^R \int_\alpha^\pi \int_0^{2\pi} (\frac{\partial\varphi}{\partial x_2})^2 h^2 \sin\theta d\phi d\theta dh = \\
&\frac{\rho}{2}\int_r^R (\int_\alpha^\pi (\int_0^{2\pi} (-\frac{1}{4}\frac{\cos^2\phi\cos^2\theta - \cos^2\phi\cos\theta + 1 - 2\cos^2\phi}{(-1+\cos\theta)\,\pi\rho U h^2})^2 d\phi) \sin^3\theta d\theta) h^2 dh \\
&= \frac{1}{240}\frac{R-r}{\pi\rho^2 U^2 Rr}\cos^{10}\frac{1}{2}\alpha\{30\ln(1+\tan^2\frac{1}{2}\alpha) - 60\ln(\tan\frac{1}{2}\alpha) \\
&- 115\tan^2\frac{1}{2}\alpha - 17 - 245\tan^4\frac{1}{2}\alpha \\
&- 105\tan^6\frac{1}{2}\alpha - 30\tan^8\frac{1}{2}\alpha - 300\ln(\tan\frac{1}{2}\alpha)\tan^2\frac{1}{2}\alpha - 600\ln(\tan\frac{1}{2}\alpha)\tan^4\frac{1}{2}\alpha \\
&- 600\ln(\tan\frac{1}{2}\alpha)\tan^6\frac{1}{2}\alpha - 300\ln(\tan\frac{1}{2}\alpha)\tan^8\frac{1}{2}\alpha - 60\ln(\tan\frac{1}{2}\alpha)\tan^{10}\frac{1}{2}\alpha \\
&+ 150\ln(1+\tan^2\frac{1}{2}\alpha)\tan^2\frac{1}{2}\alpha + 300\ln(1+\tan^2\frac{1}{2}\alpha)\tan^4\frac{1}{2}\alpha \\
&+ 300\ln(1+\tan^2\frac{1}{2}\alpha)\tan^6\frac{1}{2}\alpha + 150\ln(1+\tan^2\frac{1}{2}\alpha)\tan^8\frac{1}{2}\alpha \\
&+ 30\ln(1+\tan^2\frac{1}{2}\alpha)\tan^{10}\frac{1}{2}\alpha\} = I(\alpha),
\end{aligned}
$$

since $\ln\left(\tan\frac{1}{2}\alpha\right)\tan^m\frac{1}{2}\alpha \approx (\frac{\alpha}{2})^m \ln\left(\frac{1}{2}\alpha\right)$ as $\alpha \to 0^+$, and $\lim_{\alpha\to 0}(\frac{\alpha}{2})^m \ln\left(\frac{1}{2}\alpha\right) = \lim_{\alpha\to 0}(-\frac{\alpha^m}{m2^m}) = 0$ for all positive values m. The dominant term in the solution of this integral (which we denoted it by $I(\alpha)$) for small positive value of α is $-60\ln\left(\tan\frac{1}{2}\alpha\right)$, so

$$\lim_{\alpha\to 0} I(\alpha) = \lim_{\alpha\to 0}\frac{1}{240}\frac{R-r}{\pi\rho^2U^2Rr}\cos^{10}(\tfrac{1}{2}\alpha)(-60\ln\left(\tan\tfrac{1}{2}\alpha\right)) = +\infty.$$

Hence

$$K.E|_V \geq \lim_{\alpha\to 0} K.E|_{V_{R-r}} = +\infty.$$

Chapter 5

The jump in lift at the trailing edge of a thin wing in potential flow

5.1 Introduction

In many computational potential flow aerodynamic models, the lift is calculated from the pressure distribution over the top and bottom surfaces of the wing (rather than by calculating the lift from horseshoe vortex distribution representing the trailing wake sheet) and these results agree with experiment. This is the starting point of the research arising from this chapter. In this chapter we shall consider exclusively the standard aerodynamic potential flow model (and not quasi-potential or Oseen flow), in order to investigate how the lift is calculated from the pressure distribution over the wing in the standard approach. In particular we shall show that standard text book approach overcalculates the lift by a factor of two as there is an omitted calculation, a discontinuous jump in the lift integral at the trailing edge.

5.2 Statement of problem

For the structure of the lift force we here also follow all conditions and assumptions that has been considered in (§4.2.1). Then we develop a wing representation in potential flow and give an expression for the lift force on the wing . The lift force is then evaluated from the pressure distribution over the top and bottom surfaces of the wing, and also across the trailing edge of the wing.

5.2.1 Wing representation

The classical approach is developed by thinking of a discretisation of the vortex sheet by a number of horseshoe vortices: Lighthill [35] figure 86 p. 216, Batchelor [21] figure 7.8.4 p. 585, and Katz and Plotkin [36] figure 8.2 p. 169 distribute a spanwise number of horseshoe vortices of varying strength and in the limit let the span of each tend to zero; Newman [37] figure 5.18 p.195, and Katz and Polkin [36] figure 8.17 p.186 distribute a spanwise and chordwise distribution of horseshoe vortices of varying and in the limit again let the span of each tend to zero. We therefore represent the flow around a slender wing by a distribution of bound and free vortices over an area A within the slender wing. For simplicity, let us restrict our attention to an area A that lies on the rectangular area $0 \leq x_1 \leq X_1,\ x_2 = 0$ and $0 \leq x_3 \leq X_3$, and let the uniform stream U flow past the body predominantly in the x_1 direction. This distribution is approximated by a finite number of horseshoe vortices distributed over the area A, and such that the horseshoe vortices are regularly spaced with span Δx_3 in the x_3 direction and separated by distance Δx_1 in the x_1 direction as shown in figure 5.1.

The circulation vortex strength on the vortex sheet $\Gamma(x_1, x_3)$ is approximated at a finite number of points with coordinates $(i\Delta x_1, 0, (j + 1/2)\Delta x_3)$ for some integer value of i and j, and related to the strength of the horseshoe vortex at that point. In the limit as both Δx_1 and $\Delta x_3 \to 0$, then the circulation function Γ is determined. Hence, in this limit the span of each horseshoe vortex tends to zero. This means we take $\frac{\Gamma}{U\Delta x_3} \to \infty$.

Expressing in terms of the perturbation velocity $u_i = \frac{\partial \phi}{\partial x_i}$ to the uniform stream $U\delta_{i1} + V\delta_{i2}$ where $U \gg V$ such that

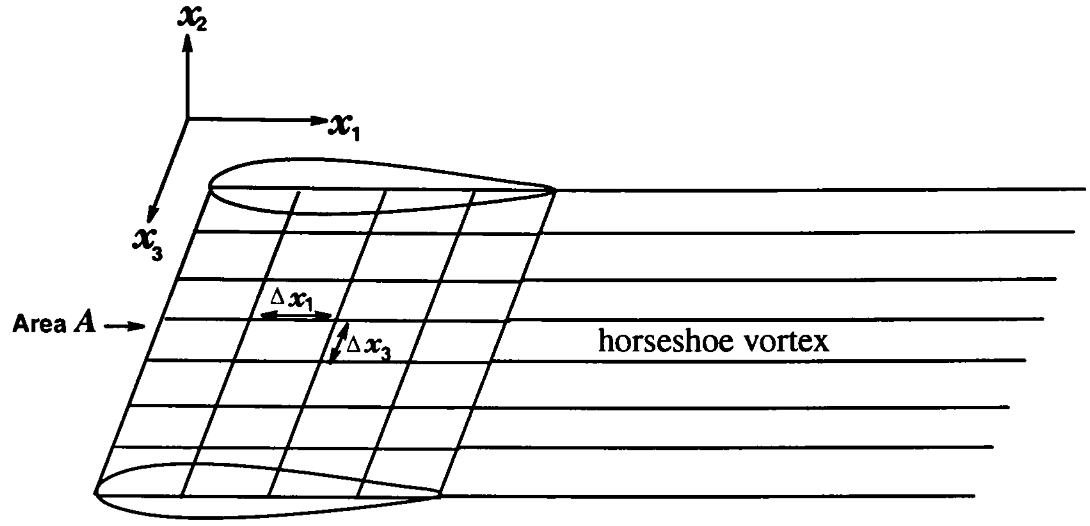

Figure 5.1: Distribution of horseshoe vortices which make up the vortex sheet.

$$u_i = u_i^\dagger - U\delta_{i1} - V\delta_{i2}, \tag{5.2.1}$$

then in [1], this is shown to give

$$\phi(x_1, x_2, x_3) = \iint\limits_A \frac{\ell_{13}(y_1, y_3)}{4\pi\rho U} \frac{\partial}{\partial x_2} \ln(R_{13} - x_{11}) dy_1 dy_3, \tag{5.2.2}$$

where $R_{13} = \{(x_1 - y_1)^2 + x_2^2 + (x_3 - y_3)^2\}^{\frac{1}{2}}$, $x_{11} = x_1 - y_1$.

Thwaites and Prandtl [8] p. 301 eqns. (21) and (22) give similar expressions to (5.2.2), but for $\frac{\partial\phi}{\partial x_2}$ and restricted to when $x_2 = 0$. Thwaites' result is obtained by replacing the integrand expression with

$$\frac{\partial^2}{\partial x_2^2} \ln(R_{13} - x_{11})|_{x_2=0} = \frac{1}{x_{33}^2} \left(1 + \frac{x_{11}}{r_{13}}\right), \tag{5.2.3}$$

where $x_{33} = x_3 - y_3$ and $r_{13} = \sqrt{x_{11}^2 + x_{33}^2}$. Similarly Prandtl's result [4] is obtained by replacing the integrand expression with

$$\frac{\partial^2}{\partial x_2^2} \ln(R_{13} - x_{11})|_{x_2=0} = -\frac{\partial}{\partial x_3} \left\{ \frac{1}{x_{33}} \left(1 + \frac{r_{13}}{x_{11}}\right) \right\}. \tag{5.2.4}$$

Thwaites describes the function ℓ_{13} as the load function, and it is related to the circulation strength of the vortex Γ such that $\ell_{13}(y_1, y_3) = \partial\ell_3(y_1, y_3)/\partial y_1$ and $\ell_3(y_1, y_3) = \rho U \Gamma(y_1, y_3)$

[1]. Hence, ℓ_{13} is a singularity strength distribution over the area A. The vortex strength in the x_1 direction is given by $\gamma_1 = -\ell_{33}/(\rho U)$ and in the x_3 direction is given by $\gamma_3 = \ell_{13}/(\rho U)$ where $\ell_{33}(y_1, y_3) = \partial\ell_3(y_1, y_3)/\partial y_3$. Hence, (5.2.2) represents an integral distribution of infinitesimal horseshoe vortices. This also agrees with the infinitesimal horseshoe vortex potential given by Thwaites [8] p. 391 eqn 76. Similarly, the shed vortex wake is also a singular sheet which we present by an equivalent singularity distribution $\ell_{13}(y_1, y_3)$, see figure 5.2.

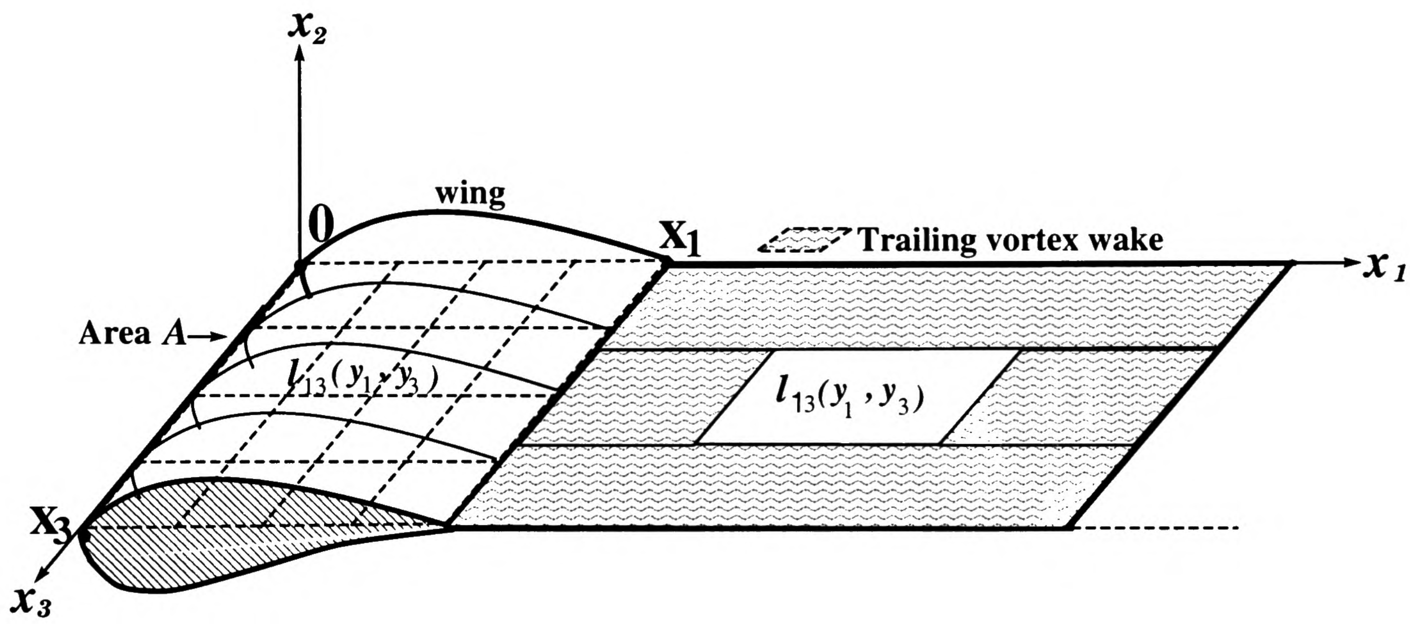

Figure 5.2: Strength of vortex sheet inside and outside the body.

Let us also define the quantity L by

$$L = \iint_A \ell_{13}(y_1, y_3) dy_1 dy_3. \tag{5.2.5}$$

(Hence, for a single horseshoe vortex of strength Γ, $L = \rho U \Gamma s$ where s is the span of the horseshoe vortex.)

5.2.2 Force integral representation

The force is represented by an integral distribution of the surface pressure. however, since the pressure is undefined on the vortex sheet, and this sheet intersects the wing surface at the trailing edge, then the integral cannot be determined at the trailing edge. Therefore, a contour C_δ is considered (which is defined later) and which lies on the wing near to and enclosing the trailing edge a distance δ away from the vortex sheet. The force is then given as an integral over all the body surface S_B except for the surface on the body S_δ (which is the surface enclosed by the contour C_δ), in the limit as $\delta \rightarrow 0$. Finally the force integral is evaluated over a symmetric surface S_{symm} in order to simplify the representation. So before proceeding with the force representation, the surface S_{symm} is defined and from this the contour C_δ is defined.

Consider the surface S_{symm} defined as the surface a distance ε away from the rectangular area A. (A is defined as lying in the region $0 \leq x_1 \leq X_1 - \varepsilon,\ x_2 = 0,\ 0 \leq x_3 \leq X_3 - \varepsilon$.) Then S_{symm} consists of: the top and bottom surface S_{tb}; the side surface S_{side}; the trailing edge surface S_{te} and the front edge surface S_{fe}.

The top and bottom surfaces S_{tb} consist of: the top surface S_t parameterised by (p, ε, q) where $0 \leq p \leq X_1 - \varepsilon,\ 0 \leq q \leq X_3 - \varepsilon$; and the bottom surface S_b parametrised by $(p, -\varepsilon, q)$ where $0 \leq p \leq X_1 - \varepsilon,\ 0 \leq q \leq X_3 - \varepsilon$.

The side surfaces S_{side} consist of: the left side surface parameterised by $(p, \varepsilon\cos\beta, \varepsilon\sin\beta)$ where $0 \leq p \leq X_1 - \varepsilon,\ -\pi \leq \beta \leq 0$; and the right side surface parameterised by $(p, \varepsilon\cos\beta, X_3 - \varepsilon + \varepsilon\sin\beta)$ where $0 \leq p \leq X_1 - \varepsilon,\ 0 \leq \beta \leq \pi$.

The trailing edge surface S_{te} consists of: the cylindrical surface parameterised by $(X_1 - \varepsilon + \varepsilon\cos\alpha, \varepsilon\sin\alpha, q)$ where $-\frac{\pi}{2} \leq \alpha \leq \frac{\pi}{2},\ 0 \leq q \leq X_3 - \varepsilon$; the quarter sphere parameterised by $(X_1 - \varepsilon + \varepsilon\sin\alpha\sin\beta, \varepsilon\cos\alpha, \varepsilon\sin\alpha\cos\beta)$ where $0 \leq \alpha \leq \pi,\ \frac{\pi}{2} \leq \beta \leq \pi$; and the quarter sphere parameterised by $(X_1 - \varepsilon + \varepsilon\sin\alpha\sin\beta, \varepsilon\cos\alpha, X_3 - \varepsilon + \varepsilon\sin\alpha\cos\beta)$ where $0 \leq \alpha \leq \pi,\ 0 \leq \beta \leq \frac{\pi}{2}$.

The front edge surface S_{fe} consists of: the half cylinderical surface parameterised by $(\varepsilon\cos\alpha, \varepsilon\sin\alpha, q)$ where $\frac{\pi}{2} \leq \alpha \leq \frac{3\pi}{2},\ 0 \leq q \leq X_3 - \varepsilon$; the quarter sphere parameterised by $(\varepsilon\sin\alpha\sin\beta, \varepsilon\cos\alpha, \varepsilon\sin\alpha\cos\beta)$ where $0 \leq \alpha \leq \pi,\ \pi \leq \beta \leq \frac{3\pi}{2}$; and the quarter sphere parameterised by $(\varepsilon\sin\alpha\sin\beta, \varepsilon\cos\alpha, X_3 - \varepsilon + \varepsilon\sin\alpha\cos\beta)$ where $0 \leq \alpha \leq \pi,\ \frac{3\pi}{2} \leq \beta \leq 2\pi$. See figure 5.3.

Then let the contour C_ε be where the plane $x_1 = X_1 - \varepsilon$ intersects the surface S_{symm} (see figures 5.4, and 5.5). Similarly the contour C_δ be where the plane $x_1 = X_1 - \varepsilon + \sqrt{\varepsilon^2 - \delta^2}$ intersects the surface S_{symm}, where $\delta \ll \varepsilon$ (see figures 5.4, and 5.5). Hence, to first order the contour C_δ is a distance δ away from the vortex sheet.

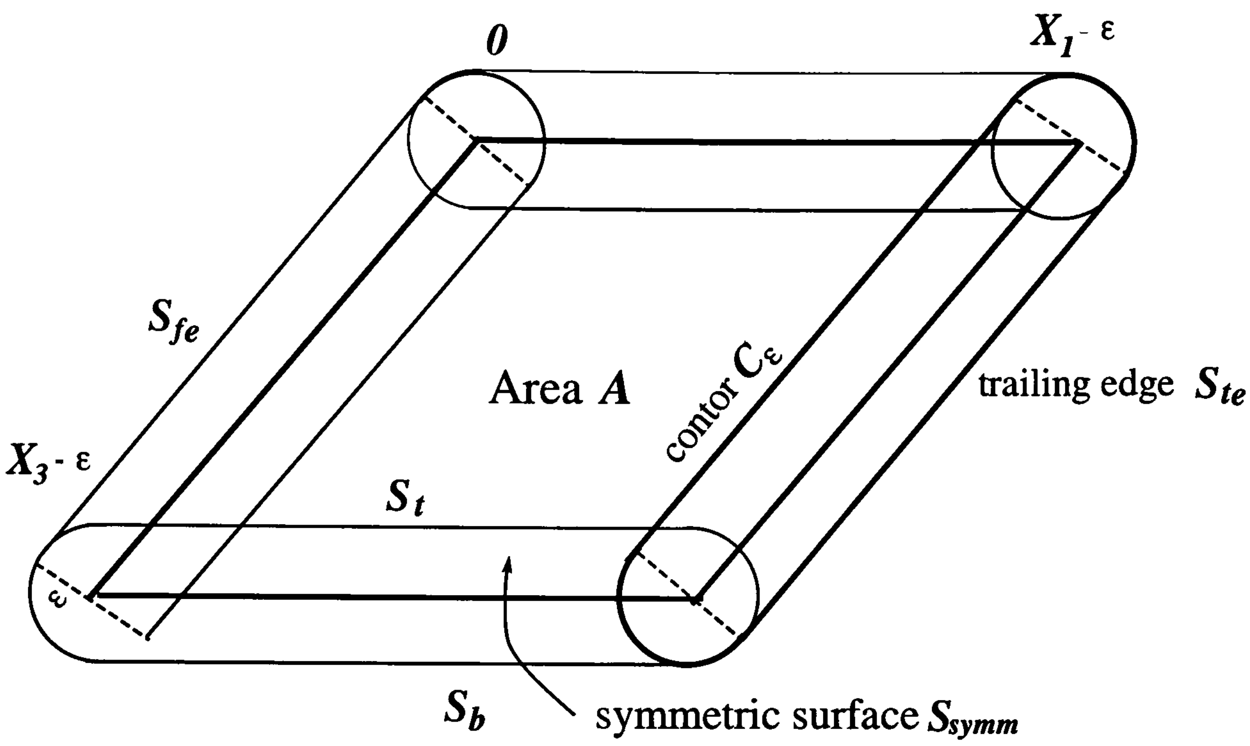

Figure 5.3: Surface symmetric about x_2 around the area A.

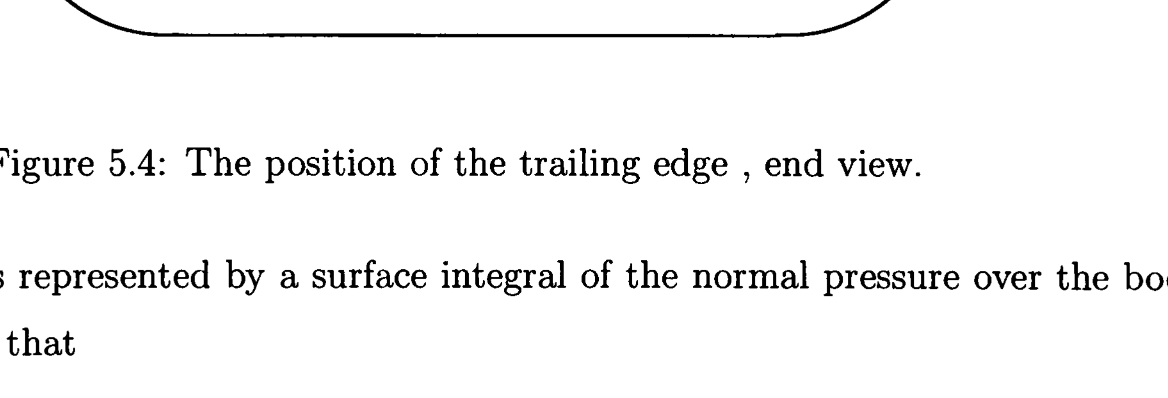

Figure 5.4: The position of the trailing edge , end view.

Then the force is represented by a surface integral of the normal pressure over the body surface [27] such that

$$f_i = \lim_{\delta \to 0} \{ - \iint_{S_B - S_\delta} P^\dagger n_i ds \}, \tag{5.2.6}$$

where f_i is the force on the body due to the fluid; ds is surface element; and $S_B - S_\delta$ is part of the body surface not lying on S_δ. (Standard calculation essentially calculate the force integral over the body surface $S_B - S_\varepsilon$, but we claim that this is incorrect as the contribution to the force integral across the trailing edge is not then considered.)

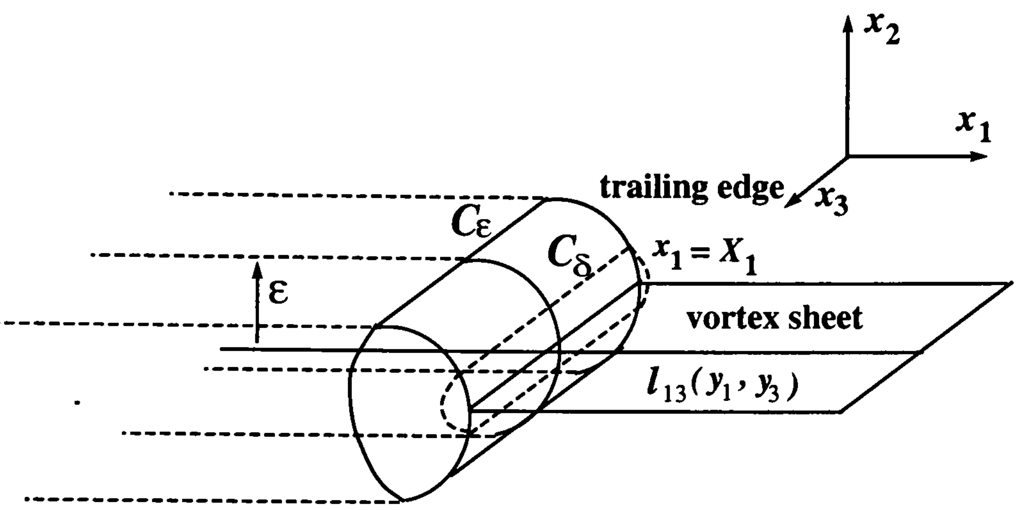

Figure 5.5: The position of the trailing edge , side view.

Since $u_j^\dagger n_j = 0$ on the body surface, then

$$\begin{aligned} f_i &= \lim_{\delta \to 0} \{- \iint\limits_{S_B - S_\delta} (P^\dagger n_i + \rho u_i^\dagger u_j^\dagger n_j) ds\} \\ &= \lim_{\delta \to 0} \{- \iint\limits_{S - S_\delta} (P^\dagger n_i + \rho u_i^\dagger u_j^\dagger n_j) ds\}, \end{aligned} \tag{5.2.7}$$

where S is a general surface enclosing the body except for the constraint that S_δ must lie on S. We have used the result that the integrand of the volume integral enclosing the two surfaces $S - S_\delta$ and $S_B - S_\delta$ is identically zero from Green's integral theorem.

The second component of force, f_2 is therefore given by

$$\begin{aligned} f_2 = \lim_{\delta \to 0} \iint\limits_{S - S_\delta} &\{\rho U u_1 n_2 + \rho V u_2 n_2 + \frac{1}{2}\rho u_1 u_1 n_2 + \frac{1}{2}\rho U u_2 u_2 n_2 \\ &+ \frac{1}{2}\rho U u_3 u_3 n_2 - \rho(V + u_2)(U + u_1) n_1 \\ &- \rho(V + u_2)(V + u_2) n_2 - \rho(V + u_2) u_3 n_3\} ds. \end{aligned} \tag{5.2.8}$$

Consider the integral over the surface such that $S = S_{symm}$ which is symmetric about $x_2 = 0$.

All terms in the integrand that are antisymmetric in x_2 give zero integral contribution.

Also, the term in the integrand $-\rho U V n_1$ give zero contribution over the closed surface. So, from the form of u_i given in (5.2.2), then equation for f_2 reduces to

$$f_2 = \lim_{\delta \to 0} \{ \rho U \iint_{S_{symm} - S_\delta} (u_1 n_2 - u_2 n_1) ds \}. \tag{5.2.9}$$

5.3 Lift force over top and bottom surfaces of the wing

The top and bottom surfaces S_{tb} defined as part of S_{symm}, are shown in figure 5.6 as the solid line. Hence the surface on the body S_ε which contains the trailing edge and is enclosed by the contour C_ε is not included in the standard approach.

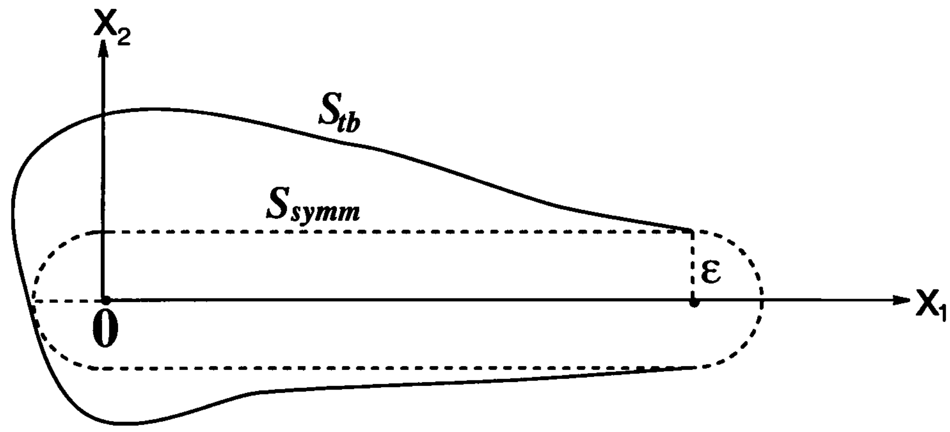

Figure 5.6: The top and bottom surfaces.

A near field approximation ϕ^{nf} is first calculated for ϕ. The inner integral of (5.2.2) is given in slender body theory [15] and the near field approximation discussed extensively in [16]. (Note that the standard form of the slender body integral, $\int \frac{m(y_1)}{R_{13} - x_{11}} dy_1$, can be rewritten as $-\frac{\partial}{\partial x_1} \int m(y_1) \ln(R_{13} - x_{11}) dy_1$.) Applying slender body analysis, a near field approximation ϕ^{nf} for ϕ is given as

$$\phi \sim \phi^{nf} = \frac{1}{2\pi\rho U} \int_0^{X_3 - \varepsilon} \ell_3(x_1, y_3) \frac{\partial}{\partial x_2} \ln(r_3) dy_3, \tag{5.3.1}$$

where $r_3 = \sqrt{(x_3 - y_3)^2 + x_2^2}$. The force integral in 2-direction over the top and bottom surfaces, which we shall denote by f_2^{tb}, is over the top surface S_t and bottom surface S_b. From (5.3.1), it is clear from symmetry arguments that the contribution from the bottom surface is the same as from the top surface.

Therefore, substituting (5.3.1) into (5.2.9) gives

$$\begin{aligned} f_2^{tb} &= 2\rho U \int_0^{X_3}\int_0^{X_1} u_1(x_1,\varepsilon,x_3)dx_1dx_3 \\ &= 2\rho U \lim_{\varepsilon\to 0}\{\int_0^{X_3}\int_0^{X_1}\int_0^{X_3} \frac{\partial \ell_3(x_1,y_3)}{\partial x_1}\frac{1}{2\pi\rho U}\frac{\partial}{\partial x_2}\ln(r_3)|_{y_2=\varepsilon}dy_3dx_1dx_3\} \\ &= \frac{1}{\pi}\lim_{\varepsilon\to 0}\{\int_0^{X_3}\int_0^{X_1}\int_0^{X_3} \frac{\partial \ell_3(x_1,y_3)}{\partial x_1}\frac{\varepsilon}{\varepsilon^2+(x_3-y_3)^2}dy_3dx_1dx_3\} \\ &= \frac{1}{\pi}\lim_{\varepsilon\to 0}\{\int_0^{X_3}\int_0^{X_1} \frac{\partial \ell_3(x_1,y_3)}{\partial x_1}[\arctan(\frac{x_3-y_3}{\varepsilon})]_{x_3=0}^{x_3=X_3}{}_1dy_3dx_1\} \\ &= \int_0^{X_3}[\ell_3(x_1,y_3)]_{x_1=0}^{x_1=X_1}dy_3 = \int_0^{X_3}\ell_3(X_1,y_3)dy_3 = L. \end{aligned} \tag{5.3.2}$$

The force over the top and bottom surfaces of the wing is therefore L. However, there is an additional contribution to the lift force across the trailing edge of the wing.

5.4 Lift force across the trailing edge of the wing

It is noted that u_i is not singular at the trailing edge, and so there is no contribution to the integral from the term u_1n_1 at the trailing edge in the limit as $\delta \to 0$. So, from (5.2.9), the force in the 2-direction across the trailing edge of the wing is given is

$$\begin{aligned} f_2^{te} &= \lim_{\varepsilon\to 0}\lim_{\delta\to 0}(-\rho U \iint\limits_{S_{te}-S_\delta} \frac{\partial \phi}{\partial x_2}n_1ds) \\ &= \lim_{\varepsilon\to 0}\lim_{\delta\to 0}(-\rho U \iint\limits_{A_{te}-A_\delta} \frac{\partial \phi}{\partial x_2}dA), \end{aligned} \tag{5.4.1}$$

where the inner limit is taken first. Also, A_{te} is the projection of the surface S_{te} onto the plane of constant x_1, similarly with A_δ, and dA is an element of area in the x_1 plane.

Hence, we have assumed that ℓ_3 is slowly varying function in x_1. Applying the divergence theorem, the area integral is changed to a contour integral such that

$$f_2^{te} = \lim_{\varepsilon\to 0}\lim_{\delta\to 0}\{-\rho U \oint_{C_\varepsilon} \phi n_2 dl + \rho U \oint_{C_\delta} \phi n_2 dl\}, \tag{5.4.2}$$

where C_ε and C_δ are given in figures 5.4 and 5.5, and $\oint$ is an integration around a closed contour in the anti-clockwise sense.

Substituting for ϕ^{nf} from (5.3.1), and changing the order of integration gives

$$f_2^{te} = \lim_{\varepsilon\to 0}\lim_{\delta\to 0}(\frac{1}{2\pi}\int_0^{X_3} \ell_3(X_1, y_3)\{-\rho U \oint_{C_\varepsilon} \frac{\partial}{\partial x_2}\ln(r_3) n_2 dl + \rho U \oint_{C_{r\delta}} \frac{\partial}{\partial x_2}\ln(r_3) n_2 dl\}, \tag{5.4.3}$$

where the contour C_δ can now be replaced by the circular contour $C_{r\delta}$ of radius δ at $y_3 = x_3$, see figure 5.7.

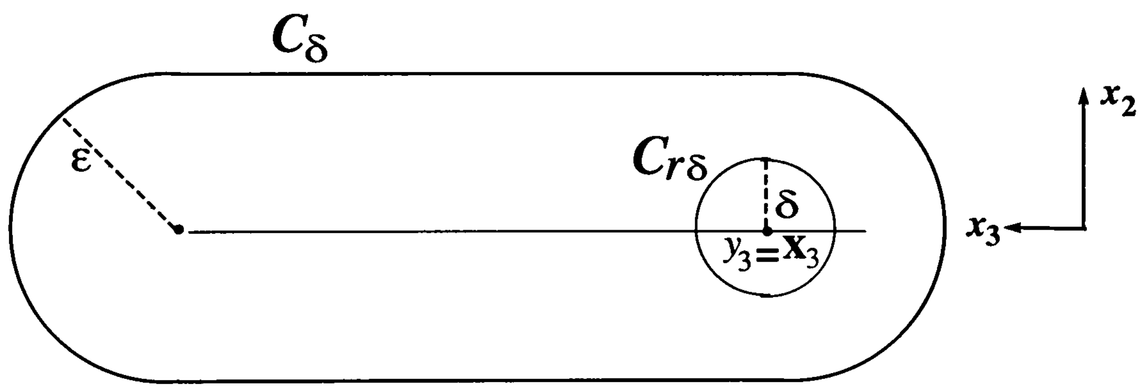

Figure 5.7: The contour $C\delta$ and $C_{r\delta}$.

5.4.1 Contribution from contour $C_{r\delta}$

The contribution to (5.4.3) from the contour $C_{r\delta}$ denoted by f_2^δ is

$$
\begin{aligned}
f_2^\delta &= \lim_{\delta\to 0}(\frac{1}{2\pi}\int_0^{X_3}[\ell_3(X_1,y_3)\{\int_0^{2\pi}\frac{\cos\theta_3}{r_3}\cos\theta_3 r_3 d\theta_3\}dy_3 \\
&= \frac{1}{2}\int_0^{X_3}\ell_3(X_1,y_3)dy_3 = \frac{L}{2},
\end{aligned} \tag{5.4.4}
$$

where $r_3 = \{x_2^2 + (x_3 - y_3)^2\}^{\frac{1}{2}}$, $x_2 = r_3\cos\theta_3$ and $x_3 = r_3\sin\theta_3$.

5.4.2 Contribution from contour C_ε

Let the contribution to the force integral over the contour C_ε be denoted by f_2^ε. Due to symmetry, the contribution from the upper half contour $x_2 \geq 0$ is equal to the contribution from the lower half contour $x_2 \leq 0$. Also, the contribution from the semi-circular contours are of lower order for small ε. Therefore,

$$
\begin{aligned}
f_2^\varepsilon &= \lim_{\varepsilon\to 0}(-2\rho U\int_0^{X_3}\phi^{nf}|_{x_2=\varepsilon}dx_3) \\
&= \lim_{\varepsilon\to 0}\{-\frac{1}{\pi}\int_0^{X_3}\int_0^{X_3}\ell_3(X_1,y_3)\frac{\varepsilon}{\varepsilon^2+(x_3-y_3)^2}dy_3dx_3\} \\
&= \lim_{\varepsilon\to 0}\{-\frac{1}{\pi}\int_0^{X_3}\ell_3(X_1,y_3)[\arctan(\frac{x_3-y_3}{\varepsilon})]_{x_3=0}^{x_3=X_3}dy_3\} \\
&= -\frac{1}{\pi}\int_0^{X_3}\ell_3(X_1,y_3)\{\frac{\pi}{2}-(-\frac{\pi}{2})\}dy_3 = -L.
\end{aligned} \tag{5.4.5}
$$

Therefore at the trailing edge there is a jump in the lift force of value $f_2^{te} = f_2^\delta + f_2^\varepsilon = L/2 - L = -L/2$.

5.4.3 Total lift force on the wing

We have seen in the previous section that the total lift force on the wing is $f_2^{tb} + f_2^{te} = L - L/2 = L/2$, half that expected by considering the pressure distribution over the top and bottom surface of the wing only.

The total lift force is given by an integral involving the pressure over the body surface. From (5.2.7) by using Green's theorem it is shown that this integral is equivalent to an integral over a general surface S enclosing the body, for a particular integral involving pressure and velocity. Here, a spherical surface in the far filed is considered.

The force can also be calculated from a far field integral enclosing the body: consider a closed surface enclosing a volume of fluid which the integral given in (5.2.9). From Green's integral theorem, this is identically zero, and so the lift force can be represented by an integral over a surface enclosing the shed vortex wake and over a far field surface enclosing the body, see figure 5.8. It shall be shown next that the first of these integral is zero and then the force shall be calculated from a far field integral enclosing the body.

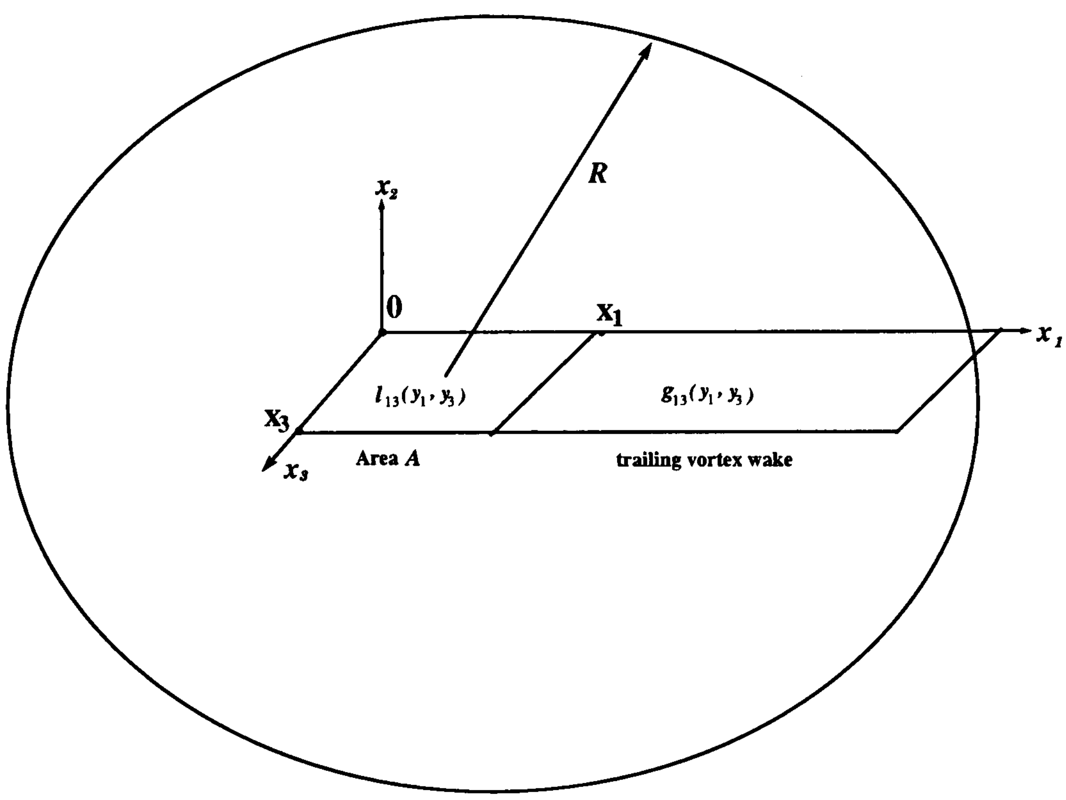

Figure 5.8: Far field

5.4.4 The force integral over a surface enclosing the shed vortex wake

First, we determine the form of the potential in the near field of the shed vortex wake ϕ^{nf}_{wake}.

The potential is given from (5.2.2) as

$$\phi = \iint_A \frac{\ell_{13}(y_1, y_3)}{4\pi\rho U}\frac{\partial}{\partial x_2}\ln(R_{13} - x_{11})dy_1dy_3. \tag{5.4.6}$$

Applying the Taylor expansion gives

$$\frac{\partial}{\partial x_2}\ln(R_{13} - x_{11}) \sim \frac{2x_2}{x_2^2 + x_{33}^2}. \tag{5.4.7}$$

Substituting this expansion for $\frac{\partial}{\partial x_2}\ln(R_{13} - x_{11})$ into (5.2.2) gives

$$\phi_{wake}^{nf} \approx \frac{1}{2\pi\rho U}\int_0^{X_3} \ell_3(X_1, y_3)\frac{\partial}{\partial x_2}\ln(r_3)dy_3, \tag{5.4.8}$$

which gives the same result as (5.3.1) with $x_1 = X_1$. Representing the flow near the wake in the form

$$\phi_{wake}^{nf} \approx \frac{1}{2\pi\rho U}\int_0^{X_3} \ell_3(x_1, y_3)\frac{\partial}{\partial x_2}\ln(r_3)dy_3, \tag{5.4.9}$$

gives for $y_1 > X_1$

$$\ell_3(y_1, y_3) = \ell_3(X_1, y_3), \tag{5.4.10}$$

which is consistent with the standard aerodynamic horseshoe vortex description of the shed vortex wake, the vortex lines are parallel and constant strength.

The force integral over the trailing vortex wake f_2^{wake} can now be determined. To first order, from (5.2.9), substituting in for ϕ the value ϕ_{wake}^{nf} from (5.4.9) gives

.

$$\begin{aligned} f_2^{wake} &= -2\rho U\int_0^{X_3}\int_{X_1}^{\infty} u_1(x_1, \delta, x_3)dx_1dx_3 \\ &= \frac{1}{\pi}\int_0^{X_3}\int_{X_1}^{\infty}\int_0^{X_3} \frac{\partial}{\partial x_1}g_3(x_1, x_3)(\frac{\delta}{\delta^2 + x_{33}^2})dx_3dx_1dy_3. \end{aligned} \tag{5.4.11}$$

However, using the result (5.4.10), then

$$\int_{X_1}^{\infty} \frac{\partial}{\partial x_1} g_3(x_1, x_3)dx_1 = [g_3(x_1, x_3)]_{x_1=x_1}^{x_1=\infty}$$
$$= \ell_3(X_1, y_3) - \ell_3(X_1, y_3) = 0, \tag{5.4.12}$$

so $f_2^{wake} = 0$.

5.4.5 The force integral over a spherical surface radius $R \to \infty$ enclosing the body

In the far field, from (5.2.2), applying the Taylor series expansion about a point $(0, 0, 0)$ centered on the body gives

$$\phi = \sum_{n=0}^{\infty} \sum_{m=0}^{\infty} a_{nm} \frac{\partial^n}{\partial x_1^n} \frac{\partial^m}{\partial x_2^m} \frac{\partial}{\partial x_2} \ln(R - x_1), \tag{5.4.13}$$

where $R = \{x_1^2 + x_2^2 + x_3^2\}^{\frac{1}{2}}$, and n and m and are non negative integers. The expansion is convergent except on the vortex wake $x_2 = 0$, $0 \leq x_3 \leq X_3$, and also the coefficient $a_{00} = \frac{L}{4\pi\rho U}$. Consider the surface S_R such that $x_1^2 + x_2^2 + x_3^2 = R^2$, and the surface S_R^δ which lies on the surface S_R such that $x_2^2 + s^2 \leq \delta^2$ where $0 \leq s \leq X_3$. Therefore the points on the surface S_R^δ are a distance at most δ away from the trailing vortex sheet. Then from (5.2.9) the force over the far field surface enclosing the body f_2^{ff} is given by

$$f_2^{ff} = \lim_{\delta \to 0} \lim_{R \to \infty} \{\rho U \iint_{S_R - S_R^\delta} (u_1 n_2 - u_2 n_1) ds\}. \tag{5.4.14}$$

On substituting the expansion for φ from (5.4.13) and (5.4.14), only the first term in the expansion, $a_{00} = \frac{L}{4\pi\rho U}$, is nonzero in the limit as $R \to \infty$, and gives

$$f_2^{ff} = L/3 + L/6 = L/2. \tag{5.4.15}$$

Hence, as expected, the total lift force on the wing is $f_2^{wake} + f_2^{ff} = 0 + L/2 = L/2$.

5.5 Chapter 5 Discussion

The standard horseshoe vortex description of a vortex wake in potential flow aerodynamics has been taken, described in for example Lighthill [35] figure 86 p. 216, Batchelor [21] figure 7.8.4 p. 585, and Katz and Plotkin [36] figure 8.2 p. 169.

The discrete summation of horseshoe vortices is then replaced by an integral distribution of potential lifting singular solusions, following [1] (and first used in a slender body context in [15]).

The force integral over the body surface is replaced by a general force integral enclosing the body, and the near field flow is determined by using asymptotic analysis similar to that used in slender body theory. From this, it is shown that the lift force from the pressure integral over the top and bottom surface is L, as given in standard theory. (This is equivalent to stopping the integration at the contour C_ε). However, there is also a lift force from the pressure integral across the trailing edge, and this is shown to give a jump in the lift at the trailing edge of value $-L/2$. (This is equivalent to stopping the integration at the contour C_δ). The lift on the body is also calculated from an integral enclosing the body in the far field. Both calculations show that the total lift force on the body is $L/2$ in inviscid potential flow theory and not L as has always been thought. This is consistent with the lift calculation obtained by considering the horseshoe vortex model given in [1].

Clearly, the potential flow model is incorrect for the following reasons: evaluated properly, the lift on a wing is given as $L/2$ and not L as given by experiment, (the assumed agreement with experiment due to an improper calculation is merely fortuitous); also the kinetic energy about a vortex line which is the fundamental building block element of a vortex model, is not bounded; and finally the far field uniform stream boundary condition is broken near the shed vortex wake because vorticity does not diffuse.

Furthermore, from a physical argument the representation must be flawed as it is impossible to have a jump in lift at trailing edge. The pressure force is such that the trailing edge would snap off. This gives an indication as to why the potential flow model is incorrect. There must be an omitted viscous resistive contribution which counterbalances the singular nature of the potential flow velocity, such that when included in the model: There is no jump in lift at the trailing edge; the kinetic energy about a vortex line is finite; and the far field uniform stream boundary condition if satisfied. The reason why the potential flow model fails is because the viscosity has been set to zero in the Navier-Stokes equations, but yet a coupled singular viscous velocity term is expected to be present in the solution. So, even at high Reynolds number, it cannot be ignored.

This naturally leads to the requirement for a new model in which these viscous terms are present, and this model is given in [15] and [1] : Consider, for example, small perturbation potential theory [36] used extensively in aerodynamics. One way of obtaining this theory is by first setting the viscosity to zero in Navier-Stokes equations (yielding potential flow) and then by assuming that the velocity perturbations to the uniform stream are small. If we re-order these approximations so that first we assume that the velocity perturbations to the uniform stream in the Navier-Stokes equations are small (yielding the Oseen equations), and then take the limit as the Reynolds number tends to infinity, then the viscous terms are retained in the model. This yields a "quasi-potential flow model", and this is believed by us to be correct flow model for aerodynamics and hydrodynamics where the Reynolds number is high and lift/side force calculations are required: there is then no jump in lift for flow past wings, and theory agrees with experiment [1], and the velocity at the center of a vortex line is finite [15].

5.6 Chapter 5 Appendix: Boundary conditions

Since we consider an integral distribution of infinitesimal horseshoe vortices over the area A, the kinematic and dynamic boundary condition applied to the wake, and also the Kutta condition, are implicity satisfied by (5.2.2). However it is important to demonstrate this explicitly, which is done in the following appendix. The kinematic condition are [36] p.87-89

$$\lim_{x_2 \to 0^+} \left(\frac{\partial \varphi^{nf}}{\partial x_1} \right) = \frac{\gamma_3}{2}, \tag{5.6.1}$$

$$\lim_{x_2 \to 0^+} \left(\frac{\partial \varphi^{nf}}{\partial x_3} \right) = -\frac{\gamma_1}{2}, \tag{5.6.2}$$

where in the notation of [36], $\gamma_x = \gamma_1$ and $\gamma_y = \gamma_3$. γ_1 is the bound vortex strength of the wake in the x_1 direction, and γ_3 is the bound vortex strength of wake in the x_3 direction such that [36], p.89

$$\frac{\partial \gamma_1}{\partial x_1} + \frac{\partial \gamma_3}{\partial x_3} = 0. \tag{5.6.3}$$

The dynamic boundary condition [36], p. 87 state that the jump in the pressure Δp and the vortex sheet strength function in the transverse direction γ_3 are

$$\Delta p = 0. \tag{5.6.4}$$

$$\gamma_3 = 0. \tag{5.6.5}$$

This is applied up to the trailing edge, and on the trailing edge satisfies the Kutta condition [36], p. 88.

Kinematic boundary conditions

From (5.3.1), near the vortex sheet we have

$$\phi \sim \phi^{nf} = \frac{1}{2\pi\rho U} \int_0^{X_3} \ell_3(x_1, y_3) \frac{\partial}{\partial x_2} \ln(r_3) dy_3, \tag{5.6.6}$$

so

$$\frac{\partial \phi^{nf}}{\partial x_1} = \frac{1}{2\pi\rho U} \int_0^{X_3} \ell_{31}(x_1, y_3) \frac{\partial}{\partial x_2} \ln(r_3) dy_3, \tag{5.6.7}$$

where $\ell_{31}(x_1, y_3) = \frac{\partial^2}{\partial x_3 \partial x_1} \ell(x_1, y_3)$. Letting $x_{33} = x_3 - y_3$, then

$$\frac{\partial \phi^{nf}}{\partial x_1} = -\frac{1}{2\pi\rho U} \int_0^{x_3 - X_3} \ell_{31}(x_1, x_3 - x_{33}) \frac{\partial}{\partial x_2} \ln(\sqrt{x_2^2 + x_{33}^2}) dx_{33}. \tag{5.6.8}$$

Let us assume that ℓ_{31} can be represented by a finite Taylor series expansion to N terms.

Then

$$\frac{\partial \phi^{nf}}{\partial x_1} = -\frac{1}{2\pi\rho U}\sum_{n=0}^{N}\frac{\partial^n}{\partial x_3^n}\ell_{31}(x_1,x_3)\int_0^{x_3-X_3}\frac{(-x_{33})^n}{n!}\frac{x_2}{x_2^2+x_{33}^2}dx_{33}. \tag{5.6.9}$$

Changing the variable of integration to β where $x_{33} = x_2\tan\beta$, then

$$\frac{\partial \phi^{nf}}{\partial x_1} = -\frac{1}{2\pi\rho U}\sum_{n=0}^{N}\frac{(-1)^n}{n!}\frac{\partial^n}{\partial x_3^n}\ell_{31}(x_1,x_3)x_2^n\int_{\arctan(\frac{x_3-X_3}{x_2})}^{\arctan(\frac{x_3}{x_2})}\tan^n\beta d\beta. \tag{5.6.10}$$

Consider

$$I_n = x_2^n\int_{\arctan(\frac{x_3-X_3}{x_2})}^{\arctan(\frac{x_3}{x_2})}\tan^n\beta d\beta. \tag{5.6.11}$$

Then

$$I_0 = \arctan(\frac{x_3}{x_2}) - \arctan(\frac{x_3-X_3}{x_2}), \tag{5.6.12}$$

and so

$$\lim_{x_2\to 0} I_0 = \lim_{x_2\to 0}\left(\arctan(\frac{x_3}{x_2}) - \arctan(\frac{x_3-X_3}{x_2})\right) = \frac{\pi}{2} - (-\frac{\pi}{2}) = \pi. \tag{5.6.13}$$

Using the result [38], p. 77 4.3.115, then

$$\lim_{x_2\to 0} I_1 = \lim_{x_2\to 0}\left\{x_2\left(\ln\left|\frac{x_3}{X_3-x_3}\right|\right)\right\} = 0. \tag{5.6.14}$$

Similarly, using the result for $n \geq 2$ given in [38], p. 77 4.3.120, then

$$I_n = x_2\left\{\frac{1}{n-1}\left(x_3^{n-1} - (x_3-X_3)^{n-1}\right)\right\} - x_2^2 I_{n-2}. \tag{5.6.15}$$

By iterating using the recursive relation, we have for $n \geq 2$ $\quad I_n = \mathcal{O}(x_2)$, and so

$$\lim_{x_2\to 0} I_n = 0. \tag{5.6.16}$$

Therefore,

$$\lim_{x_2\to 0}\left(\frac{\partial \phi^{nf}}{\partial x_1}\right) = \frac{\ell_{31}(x_1,x_3)}{2\pi\rho U}. \tag{5.6.17}$$

Similarly,

$$\frac{\partial \phi^{nf}}{\partial x_3} = -\frac{1}{2\pi\rho U}\int_0^{X_3}\ell_3(x_1,y_3)\frac{\partial}{\partial x_2}\ln(r_3)dy_3. \tag{5.6.18}$$

However, $\frac{\partial}{\partial x_3}\ln(r_3) = -\frac{\partial}{\partial y_3}\ln(r_3)$, and so, integrating by parts gives

$$\frac{\partial\phi^{nf}}{\partial x_3} = -\frac{1}{2\pi\rho U}\left\{\left[\ell_3(x_1,y_3)\frac{\partial}{\partial x_2}\ln(r_3)\right]_0^{X_3} - \int_0^{X_3}\ell_{33}(x_1,y_3)\frac{\partial}{\partial x_2}\ln(r_3)dy_3\right\}. \quad (5.6.19)$$

Applying similar arguments as for $\frac{\partial\phi^{nf}}{\partial x_1}$, we have

$$\lim_{x_2\to 0}\left(\frac{\partial\phi^{nf}}{\partial x_3}\right) = \frac{\ell_{33}(x_1,x_3)}{2\pi\rho U}. \quad (5.6.20)$$

It is more usual to express these in terms of the bound vortex strength of the wake γ_1 in the x_1 direction and γ_3 in the x_3 direction, where we let $\gamma_1 = -\ell_{33}/(\rho U)$ and $\gamma_3 = -\ell_{31}/(\rho U)$. This gives the kinematic boundary conditions

$$\lim_{x_2\to 0}\left(\frac{\partial\varphi^{nf}}{\partial x_1}\right) = \frac{\gamma_3}{2}, \quad (5.6.21)$$

and

$$\lim_{x_2\to 0}\left(\frac{\partial\varphi^{nf}}{\partial x_3}\right) = -\frac{\gamma_1}{2}. \quad (5.6.22)$$

Furthermore, since $\frac{\partial^3\ell}{\partial x_3\partial x_1\partial x_3} = \frac{\partial^3\ell}{\partial x_3\partial x_3\partial x_1}$, then the circulation condition (5.6.3)

$$\frac{\partial\gamma_1}{\partial x_1} + \frac{\partial\gamma_3}{\partial x_3} = 0.$$

holds, [36] p. 87-89.

Dynamic boundary conditions

From Bernoulli's equation and the asymmetry of the flow, the jump in pressure Δp across the vortex sheet is given by

$$\Delta p = -2\rho U\frac{\partial\varphi}{\partial x_1} = -\rho U\gamma_3. \quad (5.6.23)$$

Across the wake, from (5.4.10),

$$\frac{1}{\rho U}\frac{\partial}{\partial x_1}\ell_3(x_1,x_3) = \gamma_3 = 0, \quad \Delta p = 0, \quad (5.6.24)$$

which holds up to the trailing edge. Hence, the Kutta condition ia satisfied at the trailing edge [36], p. 88.

Chapter 6

Slender body theory

6.1 Introduction

In this chapter, we give the complete slender body expansion over a finite line for the generator potential defined as $\varphi = \ln(R - x_1)$. The integral splitting technique is used but applied to the generator potential rather than the source potential. The advantage of starting with the generator potential is immediately clear if the near field approximation for $r \to 0$, $x_1 > 0$ is considered; Then $R - x_1 \sim r^2/2x_1$, and $\ln(R - x_1) \sim 2\ln r - ln2x_1$. The separation into transverse plane and stream-wise variables is immediate and does not require involved integration by parts, or application of restrictive end conditions. In this way, an expansion to all orders is obtained but over a finite length body rather than the infinite length of the transform methods. A check for the expansion is that when the ends are taken in the limits to infinity and the equation is differentiated through with respect to x_1, then the resulting expansion is equivalent to that given by Fourier transform method for a distribution of sources over an infinite length. However, it is shown by subsequent differentiations of the generator potential that different far field distributions yield the same leading order near field solution. The implications of this non-uniqueness are discussed for several fluid applications.

6.2 Subsonic flow

We consider a flow past a body of revolution at zero yaw by the method of sources. It is of some mathematical interest to obtain the approximate solution for flow past a body of revolution by the method of sources [39]. Here we consider irrotational flow with constant entropy with an undisturbed flow U in the x_1-axis direction, if the velocity potential is $\phi^{\dagger} = Ux_1 + \varphi$, the linearised equation for φ is

$$\frac{\partial^2\varphi}{\partial x_1^2} + \frac{\partial^2\varphi}{\partial x_2^2} + \frac{\partial^2\varphi}{\partial x_3^2} = 0. \tag{6.2.1}$$

Corresponding with a source at the origin in incompressible flow, we may consider

$$\varphi = A/R \text{ where } R = \sqrt{x_1^2 + x_2^2 + x_3^2}. \tag{6.2.2}$$

The mass flux out of any closed surface S for which the origin is an interior point is [5]

$$F = \int_S \rho \nabla\phi \cdot \hat{\mathbf{n}} ds, \tag{6.2.3}$$

where ρ is density. If ρ_0 is the density in the undisturbed flow, then

$$\frac{F}{\rho_0} = \int_S (n_1\frac{\partial\varphi}{\partial x_1} + n_2\frac{\partial\varphi}{\partial x_2} + n_3\frac{\partial\varphi}{\partial x_3})ds. \tag{6.2.4}$$

Now let S to be a sphere (of radius R), then $n_i = \frac{x_i}{R}$ and then,

$$\int_S n_i\frac{\partial\varphi}{\partial x_i}ds = \int_S \frac{x_i}{R}\frac{-x_i}{R^3}ds = \frac{-1}{R^2}(4\pi R^2) = -4\pi,$$

$$\frac{F}{\rho_0} = -4\pi A,$$

For source of strength, m which supposed to be infinitely many times differentiable, in a fluid of constant density ρ_0 the mass flux out of a surface enclosing the source is $4\pi\rho_0 m$ and the velocity potential is $-m/(x_1^2 + x_2^2 + x_3^2)^{\frac{1}{2}}$. We may therefore say that in linearized subsonic flow, the perturbation potential for the source of strength m at the origin is $-m/R$, where R is given by (6.2.2).

Now consider the flow with an undisturbed velocity U along the x_1-axis, past an elongated body of revolution of length l, at zero yaw (in other words with its axis along the undisturbed flow). Let us try to find a distribution of sources, of strength $m(x_1)$ per unit length which gives, to a sufficient approximation, the same perturbation as the given body. Then if the origin is at the upstream end of the body, we should define

$$\varphi(x_1, x_2, x_3) = -\int_0^\ell \frac{m(y_1)dy_1}{\sqrt{(x_1 - y_1)^2 + r^2}}, \text{ where } r^2 = x_2^2 + x_3^2. \tag{6.2.5}$$

However it is only in exceptional cases that there is a solution of this form of equation (6.2.1) with the necessary boundary conditions. But it appears that to the order of approximation to which we shall proceed, this is a sufficiently accurate, and the value of m may be found by an elementary argument. Take two sections normal to the axis at x_1 and $x_1 + dx_1$ and consider the flux out of the surface formed by these sections and the part of the surface of the body connecting them. This flux must be $4\pi\rho_0 m(x_1)dx_1$. The flow is to be tangential to the body surface, so there is no flow across it. Let $S(x_1)$ be the area of the cross-section at x_1. To the lowest approximation the flux out through the two cross-sections is

$$\rho_0 US(x_1 + dx_1) - \rho_0 US(x_1) = \rho_0 US'(x_1)dx_1, \tag{6.2.6}$$

so we must take

$$4\pi m(x_1) = US'(x_1), \tag{6.2.7}$$

and substituting in (6.2.5) gives

$$\varphi = -\frac{U}{4\pi}\int_0^\ell \frac{S'(y_1)dy_1}{\sqrt{(x_1 - y_1)^2 + r^2}}. \tag{6.2.8}$$

To find φ on and near the surface of the body, we require only an approximation when r is small. But if we put $r = 0$ in the integrand, the integral becomes an improper integral, and care is needed in finding the correct form for small r. In what follows, we shall assume that $S(x_1)$ has a bounded second derivative. With the above value of m, we write $-\varphi = I_1 + I_2$, where,

$$I_1 = \int_0^{x_1} \frac{m(y_1)dy_1}{\sqrt{(x_1-y_1)^2+r^2}}, \quad I_2 = \int_{x_1}^{\ell} \frac{m(y_1)dy_1}{\sqrt{(x_1-y_1)^2+r^2}}. \tag{6.2.9}$$

and

$$m(y_1) - m(x_1) = (y_1 - x_1)G(y_1, x_1), \tag{6.2.10}$$

where G is bounded. Then

$$\begin{aligned} I_1 &= m(x_1)\int_0^{x_1} \frac{dy_1}{\sqrt{(x_1-y_1)^2+r^2}} + \int_0^{x_1} \frac{(y_1-x_1)G}{\sqrt{(x_1-y_1)^2+r^2}}dy_1 \\ &= m(x_1)\sinh^{-1}\frac{x_1}{Br} + \int_0^{x_1} \frac{(y_1-x_1)G}{\sqrt{(x_1-y_1)^2+r^2}}dy_1, \end{aligned}$$

and similarly

$$I_2 = m(x_1)\sinh^{-1}\frac{(\ell - x_1)}{Br} + \int_{x_1}^{\ell} \frac{(y_1-x_1)G}{\sqrt{(x_1-y_1)^2+r^2}}dy_1.$$

Since for sufficiently small r:

$$\sinh^{-1}\frac{x_1}{Br} = \log\left((\frac{x_1}{Br}) + \sqrt{(\frac{x_1}{Br})^2 + 1} \right) \sim \log\frac{2x_1}{Br},$$

$$\sinh^{-1}(\frac{\ell - x_1}{Br}) \sim \log\frac{2(\ell - x_1)}{Br},$$

$$\int_0^{x_1} \frac{(y_1-x_1)G}{\sqrt{(x_1-y_1)^2+r^2}}dy_1 \sim \int_0^{x_1} \frac{(y_1-x_1)G}{x_1-y_1}dy_1 = -\int_0^{x_1} G dy_1 ,$$

$$\int_{x_1}^{\ell} \frac{(y_1-x_1)G}{\sqrt{(x_1-y_1)^2+r^2}}dy_1 \sim \int_{x_1}^{\ell} \frac{(y_1-x_1)G}{y_1-x_1}dy_1 = \int_{x_1}^{\ell} G dy_1.$$

So as r tends to zero,

$$
\begin{aligned}
I_1 + I_2 \to & \left(m(x_1)\log\frac{2x_1}{Br} - \int_0^{x_1} G dy_1\right) + \left(m(x_1)\log\frac{2(\ell - x_1)}{Br} + \int_{x_1}^{\ell} G dy_1\right) \\
& = m(x_1)\log x_1(\ell - x_1) - 2m(x_1)\log\frac{Br}{2} - \int_0^{x_1} G dy_1 + \int_{x_1}^{\ell} G dy_1.
\end{aligned}
\tag{6.2.11}
$$

So an approximation for φ in (6.2.5) is

$$
\varphi \sim -\{m(x_1)\log x_1(\ell - x_1) - 2m(x_1)\log\frac{Br}{2} - \int_0^{x_1} G dy_1 + \int_{x_1}^{\ell} G dy_1\}.
$$

Now we construct

$$
J = \int_0^{x_1 - \frac{1}{2}Br} \frac{m(y_1)dy_1}{x_1 - y_1} + \int_{x_1 + \frac{1}{2}Br}^{\ell} \frac{m(y_1)dy_1}{y_1 - x_1},
$$

and replace $m(y_1)$ from (6.2.10) to get

$$
\begin{aligned}
\int_0^{x_1 - \frac{1}{2}Br} \frac{m(y_1)dy_1}{x_1 - y_1} &= \int_0^{x_1 - \frac{1}{2}Br} \frac{(m(x_1) + (y_1 - x_1)G)dy_1}{x_1 - y_1} \\
&= m(x_1)\log x_1 - m(x_1)\log\frac{Br}{2} - \int_0^{x_1 - \frac{1}{2}Br} G dy_1,
\end{aligned}
$$

similarly,

$$
\int_{x_1 + \frac{1}{2}Br}^{\ell} \frac{m(y_1)dy_1}{y_1 - x_1} = m(x_1)\log(\ell - x_1) - m(x_1)\log\frac{Br}{2} + \int_{x_1 + \frac{1}{2}Br}^{\ell} G dy_1.
$$

So

$$
J = m(x_1)\log x_1(\ell - x_1) - 2m(x_1)\log\frac{Br}{2} - \int_0^{x_1 - \frac{1}{2}Br} G dy_1 + \int_{x_1 + \frac{1}{2}Br}^{\ell} G dy_1 .
$$

Now since G is bounded with bound M, so we suppose $M_r = \max_{y_1 \in [x_1 - Br/2, x_1 + Br/2]} G(y_1, x_1)$ and therefore $M_r \leq M$ so,

$$
\begin{aligned}
|J-(I_1+I_2)| &= \left|\int_{x_1-\frac{1}{2}Br}^{x_1} G dy_1 - \int_{x_1}^{x_1+\frac{1}{2}Br} G dy_1\right| \\
&\le \left|\int_{x_1-\frac{1}{2}Br}^{x_1} G dy_1\right| + \left|\int_{x_1}^{x_1+\frac{1}{2}Br} G dy_1\right| \\
&\le M_r Br \le MBr.
\end{aligned}
\tag{6.2.12}
$$

It can be seen in (6.2.12) that $(I_1+I_2)-J \to 0$ as $r \to 0$. On the other hand by integration by parts we'll have

$$
\int_0^{x_1-\frac{1}{2}Br} \frac{m(y_1)dy_1}{x_1-y_1} = m(0)\log(x_1) - m(x_1-\frac{1}{2}Br)\log\frac{Br}{2} + \int_0^{x_1-\frac{1}{2}Br} m'(y_1)\log(x_1-y_1)dy_1,
$$

and,

$$
\int_{x_1+\frac{1}{2}Br}^{\ell} \frac{m(y_1)dy_1}{y_1-x_1} = m(\ell)\log(\ell-x_1) - m(x_1+\frac{1}{2}Br)\log\frac{Br}{2} - \int_{x_1+\frac{1}{2}Br}^{\ell} m'(y_1)\log(y_1-x_1)dy_1.
$$

Hence as $r \to 0$, we will have

$$
\begin{aligned}
(I_1+I_2) \;\sim\; J = \{&m(0)\log(x_1) + m(\ell)\log(\ell-x_1) - 2m(x_1)\log\frac{Br}{2} \\
&+ \int_0^{x_1} m'(y_1)\log(x_1-y_1)dy_1 - \int_{x_1}^{\ell} m'(y_1)\log(y_1-x_1)dy_1\}.
\end{aligned}
$$

Now we substitute m from (6.2.7) and for small r we get an approximation for φ in (6.2.8) that is

$$
\begin{aligned}
\varphi \sim -\frac{U}{4\pi}\{&S'(0)\log(x_1) + S'(\ell)\log(\ell-x_1) - 2S'(x_1)\log\frac{Br}{2} \\
&+ \int_0^{x_1} S''(y_1)\log(x_1-y_1)dy_1 - \int_{x_1}^{\ell} S''(y_1)\log(y_1-x_1)dy_1\}.
\end{aligned}
\tag{6.2.13}
$$

The interest of above method in finding an approximation for (6.2.8) is that it relates the limiting value, as $r \to 0$, of I_1+I_2 to a particular "principal value" of the integral of $m(y_1)/|x_1-y_1|$ from 0 to ℓ.

If the body is pointed at the forward end, $S'(0) = 0$, and if it is pointed at the rear end $S'(\ell) = 0$. Note that φ is logarithmically infinite at the forward end unless $S'(0) = 0$, and at the rear unless $S'(\ell) = 0$. By considering these assumption we may have

$$\varphi \sim \frac{U}{4\pi}\{2S'(x_1)\log\frac{Br}{2} - \int_0^{x_1} S''(y_1)\log(x_1 - y_1)dy_1 + \int_{x_1}^{\ell} S''(y_1)\log(y_1 - x_1)dy_1\}. \quad (6.2.14)$$

6.3 Proceeding by Fourier transform method

In this section we apply the Fourier transform to find an approximation for φ as a distribution of sources $m(x_1)$ along x_1-axis [40], such that

$$\varphi(x_1, x_2, x_3) = \varphi(x_1, r) = -\frac{1}{4\pi}\int_{-\infty}^{\infty} \frac{m(y_1)dy_1}{\sqrt{(x_1 - y_1)^2 + r^2}}. \quad (6.3.1)$$

We show that when $r \longrightarrow 0$,

$$-\frac{1}{4\pi}\int_{-\infty}^{\infty} \frac{m(y_1)dy_1}{\sqrt{(x_1 - y_1)^2 + r^2}} = \frac{m(x_1)}{2\pi}\log r + f(x_1) + \mathcal{O}(r^2\log r), \quad (6.3.2)$$

where,

$$f(x_1) = -\frac{1}{4\pi}\int_{-\infty}^{\infty} m'(y_1)\,\text{sgn}\,(x_1 - y_1)\ln 2\,|x_1 - y_1|\,. \quad (6.3.3)$$

To prove (6.3.2) , we define

$$g(x_1) = \frac{1}{\sqrt{x_1^2 + r^2}},$$

and now (6.7.3) yields

$$g * m\,(x_1) = \int_{-\infty}^{\infty} m(y_1)g(x_1 - y_1)dy_1 = \int_{-\infty}^{\infty} \frac{m(y_1)dy_1}{\sqrt{(x_1 - y_1)^2 + r^2}}, \quad (6.3.4)$$

Thm. (6.7.2) implies that $F\,(g * m, \omega) = \hat{g}(\omega)\hat{m}(\omega)$.

But,

$$\begin{aligned}\hat{g}(\omega) &= \int_{-\infty}^{\infty}\frac{1}{\sqrt{u^2+r^2}}e^{-i\omega u}du = \int_{-\infty}^{\infty}\frac{\cos\omega u}{\sqrt{u^2+r^2}}du + i\int_{-\infty}^{\infty}\frac{\sin\omega u}{\sqrt{u^2+r^2}}du \\ &= 2\int_0^{\infty}\frac{\cos\omega u}{\sqrt{u^2+r^2}}du = 2\int_0^{\infty}\frac{\cos\omega rt}{\sqrt{1+t^2}}dt,\end{aligned}$$

comparing with (6.7.28) shows that

$$\hat{g}(\omega) = 2K_0(\omega r). \tag{6.3.5}$$

Combining (6.7.25) and (6.7.26) together yields that

$$K_0(z) = (\ln(\frac{2}{z}) - \gamma)\left(1 + \sum_{n=1}^{\infty}\frac{(\frac{1}{4}z^2)^n}{(n!)^2}\right) + \sum_{n=1}^{\infty}\sigma_n\frac{(\frac{1}{4}z^2)^n}{(n!)^2}, \tag{6.3.6}$$

where, $\sigma_n = \sum_{k=1}^{n}\frac{1}{k}$.

$K_0(z)$ is an analytic (holomorphic) function through the $z-$plane cut along the negative real axis [38], which guaranties [41] uniformly convergence of series in (6.3.6) and therefore can be integrated term by term [41]. Therefore the Fourier transform and its inverse can be applied term by term, so for any positive ω we would have following results:

$$\begin{aligned}K_0(\omega r) &= (\ln(\frac{2}{\omega r}) - \gamma)\left(1 + \sum_{n=1}^{\infty}\frac{(\frac{1}{4}\omega^2 r^2)^n}{(n!)^2}\right) + \sum_{n=1}^{\infty}\sigma_n\frac{(\frac{1}{4}\omega^2 r^2)^n}{(n!)^2} \\ &= \ln(\frac{2}{\omega r}) - \gamma + \sum_{n=1}^{\infty}(\ln(\frac{2}{\omega r}) - \gamma + \sigma_n)\frac{(\frac{1}{4}\omega^2 r^2)^n}{(n!)^2} \\ &= \sum_{n=0}^{\infty}\frac{(\frac{r^2}{4})^n}{(n!)^2}(\sigma_n - \ln r)\,\omega^{2n} + \sum_{n=0}^{\infty}\frac{(\frac{r^2}{4})^n}{(n!)^2}(\ln(\frac{2}{\omega}) - \gamma)\omega^{2n}.\end{aligned}$$

where $\sigma_0 = 0$.

Therefore,

$$\hat{g}(\omega)\hat{m}(\omega) = 2\sum_{n=0}^{\infty}\frac{(\frac{r^2}{4})^n}{(n!)^2}(\sigma_n - \ln r)\,\omega^{2n}\hat{m}(\omega) + 2\sum_{n=0}^{\infty}\frac{(\frac{r^2}{4})^n}{(n!)^2}(\ln(\frac{2}{\omega}) - \gamma)\omega^{2n}\hat{m}(\omega). \quad (6.3.7)$$

According to Thm.6.7.3

$$\omega^{2n}\hat{m}(\omega) = (-1)^n\,(i\omega)^{2n}\,\hat{m}(\omega) = (-1)^n F(\frac{d^{2n}m}{dx_1^{2n}}, \omega), \quad (6.3.8)$$

gives the inverse Fourier transform of terms $\omega^{2n}\hat{m}(\omega)$.

Also from Thm.6.7.3 we have

$$i\omega\hat{m}(\omega) = F\,(m', \omega)\,,$$

then applying Thm.6.7.2 gives

$$\begin{aligned}&\frac{1}{2\pi}\int_{-\infty}^{\infty}\hat{m}(\omega)\left(\ln\frac{2}{|\omega|} - \gamma\right)e^{i\omega x_1}d\omega = \\ &\frac{1}{2\pi}\int_{-\infty}^{\infty}((i\omega)\hat{m}(\omega))\left(\frac{-i}{\omega}\left(\ln\frac{2}{|\omega|} - \gamma\right)\right)e^{i\omega x_1}d\omega = (m' * f_1)\,(x_1),\end{aligned} \quad (6.3.9)$$

where f_1 is the inverse Fourier transform of $\left(\frac{-i}{\omega}\left(\ln\frac{2}{|\omega|} - \gamma\right)\right)$ and by applying (6.7.2) and using (6.7.7), (6.7.5) and (6.7.6) it can be found as follows:

$$\begin{aligned}f_1(x_1) &= \frac{1}{2\pi}\int_{-\infty}^{\infty}\frac{-i}{\omega}\left(\ln\frac{2}{|\omega|} - \gamma\right)e^{i\omega x_1}d\omega = \frac{1}{2\pi}\int_{-\infty}^{\infty}\frac{1}{\omega}\left(\ln\frac{2}{|\omega|} - \gamma\right)\sin(\omega x_1)d\omega \\ &= \frac{1}{2\pi}\int_{-\infty}^{\infty}\frac{1}{\omega}(\ln 2 - \gamma)\sin(\omega x_1)d\omega - \frac{1}{2\pi}\int_{-\infty}^{\infty}\frac{\ln|\omega|}{\omega}\sin(\omega x_1)d\omega \\ &= \frac{1}{\pi}\int_{0}^{\infty}\frac{1}{\omega}(\ln 2 - \gamma)\sin(\omega x_1)d\omega - \frac{1}{\pi}\int_{0}^{\infty}\frac{\ln\omega}{\omega}\sin(\omega x_1)d\omega \\ &= \frac{1}{\pi}\left(\frac{\pi}{2}\operatorname{sgn}(x_1)(\ln 2 - \gamma)\right) - \frac{1}{\pi}\left(\operatorname{sgn}(x_1)\left(-\frac{\pi}{2}\gamma - \frac{\pi}{2}(\ln|x_1|)\right)\right) \\ &= \frac{1}{2}\operatorname{sgn}(x_1)\ln(2|x_1|),\end{aligned}$$

(6.3.10)

and hence,

$$(m' * f_1)(x_1) = \frac{1}{2}\int_{-\infty}^{\infty}m'(y_1)\operatorname{sgn}(x_1 - y_1)\ln(2|x_1 - y_1|)dy_1. \quad (6.3.11)$$

Now let us define

$$f(x_1) = -\frac{1}{2\pi}(m' * f_1)(x_1). \tag{6.3.12}$$

Now we find the inverse transform of the terms

$$(\ln(\frac{2}{\omega}) - \gamma)\omega^{2n}\hat{m}(\omega).$$

Rewriting (6.3.7) by (6.3.8), and using Thm(6.7.2) will give

$$(-\frac{1}{4\pi})(\ln(\frac{2}{\omega}) - \gamma)\omega^{2n}\hat{m}(\omega) = (-1)^n F(\frac{d^{2n}f}{dx_1^{2n}}, \omega). \tag{6.3.13}$$

Eventually

$$\begin{aligned} -\frac{1}{4\pi}\int_{-\infty}^{\infty}\frac{m(y_1)dy_1}{\sqrt{(x_1-y_1)^2+r^2}} &= -\frac{1}{4\pi}(g * m)(x_1) \\ &= \sum_{n=0}^{\infty}\frac{(-1)^n(\frac{r^2}{4})^n}{(n!)^2}\frac{d^{2n}}{dx_1^{2n}}\left[\frac{1}{2\pi}(\ln r - \sigma_n)\, m(x_1) + f(x_1)\right], \end{aligned} \tag{6.3.14}$$

and

$$f(x_1) = -\frac{1}{4\pi}\int_{-\infty}^{\infty} m'(y_1)\,\mathrm{sgn}\,(x_1 - y_1)\ln(2\,|x_1 - y_1|)dy_1. \tag{6.3.15}$$

So (6.3.14) implies (6.3.2) which is the derived result .

6.4 Proceeding by splitting method

Tuck [40] has suggested splitting method to find an asymptotic for the potential flow φ. But we follow quasi-potential flow (logarithmic distribution) rather than 3-D dipole distribution with the same source $m(x)$. It is expected this method and Fourier transform method give same results over the infinite line since,

$$\frac{\partial}{\partial x_1}\int_{x_a}^{x_b} m(y_1)\ln(R_1 - x_{11})dy_1 = -\int_{x_a}^{x_b} m(y_1)\frac{1}{R_1}dy_1, \tag{6.4.1}$$

where, $R_1 = \sqrt{x_{11}^2 + r^2}$, $x_{11} = x_1 - y_1$. We consider x_1 as a point in the integrating domain and therefore the integral

$$I = \int_{x_a}^{x_b} m(y_1) \ln(R_1 - x_{11}) dy_1 \tag{6.4.2}$$

will contain a semi infinite line singularity. To evaluate I, we split the integral into four integrals

$$I_1 = \int_{x_a}^{x_1-\delta} m(y_1) \left\{ \ln(R_1 - x_{11}) - \ln r^2 \right\} dy_1,$$

$$I_2 = \int_{x_a}^{x_1-\delta} m(y_1) 2 \ln r dy_1,$$

$$I_3 = \int_{x_1-\delta}^{x_1+\delta} m(y_1) \ln(R_1 - x_{11}) dy_1,$$

$$I_4 = \int_{x_1+\delta}^{x_b} m(y_1) \ln(R_1 - x_{11}) dy_1.$$

As it can be seen in the first integral by adding $-\ln r^2$ to the integrand we intend to remove the singularity but still this problem remains around the lower bound of I_3, and fortunately the other two integrals I_2 and I_4 are definite. We calculate each integral in turn.

I_1 :

Firstly we show the singularity in the integrand is removable.

Consider

$$g(x, r) = \ln(\sqrt{x^2 + r^2} - x) - \ln r^2. \tag{6.4.3}$$

According to

$$(1+t)^{\frac{1}{2}} = 1 + \sum_{n=1}^{\infty} \frac{(-1)^{n-1}(2n)!}{2^{2n}(2n-1)(n!)^2} t^n, \tag{6.4.4}$$

and assuming $x \gg r > 0$,

$$\begin{aligned} g(x,r) &= \ln\left(\frac{(\sqrt{x^2+r^2}-x)}{r^2}\right) = \ln\left(\frac{1}{r^2}(x(1+\frac{r^2}{x^2})^{\frac{1}{2}}-x)\right) \\ &= \ln\left(\sum_{n=1}^{\infty}\frac{(-1)^{n-1}(2n)!}{2^{2n}(2n-1)(n!)^2}\frac{r^{2n-2}}{x^{2n-1}}\right) \\ &= -\ln 2x + \ln(\sum_{n=1}^{\infty}\frac{(-1)^{n-1}(2n)!}{2^{2n-1}(2n-1)(n!)^2}\frac{r^{2n-2}}{x^{2n-2}}), \end{aligned}$$

therefore,

$$g(x,0) = \lim_{r\to 0} g(x,r) = -\ln 2x. \tag{6.4.5}$$

This shows that g has a removable singularity as r tends to 0 and hence it can be expressed by a power series in terms of r.

Since,

$$\frac{\partial}{\partial x_{11}} g(x_{11}, r) = -\frac{1}{R_1} = -\frac{1}{x_{11}}(1+\frac{r^2}{x_{11}^2})^{-\frac{1}{2}}. \tag{6.4.6}$$

Since

$$(1+t)^{-\frac{1}{2}} = 1 + \sum_{n=1}^{\infty}\frac{(-1)^n(2n)!}{2^{2n}(n!)^2}t^n. \tag{6.4.7}$$

So applying (6.4.7) to (6.4.6) yields

$$\frac{\partial}{\partial x_{11}} g(x_{11}, r) = -\frac{1}{x_{11}}\left(1+\sum_{n=1}^{\infty}\frac{(-1)^n(2n)!}{2^{2n}(n!)^2}\frac{r^{2n}}{x_{11}^{2n}}\right).$$

Integrating with respect to x_{11} gives

$$\begin{aligned} g(x_{11}, r) &= \int \frac{\partial}{\partial x_{11}} g(x_{11}, r)dx_{11} + h(r) \\ &= \int(-\frac{1}{x_{11}} - \sum_{n=1}^{\infty}\frac{(-1)^n(2n)!}{2^{2n}(n!)^2}\frac{r^{2n}}{x_{11}^{2n+1}})dx_{11} + h(r) \\ &= -\ln x_{11} + \sum_{n=1}^{\infty}\frac{(-1)^n(2n)!}{(2n)2^{2n}(n!)^2}\frac{r^{2n}}{x_{11}^{2n}} + h(r). \end{aligned}$$

But $g(x_{11}, 0) = -\ln 2x_{11}$ and so

$$g(x_{11}, r) = -\ln 2x_{11} + \sum_{n=1}^{\infty} \frac{(-1)^n (2n)!}{(2n)2^{2n}(n!)^2} \frac{r^{2n}}{x_{11}^{2n}}. \tag{6.4.8}$$

However from (6.4.8),

$$\frac{\partial^{2n}}{\partial x_{11}^{2n}} g(x_{11}, 0) = \frac{(2n-1)!}{x^{2n}} \quad \text{for } n \geq 1. \tag{6.4.9}$$

and so

$$g(x_{11}, r) = \sum_{n=0}^{\infty} \frac{(-1)^n r^{2n}}{2^{2n}(n!)^2} \frac{\partial^{2n}}{\partial x_{11}^{2n}} g(x_{11}, 0). \tag{6.4.10}$$

we now use the Leibnitz rule for differentiation, given below:

If $\varphi(\alpha) = \int_{u_1(\alpha)}^{u_2(\alpha)} f(x, \alpha) dx$, then,

$$\frac{d\varphi}{d\alpha} = \int_{u_1(\alpha)}^{u_2(\alpha)} \frac{\partial f(x, \alpha)}{\partial \alpha} dx + f(u_2(\alpha), \alpha) \frac{du_2(\alpha)}{d\alpha} - f(u_1(\alpha), \alpha) \frac{du_1(\alpha)}{d\alpha}. \tag{6.4.11}$$

Now using Leibnitz rule (6.4.11) gives

$$\frac{\partial}{\partial x_1} \int_{x_a}^{x_1 - \delta} m(y_1) g(x_{11}, 0) dy_1 = m(x_1 - \delta)(-\ln 2\delta) + \int_{x_a}^{x_1 - \delta} m(y_1) \frac{\partial}{\partial x_1} g(x_{11}, 0) dy_1,$$

$$\frac{\partial^2}{\partial x_1^2} \int_{x_a}^{x_1 - \delta} m(y_1) g(x_{11}, 0) dy_1 = m'(x_1 - \delta)(-\ln 2\delta) + m(x_1 - \delta)(\tfrac{(-1)}{\delta})$$

$$+ \int_{x_a}^{x_1 - \delta} m(y_1) \frac{\partial^2}{\partial x_1^2} g(x_{11}, 0) dy_1,$$

$$\frac{\partial^3}{\partial x_1^3} \int_{x_a}^{x_1 - \delta} m(y_1) g(x_{11}, 0) dy_1 = m''(x_1 - \delta)(-\ln 2\delta) + m'(x_1 - \delta)(\tfrac{(-1)}{\delta}) + m(x_1 - \delta)(\tfrac{(-1)^2}{\delta^2})$$

$$+ \int_{x_a}^{x_1 - \delta} m(y_1) \frac{\partial^3}{\partial x_1^3} g(x_{11}, 0) dy_1,$$

and applying induction gives

$$\begin{aligned} \int_{x_a}^{x_1 - \delta} m(y_1) \frac{\partial^{2n}}{\partial x_1^{2n}} g(x_{11}, 0) dy_1 = \frac{\partial^{2n}}{\partial x_1^{2n}} \int_{x_a}^{x_1 - \delta} m(y_1) g(x_{11}, 0) dy_1 + \\ m^{(2n-1)}(x_1 - \delta)(\ln 2\delta) - \sum_{k=1}^{2n-1} \frac{(-1)^k (k-1)! m^{(2n-1-k)}(x_1 - \delta)}{\delta^k}, \end{aligned} \tag{6.4.12}$$

where we denoted $m^k(x_1-\delta)=\frac{\partial^k}{\partial x_1^k}m(x_1-\delta)$.

From (6.4.10) and (6.4.12) and applying Taylor expansion for $m^{(2n-1)}(x_1-\delta)$ and $m^{(2n-1-k)}(x_1-\delta)$ about x_1 we deduce that

$$
\begin{aligned}
I_1 \;=\; & \int_{x_a}^{x_1-\delta} m(y_1)g(x_{11},r)dy_1 = \sum_{n=0}^{\infty}\frac{(-1)^n r^{2n}}{2^{2n}(n!)^2}\frac{\partial^{2n}}{\partial x_1^{2n}}\int_{x_a}^{x_1-\delta} m(y_1)g(x_{11},0)dy_1 \\
& +(\ln 2\delta)\sum_{n=1}^{\infty}\frac{(-1)^n r^{2n}M^{(2n)}(x_1)}{2^{2n}(n!)^2}+(\ln 2\delta)\sum_{n=1}^{\infty}\frac{(-1)^n r^{2n}}{2^{2n}(n!)^2}\sum_{k=1}^{\infty}\frac{(-1)^k M^{(2n+k)}(x_1)\delta^k}{(k!)} \\
& -\sum_{n=1}^{\infty}\frac{(-1)^n r^{2n}}{2^{2n}(n!)^2}\sum_{k=1}^{2n-1}\frac{(-1)^k(k-1)!M^{(2n-k)}(x_1)}{\delta^k} \\
& -\sum_{n=1}^{\infty}\frac{(-1)^n r^{2n}}{2^{2n}(n!)^2}\sum_{k=1}^{2n-1}\frac{(-1)^k(k-1)!}{\delta^k}\sum_{j=1}^{\infty}\frac{(-1)^j M^{(2n-k+j)}(x_1)\delta^j}{(j!)}.
\end{aligned}
$$

I_4 :

Since,

$$\ln(R_1-x_{11})=-g(-x_{11},r)=\sum_{n=0}^{\infty}\frac{(-1)^{n+1}r^{2n}}{2^{2n}(n!)^2}\frac{\partial^{2n}}{\partial x_{11}^{2n}}g(-x_{11},0),\ x_{11}<0,$$

and $-g(-x_{11},0)=\ln(-2x_{11})$ therefore as we used Leibnitz rule for I_1 here we have

$$-g(-x_{11},0)=\ln 2(y_1-x_1),$$

and therefore,

$$\frac{\partial}{\partial x_1}\int_{x_1+\delta}^{x_b} m(y_1)\left(-g(-x_{11},0)\right)dy_1=-m(x_1+\delta)(\ln 2\delta)+\int_{x_1+\delta}^{x_b} m(y_1)\frac{\partial}{\partial x_1}\left(-g(-x_{11},0)\right)dy_1,$$

$$\frac{\partial^2}{\partial x_1^2}\int_{x_1+\delta}^{x_b} m(y_1)\left(-g(-x_{11},0)\right)dy_1=-m'(x_1+\delta)(\ln 2\delta)-m(x_1+\delta)(\tfrac{(-1)}{\delta})$$

$$+\int_{x_1+\delta}^{x_b} m(y_1)\frac{\partial^2}{\partial x_1^2}\left(-g(-x_{11},0)\right)dy_1,$$

$$\frac{\partial^3}{\partial x_1^3}\int_{x_1+\delta}^{x_b} m(y_1)\left(-g(-x_{11},0)\right)dy_1=-m''(x_1+\delta)(\ln 2\delta)-m'(x_1+\delta)(\tfrac{-1}{\delta})-m(x_1+\delta)(\tfrac{-1}{\delta^2})$$

$$+\int_{x_1+\delta}^{x_b} m(y_1)\frac{\partial^3}{\partial x_1^3}\left(-g(-x_{11},0)\right)dy_1.$$

Again applying induction gives

$$\int_{x_1+\delta}^{x_b} m(y_1)\frac{\partial^{2n}}{\partial x_1^{2n}}\left(-g(-x_{11},0)\right)dy_1 = \frac{\partial^{2n}}{\partial x_1^{2n}}\int_{x_1+\delta}^{x_b} m(y_1)\left(-g(-x_{11},0)\right)dy_1 + m^{(2n-1)}(x_1+\delta)(\ln 2\delta) - \sum_{k=1}^{2n-1}\frac{(k-1)!m^{(2n-1-k)}(x_1+\delta)}{\delta^k}.$$

Using Taylor expansion for $m^{(2n-1)}(x_1+\delta)$ and $m^{(2n-1-k)}(x_1+\delta)$ about x_1 gives

$$\begin{aligned} I_4 &= \sum_{n=0}^{\infty}\frac{(-1)^n r^{2n}}{2^{2n}(n!)^2}\int_{x_1+\delta}^{x_b} m(y_1)\frac{\partial^{2n}}{\partial x_1^{2n}}\left(-g(-x_{11},0)\right)dy_1 = \\ &\sum_{n=0}^{\infty}\frac{(-1)^n r^{2n}}{2^{2n}(n!)^2}\frac{\partial^{2n}}{\partial x_1^{2n}}\int_{x_1+\delta}^{x_b} m(y_1)\left(-g(-x_{11},0)\right)dy_1 \\ &+(\ln 2\delta)\sum_{n=1}^{\infty}\frac{(-1)^n r^{2n}M^{(2n)}(x_1)}{2^{2n}(n!)^2} + (\ln 2\delta)\sum_{n=1}^{\infty}\frac{(-1)^n r^{2n}}{2^{2n}(n!)^2}\left[\sum_{k=1}^{\infty}\frac{M^{(2n+k)}(x_1)\delta^k}{k!}\right] \\ &-\sum_{n=1}^{\infty}\frac{(-1)^n r^{2n}}{2^{2n}(n!)^2}\sum_{k=1}^{2n-1}\frac{(k-1)!M^{(2n-k)}(x_1)}{\delta^k} \\ &-\sum_{n=1}^{\infty}\frac{(-1)^n r^{2n}}{2^{2n}(n!)^2}\sum_{k=1}^{2n-1}\frac{(k-1)!}{\delta^k}\sum_{j=1}^{\infty}\frac{M^{(2n-k+j)}(x_1)\delta^j}{j!}. \end{aligned}$$

I_2 :

Computation of I_2 is straight forward such that

$$\begin{aligned} I_2 &= 2\ln r\int_{x_a}^{x_1-\delta} m(y_1)dy_1 = 2\{M(x_1-\delta) - M(x_a)\}\ln r \\ &= 2M(x_1)\ln r - 2M(x_a)\ln r + 2\ln r\sum_{n=1}^{\infty}\frac{(-1)^n M^{(n)}(x_1)}{(n)!}\delta^n, \end{aligned}$$

where we have supposed $\frac{d}{dx_1}M(x_1) = m(x_1)$.

I_3 :

Computation I_3 is involved, and relies as use of the Taylor series expansion, such that

$I_3 = \int_{x_1-\delta}^{x_1+\delta} m(y_1)\ln(R_1 - x_{11})dy_1$

$= \int_{-\delta}^{+\delta} m(x_1 - x_{11}) \ln(\sqrt{x_{11}^2 + r^2} - x_{11}) dx_{11}$

$= \sum_{n=0}^{\infty} \frac{(-1)^n m^n(x_1)}{n!} \int_{-\delta}^{+\delta} x_{11}^n \ln(\sqrt{x_{11}^2 + r^2} - x_{11}) dx_{11} =$

$\sum_{n=0}^{\infty} \frac{m^{2n}(x_1)}{(2n)!} \int_{-\delta}^{+\delta} x_{11}^{2n} \ln(\sqrt{x_{11}^2 + r^2} - x_{11}) dx_{11}$

$- \sum_{n=1}^{\infty} \frac{m^{2n-1}(x_1)}{(2n-1)!} \int_{-\delta}^{+\delta} x_{11}^{2n-1} \ln(\sqrt{x_{11}^2 + r^2} - x_{11}) dx_{11}.$

Denote

$I_3^{even} = \sum_{n=0}^{\infty} \frac{m^{2n}(x_1)}{(2n)!} \int_{-\delta}^{+\delta} x_{11}^{2n} \ln(\sqrt{x_{11}^2 + r^2} - x_{11}) dx_{11},$

$I_3^{odd} = \sum_{n=1}^{\infty} \frac{m^{2n-1}(x_1)}{(2n-1)!} \int_{-\delta}^{+\delta} x_{11}^{2n-1} \ln(\sqrt{x_{11}^2 + r^2} - x_{11}) dx_{11},$

such that

$$I_3 = I_3^{even} - I_3^{odd}.$$

I_3^{even} for $n \geq 0$:

$\int_{-\delta}^{+\delta} x_{11}^{2n} \ln(\sqrt{x_{11}^2 + r^2} - x_{11}) dx_{11} =$

$\frac{\delta^{2n+1}}{2n+1} \ln\left(\sqrt{\delta^2 + r^2} - \delta\right) - \frac{(-\delta)^{2n+1}}{2n+1} \ln\left(\sqrt{\delta^2 + r^2} + \delta\right)$

$+ \frac{1}{2n+1} \int_{-\delta}^{\delta} \frac{x_{11}^{2n+1} dx_{11}}{\sqrt{x_{11}^2 + r^2}} = \frac{2\delta^{2n+1}}{2n+1} \ln r.$

So,

$I_3^{even} = \sum_{n=0}^{\infty} \frac{m^{2n}(x_1)}{(2n)!} \frac{2\delta^{2n+1}}{2n+1} \ln r = (2 \ln r) \sum_{n=0}^{\infty} \frac{m^{2n}(x_1)}{(2n+1)!} \delta^{2n+1},$

or,

$$I_3^{even} = (2 \ln r) \sum_{n=0}^{\infty} \frac{M^{2n+1}(x_1)}{(2n+1)!} \delta^{2n+1}.$$

I_3^{odd} for $n \geq 1$:

Since

$$\ln\left(\sqrt{\delta^2+r^2}-\delta\right)-\ln\left(\sqrt{\delta^2+r^2}+\delta\right)=2\ln\left(\sqrt{\delta^2+r^2}-\delta\right)-2\ln r=2g(\delta,r)+2\ln r,$$

then

$$\int_{-\delta}^{+\delta} x_{11}^{2n-1}\ln(\sqrt{x_{11}^2+r^2}-x_{11})dx_{11}=\tfrac{\delta^{2n}}{2n}\left[2g(\delta,r)+2\ln r\right]+\tfrac{1}{n}\int_0^{\delta}\tfrac{x_{11}^{2n}}{\sqrt{x_{11}^2+r^2}}\,dx_{11},$$

and

$$\int_0^{\delta}\tfrac{x_{11}^{2n}}{\sqrt{x_{11}^2+r^2}}\,dx_{11}=\int_0^{\tan^{-1}(\frac{\delta}{r})}\tfrac{r^{2n}\tan^{2n}\theta}{\sqrt{r^2\tan^2\theta+r^2}}r\sec^2\theta\,d\theta$$

$$=r^{2n}\int_0^{\tan^{-1}(\frac{\delta}{r})}\tfrac{\tan^{2n}\theta}{r\sec\theta}r\sec^2\theta\,d\theta=r^{2n}\int_0^{\tan^{-1}(\frac{\delta}{r})}\tan^{2n}\theta\sec\theta\,d\theta.$$

denote $\mathbf{J}_n=\int_0^{\tan^{-1}(\frac{\delta}{r})}\tan^{2n}\theta\sec\theta\,d\theta$ so,

$$\mathbf{J}_n=\int_0^{\tan^{-1}(\frac{\delta}{r})}\tan^{2n-1}\theta\tan\theta\sec\theta\,d\theta$$

$$=\left[\tan^{2n-1}\theta\sec\theta\right]_0^{\tan^{-1}(\frac{\delta}{r})}-(2n-1)\int_0^{\tan^{-1}(\frac{\delta}{r})}\tan^{2(n-1)}\theta(1+\tan^2\theta)\sec\theta\,d\theta$$

$$=(\tfrac{\delta}{r})^{2n}\sqrt{1+\tfrac{r^2}{\delta^2}}-(2n-1)(\mathbf{J}_n+\mathbf{J}_{n-1}),$$

and then,

$$\mathbf{J}_n=(\tfrac{\delta}{r})^{2n}\sqrt{1+\tfrac{r^2}{\delta^2}}-(2n-1)(\mathbf{J}_n+\mathbf{J}_{n-1}),$$

or

$$\mathbf{J}_n=\tfrac{1}{(2n)}(\tfrac{\delta}{r})^{2n}\sqrt{1+\tfrac{r^2}{\delta^2}}-(\tfrac{2n-1}{2n})\mathbf{J}_{n-1}.$$

Let $a_n=\frac{1}{(2n)}(\frac{\delta}{r})^{2n}\sqrt{1+\frac{r^2}{\delta^2}}$, and $b_n=-(\frac{2n-1}{2n})$, so, $\mathbf{J}_n=a_n+b_n\mathbf{J}_{n-1}$,

giving $I_3^{odd}=\sum\limits_{n=1}^{\infty}\frac{m^{2n-1}(x_1)}{(2n-1)!}\left[\frac{\delta^{2n}}{2n}\left[2g(\delta,r)+2\ln r\right]+\frac{1}{n}r^{2n}\mathbf{J}_n\right].$

By induction,

$$\mathbf{J}_n = \left(a_n + b_n\left(a_{n-1} + b_{n-1}\mathbf{J}_{n-2}\right)\right)$$

$$= \left(a_n + b_n a_{n-1} + b_n b_{n-1}\left(a_{n-2} + b_{n-2}\mathbf{J}_{n-3}\right)\right)$$

$$= a_n + b_n a_{n-1} + b_n b_{n-1} a_{n-2} + b_n b_{n-1} b_{n-2}\mathbf{J}_{n-3}$$

$$= \ldots$$

$$= \sum_{k=1}^{n} \frac{(b_n)^! a_k}{(b_k)^!} + (b_n)^! \, \mathbf{J}_0,$$

where $(b_k)^! = b_1 b_2 \ldots b_k = \frac{(-1)^k (2k)!}{2^{2k}(k!)^2}$ and

$$\mathbf{J}_0 = \int_0^{\tan^{-1}\left(\frac{\delta}{r}\right)} \sec\theta \, d\theta = \ln\left(\sec\theta + \tan\theta\right)\Big|_0^{\tan^{-1}\left(\frac{\delta}{r}\right)} = \ln\left(\sqrt{1 + \frac{\delta^2}{r^2}} + \frac{\delta}{r}\right) = -g(\delta, r) - \ln r.$$

Hence,

$$\mathbf{J}_n = \sum_{k=1}^{n} \frac{(-1)^{n-k}(2n)!(k!)^2}{2^{2n-2k}(n!)^2(2k)!} \frac{1}{(2k)} \left(\frac{\delta}{r}\right)^{2k} \left(\sqrt{1 + \frac{r^2}{\delta^2}}\right) + \frac{(-1)^n (2n)!}{2^{2n}(n!)^2}\left(-g(\delta, r) - \ln r\right).$$

Eventually applying the Taylor series expansion (6.4.4) to $\sqrt{1 + \frac{r^2}{\delta^2}}$ such that

$$\sqrt{1 + \frac{r^2}{\delta^2}} = 1 + \sum_{j=1}^{\infty} \frac{(-1)^{j-1}(2j)!}{2^{2j}(2j-1)(j!)^2} \frac{r^{2j}}{\delta^{2j}},$$

and replacing $g(\delta, r)$ from (6.4.8) gives

$$I_3^{odd} = \sum_{n=1}^{\infty} \frac{m^{2n-1}(x_1)}{(2n-1)!} \frac{\delta^{2n}}{2n} \left[2g(\delta, r) + 2\ln r\right] + \sum_{n=1}^{\infty} \frac{m^{2n-1}(x_1)}{(2n-1)!} \frac{1}{n} r^{2n} \mathbf{J}_n$$

$$= 2\sum_{n=1}^{\infty} \frac{m^{2n-1}(x_1)}{(2n-1)!} \frac{\delta^{2n}}{2n} \left[-\ln 2\delta + \sum_{k=1}^{\infty} \frac{(-1)^k (2k)!}{(2k)2^{2k}(k!)^2} \frac{r^{2k}}{\delta^{2k}} + \ln r\right]$$

$$+ \sum_{n=1}^{\infty} \frac{m^{2n-1}(x_1)}{(2n-1)!} \frac{1}{n} r^{2n} \left\{\sum_{k=1}^{n} \frac{(-1)^{n-k}(2n)!(k!)^2}{2^{2n-2k}(n!)^2(2k)!} \frac{1}{(2k)} \left(\frac{\delta}{r}\right)^{2k} \left(1 + \sum_{j=1}^{\infty} \frac{(-1)^{j-1}(2j)!}{2^{2j}(2j-1)(j!)^2} \frac{r^{2j}}{\delta^{2j}}\right)\right\}$$

$$+ \sum_{n=1}^{\infty} \frac{m^{2n-1}(x_1)}{(2n-1)!} \frac{1}{n} r^{2n} \left\{\frac{(-1)^n (2n)!}{2^{2n}(n!)^2} \left(\ln 2\delta - \sum_{k=1}^{\infty} \frac{(-1)^k (2k)!}{(2k)2^{2k}(k!)^2} \frac{r^{2k}}{\delta^{2k}} - \ln r\right)\right\},$$

or,

$$
\begin{aligned}
I_3^{odd} &= 2\,(\ln r)\sum_{n=1}^{\infty}\frac{M^{2n}(x_1)\delta^{2n}}{(2n)!} - 2\,(\ln 2\delta)\sum_{n=1}^{\infty}\frac{M^{2n}(x_1)\delta^{2n}}{(2n)!} \\
&+2\sum_{n=1}^{\infty}\frac{M^{2n}(x_1)\delta^{2n}}{(2n)!}\left(\sum_{k=1}^{\infty}\frac{(-1)^k(2k)!}{(2k)2^{2k}(k!)^2}\frac{r^{2k}}{\delta^{2k}}\right) \\
&+2\sum_{n=1}^{\infty}\frac{r^{2n}M^{2n}(x_1)}{(n!)^2}\left(\sum_{k=1}^{n}\frac{(-1)^{n-k}(k!)^2}{2^{2n-2k}(2k)!}\frac{1}{(2k)}\frac{\delta^{2k}}{r^{2k}}\right) \\
&+2\sum_{n=1}^{\infty}\frac{r^{2n}M^{2n}(x_1)}{(n!)^2}\left\{\sum_{k=1}^{n}\frac{(-1)^{n-k}(k!)^2}{2^{2n-2k}(2k)!}\frac{1}{(2k)}\frac{\delta^{2k}}{r^{2k}}\left(\sum_{j=1}^{\infty}\frac{(-1)^{j-1}(2j)!}{2^{2j}(2j-1)(j!)^2}\frac{r^{2j}}{\delta^{2j}}\right)\right\} \\
&-2\sum_{n=1}^{\infty}\frac{(-1)^n r^{2n}M^{2n}(x_1)}{2^{2n}(n!)^2}\left(\sum_{k=1}^{\infty}\frac{(-1)^k(2k)!}{(2k)2^{2k}(k!)^2}\frac{r^{2k}}{\delta^{2k}}\right) \\
&+2\,(\ln 2\delta)\sum_{n=1}^{\infty}\frac{(-1)^n r^{2n}M^{2n}(x_1)}{2^{2n}(n!)^2} - \sum_{n=1}^{\infty}\frac{(-1)^n r^{2n}M^{2n}(x_1)}{2^{2n}(n!)^2}\,(2\ln r)\,.
\end{aligned}
$$

Then

$$
\begin{aligned}
I_3 &= 2(\ln r)\sum_{n=0}^{\infty}\frac{M^{2n+1}(x_1)}{(2n+1)!}\delta^{2n+1} - 2\,(\ln r)\sum_{n=1}^{\infty}\frac{M^{2n}(x_1)\delta^{2n}}{(2n)!} + 2\,(\ln 2\delta)\sum_{n=1}^{\infty}\frac{M^{2n}(x_1)\delta^{2n}}{(2n)!} \\
&-2\sum_{n=1}^{\infty}\frac{M^{2n}(x_1)\delta^{2n}}{(2n)!}\left(\sum_{k=1}^{\infty}\frac{(-1)^k(2k)!}{(2k)2^{2k}(k!)^2}\frac{r^{2k}}{\delta^{2k}}\right) \\
&-2\sum_{n=1}^{\infty}\frac{r^{2n}M^{2n}(x_1)}{(n!)^2}\left(\sum_{k=1}^{n}\frac{(-1)^{n-k}(k!)^2}{2^{2n-2k}(2k)!}\frac{1}{(2k)}\frac{\delta^{2k}}{r^{2k}}\right) \\
&-2\sum_{n=1}^{\infty}\frac{r^{2n}M^{2n}(x_1)}{(n!)^2}\left\{\sum_{k=1}^{n}\frac{(-1)^{n-k}(k!)^2}{2^{2n-2k}(2k)!}\frac{1}{(2k)}\frac{\delta^{2k}}{r^{2k}}\left(\sum_{j=1}^{\infty}\frac{(-1)^{j-1}(2j)!}{2^{2j}(2j-1)(j!)^2}\frac{r^{2j}}{\delta^{2j}}\right)\right\} \\
&+2\sum_{n=1}^{\infty}\frac{(-1)^n r^{2n}M^{2n}(x_1)}{2^{2n}(n!)^2}\left(\sum_{k=1}^{\infty}\frac{(-1)^k(2k)!}{(2k)2^{2k}(k!)^2}\frac{r^{2k}}{\delta^{2k}}\right) \\
&-2\,(\ln 2\delta)\sum_{n=1}^{\infty}\frac{(-1)^n r^{2n}M^{2n}(x_1)}{2^{2n}(n!)^2} + \sum_{n=1}^{\infty}\frac{(-1)^n r^{2n}M^{2n}(x_1)}{2^{2n}(n!)^2}\,(2\ln r)\,.
\end{aligned}
$$

Now bring all four integrals together and pulling out all those terms independent of δ gives:

$$
\sum_{n=1}^{\infty}\frac{M^{2n}(x_1)\delta^{2n}}{(2n)!}\sum_{k=1}^{\infty}\frac{(-1)^k(2k)!}{(2k)2^{2k}(k!)^2}\frac{r^{2k}}{\delta^{2k}} = \sum_{n=1}^{\infty}\frac{(-1)^n r^{2n}M^{2n}(x_1)}{2^{2n}(n!)^2}\frac{1}{(2n)} + \sum_{n=1}^{\infty}\frac{M^{2n}(x_1)\delta^{2n}}{(2n)!}\sum_{k=1,k\neq n}^{\infty}\frac{(-1)^k(2k)!}{(2k)2^{2k}(k!)^2}\frac{r^{2k}}{\delta^{2k}},
$$

$$\sum_{n=1}^{\infty} \frac{r^{2n} M^{2n}(x_1)}{(n!)^2} \sum_{k=1}^{n} \frac{(-1)^{n-k}(k!)^2}{2^{2n-2k}(2k)!} \frac{1}{(2k)} \frac{\delta^{2k}}{r^{2k}} \sum_{j=1}^{\infty} \frac{(-1)^{j-1}(2j)!}{2^{2j}(2j-1)(j!)^2} \frac{r^{2j}}{\delta^{2j}} =$$

$$\sum_{n=1}^{\infty} \frac{(-1)^n r^{2n} M^{2n}(x_1)}{2^{2n}(n!)^2} \sum_{k=1}^{n} \frac{-1}{(2k)(2k-1)} + \sum_{n=1}^{\infty} \frac{r^{2n} M^{2n}(x_1)}{(n!)^2} \sum_{k=1}^{n} \frac{(-1)^{n-k}(k!)^2}{2^{2n-2k}(2k)!} \frac{1}{(2k)} \frac{\delta^{2k}}{r^{2k}} \sum_{j=1, j\neq k}^{\infty} \frac{(-1)^{j-1}(2j)!}{2^{2j}(2j-1)(j!)^2} \frac{r^{2j}}{\delta^{2j}},$$

$$\sum_{n=1}^{\infty} \frac{(-1)^n r^{2n}}{2^{2n}(n!)^2} \sum_{k=1}^{2n-1} \frac{(-1)^k (k-1)!}{\delta^k} \sum_{j=1}^{\infty} \frac{(-1)^j M^{(2n-k+j)}(x_1)\delta^j}{(j!)} =$$

$$\sum_{n=1}^{\infty} \frac{(-1)^n r^{2n} M^{(2n)}(x_1)}{2^{2n}(n!)^2} \sum_{k=1}^{2n-1} \frac{1}{k} + \sum_{n=1}^{\infty} \frac{(-1)^n r^{2n}}{2^{2n}(n!)^2} \sum_{k=1}^{2n-1} \frac{(-1)^k (k-1)!}{\delta^k} \sum_{j=1, j\neq k}^{\infty} \frac{(-1)^j M^{(2n-k+j)}(x_1)\delta^j}{(j!)},$$

$$\sum_{n=1}^{\infty} \frac{(-1)^n r^{2n}}{2^{2n}(n!)^2} \sum_{k=1}^{2n-1} \frac{(k-1)!}{\delta^k} \sum_{j=1}^{\infty} \frac{M^{(2n-k+j)}(x_1)\delta^j}{j!} =$$

$$\sum_{n=1}^{\infty} \frac{(-1)^n r^{2n} M^{(2n)}(x_1)}{2^{2n}(n!)^2} \sum_{k=1}^{2n-1} \frac{1}{k} + \sum_{n=1}^{\infty} \frac{(-1)^n r^{2n}}{2^{2n}(n!)^2} \sum_{k=1}^{2n-1} \frac{(k-1)!}{\delta^k} \sum_{j=1, j\neq k}^{\infty} \frac{M^{(2n-k+j)}(x_1)\delta^j}{j!},$$

so,

$$I = I_1 + I_2 + I_3 + I_4 = 2M(x_1)\ln r + \sum_{n=1}^{\infty} \frac{(-1)^n r^{2n} M^{2n}(x_1)}{2^{2n}(n!)^2} (2\ln r) +$$

$$\sum_{n=0}^{\infty} \frac{(-1)^n r^{2n}}{2^{2n}(n!)^2} \frac{\partial^{2n}}{\partial x_1^{2n}} \left[\int_{x_a}^{x_1-\delta} m(y_1) g(x_{11}, 0) dy_1 + \int_{x_1+\delta}^{x_b} m(y_1) \left(-g(-x_{11}, 0)\right) dy_1 \right]$$

$$+(\ln 2\delta) \sum_{n=1}^{\infty} \frac{(-1)^n r^{2n} M^{(2n)}(x_1)}{2^{2n}(n!)^2} - 2(\ln 2\delta) \sum_{n=1}^{\infty} \frac{(-1)^n r^{2n} M^{2n}(x_1)}{2^{2n}(n!)^2} + (\ln 2\delta) \sum_{n=1}^{\infty} \frac{(-1)^n r^{2n} M^{(2n)}(x_1)}{2^{2n}(n!)^2}$$

$$+2(\ln r) \sum_{n=0}^{\infty} \frac{M^{2n+1}(x_1)}{(2n+1)!} \delta^{2n+1} - 2(\ln r) \sum_{n=1}^{\infty} \frac{M^{2n}(x_1)\delta^{2n}}{(2n)!} + 2\ln r \sum_{n=1}^{\infty} \frac{(-1)^n M^{(n)}(x_1)}{(n)!} \delta^n$$

$$-2 \sum_{n=1}^{\infty} \frac{(-1)^n r^{2n} M^{2n}(x_1)}{2^{2n}(n!)^2} \frac{1}{(2n)} - 2 \sum_{n=1}^{\infty} \frac{M^{2n}(x_1)\delta^{2n}}{(2n)!} \left(\sum_{k=1, k\neq n}^{\infty} \frac{(-1)^k (2k)!}{(2k)2^{2k}(k!)^2} \frac{r^{2k}}{\delta^{2k}} \right)$$

$$-2 \sum_{n=1}^{\infty} \frac{(-1)^n r^{2n} M^{2n}(x_1)}{2^{2n}(n!)^2} \left\{ \sum_{k=1}^{n} \frac{-1}{(2k)(2k-1)} \right\}$$

$$-2 \sum_{n=1}^{\infty} \frac{r^{2n} M^{2n}(x_1)}{(n!)^2} \left\{ \sum_{k=1}^{n} \frac{(-1)^{n-k}(k!)^2}{2^{2n-2k}(2k)!} \frac{1}{(2k)} \frac{\delta^{2k}}{r^{2k}} \left(\sum_{j=1, j\neq k}^{\infty} \frac{(-1)^{j-1}(2j)!}{2^{2j}(2j-1)(j!)^2} \frac{r^{2j}}{\delta^{2j}} \right) \right\}$$

$$-2 \sum_{n=1}^{\infty} \frac{(-1)^n r^{2n} M^{(2n)}(x_1)}{2^{2n}(n!)^2} \sum_{k=1}^{2n-1} \frac{1}{k} - \sum_{n=1}^{\infty} \frac{(-1)^n r^{2n}}{2^{2n}(n!)^2} \sum_{k=1}^{2n-1} \frac{(-1)^k (k-1)!}{\delta^k} \sum_{j=1, j\neq k}^{\infty} \frac{(-1)^j M^{(2n-k+j)}(x_1)\delta^j}{(j!)}$$

$$- \sum_{n=1}^{\infty} \frac{(-1)^n r^{2n}}{2^{2n}(n!)^2} \sum_{k=1}^{2n-1} \frac{(k-1)!}{\delta^k} \sum_{j=1, j\neq k}^{\infty} \frac{M^{(2n-k+j)}(x_1)\delta^j}{j!}$$

$$+(\ln 2\delta) \sum_{n=1}^{\infty} \frac{(-1)^n r^{2n}}{2^{2n}(n!)^2} \sum_{k=1}^{\infty} \frac{(-1)^k M^{(2n+k)}(x_1)\delta^k}{(k!)} + (\ln 2\delta) \sum_{n=1}^{\infty} \frac{(-1)^n r^{2n}}{2^{2n}(n!)^2} \left[\sum_{k=1}^{\infty} \frac{M^{(2n+k)}(x_1)\delta^k}{k!} \right]$$

$$- \sum_{n=1}^{\infty} \frac{(-1)^n r^{2n}}{2^{2n}(n!)^2} \sum_{k=1}^{2n-1} \frac{(-1)^k (k-1)! M^{(2n-k)}(x_1)}{\delta^k} - \sum_{n=1}^{\infty} \frac{(-1)^n r^{2n}}{2^{2n}(n!)^2} \sum_{k=1}^{2n-1} \frac{(k-1)! M^{(2n-k)}(x_1)}{\delta^k}$$

$$+2(\ln 2\delta) \sum_{n=1}^{\infty} \frac{M^{2n}(x_1)\delta^{2n}}{(2n)!} - 2M(x_a)\ln r$$

$$-2 \sum_{n=1}^{\infty} \frac{(-1)^n r^{2n} M^{2n}(x_1)}{2^{2n}(n!)^2} \left(\sum_{k=1}^{n} \frac{(-1)^{-k}(k!)^2}{2^{-2k}(2k)!} \frac{1}{(2k)} \frac{\delta^{2k}}{r^{2k}} \right) + 2 \sum_{n=1}^{\infty} \frac{(-1)^n r^{2n} M^{2n}(x_1)}{2^{2n}(n!)^2} \left(\sum_{k=1}^{\infty} \frac{(-1)^k (2k)!}{(2k) 2^{2k}(k!)^2} \frac{r^{2k}}{\delta^{2k}} \right).$$

We have

$$\frac{1}{2n} + \sum_{k=1}^{n} \frac{-1}{(2k)(2k-1)} + \sum_{k=1}^{2n-1} \frac{1}{k} = \sum_{k=1}^{2n} \frac{1}{k} - \sum_{k=1}^{n} \frac{1}{2k-1} + \sum_{k=1}^{n} \frac{1}{2k} = 2\sum_{k=1}^{n} \frac{1}{2k} = \sigma_n,$$

and consider

$$F(x_1) = \lim_{\varepsilon \to 0} \frac{1}{4\pi} \left\{ \int_{x_a}^{x_1-\varepsilon} m(y_1)(-\ln 2x_{11}) dy_1 + \int_{x_1+\varepsilon}^{x_b} m(y_1) \left(\ln(-2x_{11})\right) dy_1 \right\},$$

also

$$F^\delta(x_1, \delta) = \lim_{\varepsilon \to 0} \left\{ \int_{x_1-\varepsilon}^{x_1-\delta} m(y_1)(-\ln 2x_{11}) dy_1 + \int_{x_1+\delta}^{x_1+\varepsilon} m(y_1) \left(\ln(-2x_{11})\right) dy_1 \right\},$$

where by changing variables and imposing the limit we get,

$$\begin{aligned} F^\delta(x_1, \delta) &= \lim_{\varepsilon \to 0} \left\{ \int_\varepsilon^\delta m(x_1 - x_{11})(\ln 2x_{11}) dy_1 - \int_\varepsilon^\delta m(x_1 + x_{11}) \left(\ln 2x_{11}\right) dy_1 \right\} \\ &= \int_0^\delta \{ m(x_1 - x_{11}) - m(x_1 + x_{11}) \} \ln 2x_{11} dx_{11} \\ &= -2 \sum_{k=1}^{\infty} \frac{m^{(2k-1)}(x_1)}{(2k-1)!} \int_0^\delta x_{11}^{2k-1} \ln 2x_{11} dx_{11} \\ &= 2 \sum_{k=1}^{\infty} \frac{M^{(2k)}(x_1)\delta^{2k}}{(2k)!} \frac{1}{(2k)} - 2(\ln 2\delta) \sum_{k=1}^{\infty} \frac{M^{(2k)}(x_1)\delta^{2k}}{(2k)!}. \end{aligned}$$

So

$$I=\sum_{n=0}^{\infty}\frac{(-1)^n r^{2n}M^{2n}(x_1)}{2^{2n}(n!)^2}(2\ln r)-2\sum_{n=1}^{\infty}\frac{(-1)^n r^{2n}M^{2n}(x_1)}{2^{2n}(n!)^2}\sigma_n$$

$$+\sum_{n=0}^{\infty}\frac{(-1)^n r^{2n}}{2^{2n}(n!)^2}\frac{\partial^{2n}}{\partial x_1^{2n}}[4\pi F(x_1)]-2M(x_a)\ln r$$

$$+\{2\sum_{k=1}^{\infty}\frac{M^{(2k)}(x_1)\delta^{2k}}{(2k)!}\frac{1}{(2k)}$$

$$-2\sum_{n=1}^{\infty}\frac{M^{2n}(x_1)\delta^{2n}}{(2n)!}\left(\sum_{k=1,k\neq n}^{\infty}\frac{(-1)^k(2k)!}{(2k)2^{2k}(k!)^2}\frac{r^{2k}}{\delta^{2k}}\right)$$

$$-2\sum_{n=1}^{\infty}\frac{r^{2n}M^{2n}(x_1)}{(n!)^2}\sum_{k=1}^{n}\frac{(-1)^{n-k}(k!)^2}{2^{2n-2k}(2k)!}\frac{1}{(2k)}\frac{\delta^{2k}}{r^{2k}}\left(\sum_{j=1,j\neq k}^{\infty}\frac{(-1)^{j-1}(2j)!}{2^{2j}(2j-1)(j!)^2}\frac{r^{2j}}{\delta^{2j}}\right)$$

$$-\sum_{n=1}^{\infty}\frac{(-1)^n r^{2n}}{2^{2n}(n!)^2}\sum_{k=1}^{2n-1}\frac{(-1)^k(k-1)!}{\delta^k}\sum_{j=1,j\neq k}^{\infty}\frac{(-1)^j M^{(2n-k+j)}(x_1)\delta^j}{(j!)}$$

$$-\sum_{n=1}^{\infty}\frac{(-1)^n r^{2n}}{2^{2n}(n!)^2}\sum_{k=1}^{2n-1}\frac{(k-1)!}{\delta^k}\sum_{j=1,j\neq k}^{\infty}\frac{M^{(2n-k+j)}(x_1)\delta^j}{j!}+(\ln 2\delta)\sum_{n=1}^{\infty}\frac{(-1)^n r^{2n}}{2^{2n}(n!)^2}\sum_{k=1}^{\infty}\frac{(-1)^k M^{(2n+k)}(x_1)\delta^k}{(k!)}$$

$$+(\ln 2\delta)\sum_{n=1}^{\infty}\frac{(-1)^n r^{2n}}{2^{2n}(n!)^2}\sum_{k=1}^{\infty}\frac{M^{(2n+k)}(x_1)\delta^k}{k!}-\sum_{n=1}^{\infty}\frac{(-1)^n r^{2n}}{2^{2n}(n!)^2}\sum_{k=1}^{2n-1}\frac{(-1)^k(k-1)!M^{(2n-k)}(x_1)}{\delta^k}$$

$$-\sum_{n=1}^{\infty}\frac{(-1)^n r^{2n}}{2^{2n}(n!)^2}\sum_{k=1}^{2n-1}\frac{(k-1)!M^{(2n-k)}(x_1)}{\delta^k}$$

$$-2\sum_{n=1}^{\infty}\frac{(-1)^n r^{2n}M^{2n}(x_1)}{2^{2n}(n!)^2}\sum_{k=1}^{n}\frac{(-1)^{-k}(k!)^2}{2^{-2k}(2k)!}\frac{1}{(2k)}\frac{\delta^{2k}}{r^{2k}}+2\sum_{n=1}^{\infty}\frac{(-1)^n r^{2n}M^{2n}(x_1)}{2^{2n}(n!)^2}\sum_{k=1}^{\infty}\frac{(-1)^k(2k)!}{(2k)2^{2k}(k!)^2}\frac{r^{2k}}{\delta^{2k}}\}.$$

Eventually we write I in following form

$$I=\sum_{n=0}^{\infty}\frac{(-1)^n r^{2n}}{2^{2n}(n!)^2}\frac{\partial^{2n}}{\partial x_1^{2n}}[2M(x_1)(\ln r-\sigma_n)+4\pi F(x_1))]-2M(x_a)\ln r+G(x_1,\delta). \quad (6.4.13)$$

where $G(x_1,\delta)$ is all terms that assembled inside the bracket and it is identically equal to zero because all terms in both sides of (6.4.13) are independent off δ. Now since

$\frac{\partial}{\partial x_1}\int_{x_a}^{x_1-\varepsilon}m(y_1)(-\ln 2x_{11})dy_1$

$=-m(x_1-\varepsilon)\ln 2\varepsilon+\int_{x_a}^{x_1-\varepsilon}m(y_1)\frac{\partial(-\ln 2x_{11})}{\partial x_1}dy_1$

$=-m(x_1-\varepsilon)\ln 2\varepsilon+\int_{x_a}^{x_1-\varepsilon}m(y_1)\frac{\partial(\ln 2x_{11})}{\partial y_1}dy_1$

$$= -m(x_1-\varepsilon)\ln 2\varepsilon + m(x_1-\varepsilon)\ln 2\varepsilon - m(x_a)\ln(2(x_1-x_a)) - \int_{x_a}^{x_1-\varepsilon}\tfrac{dm(y_1)}{dy_1}(\ln 2x_{11})dy_1$$

$$= -m(x_a)\ln(2(x_1-x_a)) - \int_{x_a}^{x_1-\varepsilon}\tfrac{dm(y_1)}{dy_1}(\ln 2x_{11})dy_1$$

$$= -m(x_a)\ln(2(x_1-x_a)) - \int_{x_a}^{x_1-\varepsilon}\tfrac{dm(y_1)}{dy_1}sgn(x_1-y_1)\left(\ln 2\left|x_1-y_1\right|\right)dy_1,$$

and

$$\tfrac{\partial}{\partial x_1}\int_{x_1+\varepsilon}^{x_b} m(y_1)\ln(-2x_{11})dy_1$$

$$= -m(x_1+\varepsilon)(\ln 2\varepsilon) + \int_{x_1+\varepsilon}^{x_b} m(y_1)\tfrac{\partial \ln(-2x_{11})}{\partial x_1}dy_1$$

$$= -m(x_1+\varepsilon)(\ln 2\varepsilon) - \int_{x_1+\varepsilon}^{x_b} m(y_1)\tfrac{\partial \ln(-2x_{11})}{\partial y_1}dy_1$$

$$= -m(x_1+\varepsilon)(\ln 2\varepsilon) - m(x_b)\ln(2(x_b-x_1)) + m(x_1+\varepsilon)(\ln 2\varepsilon) + \int_{x_1+\varepsilon}^{x_b}\tfrac{dm(y_1)}{dy_1}\ln(-2x_{11})dy_1$$

$$= -m(x_b)\ln(2(x_b-x_1)) + \int_{x_1+\varepsilon}^{x_b}\tfrac{dm(y_1)}{dy_1}\ln(-2x_{11})dy_1$$

$$= -m(x_b)\ln(2(x_b-x_1)) - \int_{x_1+\varepsilon}^{x_b}\tfrac{dm(y_1)}{dy_1}sgn(x_1-y_1)\left(\ln 2\left|x_1-y_1\right|\right)dy_1,$$

then,

$$\begin{aligned}\frac{\partial}{\partial x_1}F(x_1) = \lim_{\varepsilon\to 0}\frac{1}{4\pi}\{&-m(x_a)\ln(2(x_1-x_a)) - m(x_b)\ln(2(x_b-x_1)) \\ &-\int_{x_a}^{x_1-\varepsilon}\frac{dm(y_1)}{dy_1}sgn(x_1-y_1)\left(\ln 2\left|x_1-y_1\right|\right)dy_1 \\ &-\int_{x_1+\varepsilon}^{x_b}\frac{dm(y_1)}{dy_1}sgn(x_1-y_1)\left(\ln 2\left|x_1-y_1\right|\right)dy_1\}.\end{aligned} \tag{6.4.14}$$

As $x_a \to -\infty$, assuming $m(x_a)$ approaches to zero faster than $\ln 2(x_1-x_a)$ and similarly for x_b, then

$\lim_{x_a\to-\infty} m(x_a)\ln(2(x_1-x_a)) = 0$, $\lim_{x_b\to\infty} m(x_b)\ln(2(x_b-x_1)) = 0$ and in this case

$$\begin{aligned}\frac{\partial}{\partial x_1}F(x_1) &= \lim_{\varepsilon\to 0}\frac{1}{4\pi}\{-\int_{-\infty}^{x_1-\varepsilon}\frac{dm(y_1)}{dy_1}sgn(x_1-y_1)\left(\ln 2\left|x_1-y_1\right|\right)dy_1 \\ &\quad -\int_{x_1+\varepsilon}^{\infty}\frac{dm(y_1)}{dy_1}sgn(x_1-y_1)\left(\ln 2\left|x_1-y_1\right|\right)dy_1\} \\ &= -\frac{1}{4\pi}\int_{-\infty}^{\infty}\frac{dm(y_1)}{dy_1}sgn(x_1-y_1)\left(\ln 2\left|x_1-y_1\right|\right)dy_1.\end{aligned} \tag{6.4.15}$$

Integrating both sides of (6.4.2) and (6.4.13) with respect to x_1 and letting x_a tend to $-\infty$, x_b to ∞, gives

$$-\frac{1}{4\pi}\int_{-\infty}^{\infty}\frac{m(y_1)dy_1}{\sqrt{(x_1-y_1)^2+r^2}} = \sum_{n=0}^{\infty}\frac{(-1)^n r^{2n}}{2^{2n}(n!)^2}\frac{\partial^{2n}}{\partial x_1^{2n}}\left[\frac{1}{2\pi}m(x_1)\left(\ln r-\sigma_n\right)+f(x_1)\right],$$

where,

$$f(x_1)=\frac{\partial}{\partial x_1}F(x_1).$$

This is the same result as obtained for the Fourier transform method, and is a check for the analysis.

6.5 Applications

Consider using this result to determine the near field approximation for a distribution of sources, dipoles, and infinitesimal horseshoe vortices.

6.5.1 Distribution of sources

Differentiating

$$\begin{aligned}\int_{X_a}^{X_b} m(y_1)\ln(R_1-x_{11})dy_1 = &-2M(X_a)\ln r \\ &+\sum_{n=0}^{\infty}\frac{(-1)^n r^{2n}}{2^{2n}(n!)^2}\frac{\partial^{2n}}{\partial x_1^{2n}}\left\{2M(x_1)\left(\ln r-\sigma_n\right)+F(x_1)\right\}\end{aligned} \qquad (6.5.1)$$

with respect to x_1 gives

$$\int_{X_a}^{X_b} \frac{m(y_1)}{R_1} dy_1 = \sum_{n=0}^{\infty} \frac{(-1)^{n+1} r^{2n}}{2^{2n}(n!)^2} \frac{\partial^{2n}}{\partial x_1^{2n}} \left\{ 2m(x_1) (\ln r - \sigma_n) + F'(x_1) \right\}, \tag{6.5.2}$$

So, applying integration by parts gives

$$\begin{aligned} F'(x_1) &= \lim_{\varepsilon \to 0} \left\{ \int_{X_a}^{x_1 - \varepsilon} m'(y_1)(-\ln 2x_{11}) dy_1 + \int_{x_1+\varepsilon}^{X_b} m'(y_1) (\ln(-2x_{11})) \, dy_1 \right\} \\ & -m(X_a) \ln(2(x_1 - X_a)) - m(X_b) \ln(2(X_b - x_1)). \end{aligned}$$

Assuming that in the limit $X_a \to -\infty$ and $X_b \to \infty$ that $m(x_1)$ decays faster than $\ln(2\,|x_{11}|)$, then we get

$$\int_{-\infty}^{\infty} \frac{m(y_1)}{R_1} dy_1 = \sum_{n=0}^{\infty} \frac{(-1)^{n+1} r^{2n}}{2^{2n}(n!)^2} \frac{\partial^{2n}}{\partial x_1^{2n}} \left\{ 2m(x_1) (\ln r - \sigma_n) + f(x_1) \right\},$$

where

$$f(x_1) = \lim_{\varepsilon \to 0} \left\{ \int_{X_a}^{x_1 - \varepsilon} m'(y_1)(-\ln 2x_{11}) dy_1 + \int_{x_1+\varepsilon}^{X_b} m'(y_1) (\ln(-2x_{11})) \, dy_1 \right\}$$

which is equivalent to the result given in Tuck [16] which uses the Fourier transform approach of Thwaites [8] and is given for completeness in section 6.3.

6.5.2 Distribution of dipoles

Differentiating (6.5.2) with respect to x_2 then gives a distribution of 3-D dipoles

$$\int_{X_a}^{X_b} m(y_1) \frac{\partial}{\partial x_2} (\frac{1}{R_1}) dy_1 = \sum_{n=0}^{\infty} \frac{(-1)^{n+1}}{2^{2n}(n!)^2} \frac{\partial}{\partial x_2} \left\{ r^{2n} \frac{\partial^{2n}}{\partial x_1^{2n}} \left\{ 2m(x_1) (\ln r - \sigma_n) + F'(x_1) \right\} \right\}. \tag{6.5.3}$$

6.5.3 Distribution of infinitesimal horseshoe vortices

In a uniform flow field, lift is only produced by modelling the shed vortex wake; The dipole distribution (6.5.3) within the body gives no lift. In aerodynamics, the vortex wake is represented by a trailing vortex sheet which itself is approximated by a distribution of horseshoe vortices [21]. In the limit giving a continuous vortex sheet, this is equivalent to an integral distribution of infinitesimal horseshoe vortices [1], and the infinitesimal horseshoe vortex is defined in Thwaites [8]. This definition is seen to be equivalent to have given by the potential $\frac{\partial}{\partial x_2}\ln(R_1 - x_{11})$ [1]. This is also the potential part of the lift Oseenlet [15], and differentiating (6.5.1) with respect to x_2 gives

$$\begin{aligned}\int_{X_a}^{X_b} m(y_1)\frac{\partial}{\partial x_2}\ln(R_1 - x_{11})dy_1 &= -2M(X_a)\frac{\partial}{\partial x_2}\ln r \\ &+ \sum_{n=0}^{\infty}\frac{(-1)^n}{2^{2n}(n!)^2}\frac{\partial}{\partial x_2}\left\{r^{2n}\frac{\partial^{2n}}{\partial x_1^{2n}}\left\{2m(x_1)\left(\ln r - \sigma_n\right) + F(x_1)\right\}\right\}.\end{aligned} \tag{6.5.4}$$

Hence, the leading order near field term for both (6.5.3) and (6.5.4) is a two dimensional dipole term. So, different far field distributions yield the same nearfield leading order term. This is because we have allowed a discontinuity line on $x_1 > X_b$, $x_2 = x_3 = 0$. Uniqueness is restored to the matching if we apply Kutta condition of aerodynamics. Then, the solution (6.5.4) rather than (6.5.3) is obtained. Consider a distribution of infinitesimal horseshoe vortices over a span s then gives a thin body/wing representation

$$\begin{aligned}&\int_0^s\int_{X_a}^{X_b}\ell(y_1,y_3)\frac{\partial}{\partial x_2}\ln(R_{13} - x_{11})dy_1dy_3 = \\ &\sum_{n=0}^{\infty}\frac{(-1)^n}{2^{2n}(n!)^2}\frac{\partial}{\partial x_2}\int_0^s\left[r_3^{2n}\frac{\partial^{2n}}{\partial x_1^{2n}}\left\{2L(x_1,y_3)\left(\ln r_3 - \sigma_n\right) + F^{\ell}(x_1,y_3)\right\}\right]dy_3.\end{aligned} \tag{6.5.5}$$

where

$$F^{\ell}(x_1,y_3) = \lim_{\varepsilon\to 0}\left\{\int_{X_a}^{x_1-\delta}\ell(y_1,y_3)(-\ln 2x_{11})dy_1 + \int_{x_1+\varepsilon}^{X_b}\ell(y_1,y_3)\left(\ln(-2x_{11})\right)dy_1\right\}$$

and the load function $\ell(y_1,y_3) = \frac{\partial}{\partial y_1}L(y_1,y_3)$ is given in Thwaites [8]; The functions $r_3 = \sqrt{x_2^2 + (x_3 - y_3)^2}$ and $R_{13} = \sqrt{(x_1 - y_1)^2 + x_2^2 + (x_3 - y_3)^2}$. The trailing vortex wake is then defined along $x_1 > X_b$, $x_2 = 0$, $0 \le x_3 \le s$.

6.6 Chapter 6 Discussion

A distribution of generator potentials of the type $\phi = \ln(R - x_1)$ are considered over a line $X_a \le x_1 \le X_b$ $x_2 = x_3 = 0$, and using the integral splitting method near field slender body expansion is given.

Differentiating through with respect to x_1 gives a distribution of source terms, and in this way the slender body expansion for a distribution of source terms over a finite length is given. For the particular case where the ends are taken to infinity, then a distribution of source terms over an infinite length is obtained and this is shown to agree with the distribution given in Tuck [16] by using the Fourier transform method of Thwaites [8].

Differentiating through with respect to x_2 gives a distribution of infinitesimal horseshoe vortices, and the resulting potential is singular along the infinite half line $x_1 \geq 0$, $x_2 = x_3 = 0$ which defines a singular wake line. A spanwise distribution that defines a singular wake sheet, and gives a thin wing approximation. The leading near field matching term is the dipole, and this is also the leading near field matching term obtained when considering a distribution of three-dimensional dipoles. This non-uniqueness in the matching is removed if the Kutta condition is applied, and then only the distribution of infinitesimal horseshoe vortices, which provide lift in a uniform flow field, matches to the two dimensional dipole near field.

6.7 Chapter 6 Appendix: Fourier transforms requirements

The Fourier transforms definition and relevant theorems and formulas and required calculation which have been used within the chapter are presented in this section.

Definition 6.7.1. (Fourier Transform) If f is a real-valued function on $[-\infty, \infty]$, the function $\hat{f} = F(f)$ defined by the integral

$$\hat{f}(w) = F(f, w) = \int_{-\infty}^{\infty} e^{-iwu} f(u) du, \tag{6.7.1}$$

and therefore the Fourier inverse transform will be

$$f(x) = F^{-1}\left(\hat{f}, x\right) = \frac{1}{2\pi} \int_{-\infty}^{\infty} \hat{f}(w) e^{i\omega x} d\omega. \tag{6.7.2}$$

Lemma 6.7.1. *If f has Fourier transform then $F(f(x-t), w) = e^{-itw} F(f)$.*

Proof. $\int_{-\infty}^{\infty} e^{-iwu} f(u-t) du = \int_{-\infty}^{\infty} e^{-iw(\eta+t)} f(\eta) d\eta = e^{-itw} \int_{-\infty}^{\infty} e^{-iw\eta} f(\eta) d\eta$. □

Theorem 6.7.2. *(Convolution theorem for Fourier Transforms)*

Let f and g be a real-valued function over the interval $]-\infty, \infty[$, with Fourier transforms $F(\omega)$ and $G(\omega)$ respectively, then the Fourier transform of their convolution

$$f * g(x) = \int_{-\infty}^{\infty} g(t) f(x-t) dt, \tag{6.7.3}$$

exists and is equal to $F(\omega)G(\omega)$.

Proof. Since f and g have Fourier transforms then both satisfy Dirichlet's conditions and so does their convolution $f * g(x)$ which guaranties existence of $F(f * g, w)$.

For next part applying lemma (6.7.1) and also replacing $f(x-t)$ by using (6.7.2) for convolution gives:

$$
\begin{aligned}
\int_{-\infty}^{\infty} g(t)f(x-t)dt &= \int_{-\infty}^{\infty} g(t)(\frac{1}{2\pi}\int_{-\infty}^{\infty}[F\left(f(x-t)\right)]e^{i\omega x}d\omega)dt \\
&= \int_{-\infty}^{\infty} g(t)(\frac{1}{2\pi}\int_{-\infty}^{\infty}[e^{-itw}F\left(w\right)]e^{i\omega x}d\omega)dt \\
&= \frac{1}{2\pi}\int_{-\infty}^{\infty}\{F\left(w\right)(\int_{-\infty}^{\infty} e^{-i\omega t}g(t)dt)\}e^{i\omega x}d\omega \\
&= \frac{1}{2\pi}\int_{-\infty}^{\infty}\{F\left(w\right)G(\omega)\}e^{i\omega x}d\omega,
\end{aligned}
$$

now from (6.7.2) we have $F^{-1}\left(FG,x\right) = f*g\left(x\right)$ or conversely $F(\,f*g,w) = F(\omega)G(\omega)$.

□

Theorem 6.7.3. *Let $F(\omega)$ be the Fourier transforms of $f(x)$. Assume all first $(n-1)$ derivatives of $f(x)$ vanishes as $|x|\to\infty$, then, the Fourier transform of $f^{(n)}(x)$ exists and equals to*

$$
F(\frac{d^n f}{dx^n},\omega) = (i\omega)^n F(\omega). \tag{6.7.4}
$$

Proof. Applying integration by parts yields:

$$
\begin{aligned}
\int_{-\infty}^{\infty}\frac{d^n f}{du^n}(u)e^{-i\omega u}du &= \left[\frac{d^{n-1}f}{du^{n-1}}(u)e^{-i\omega u}\right]_{u=-\infty}^{u=\infty} + (i\omega)\int_{-\infty}^{\infty}\frac{d^{n-1}f}{du^{n-1}}(u)e^{-i\omega u}du \\
&= (i\omega)\int_{-\infty}^{\infty}\frac{d^{n-1}f}{du^{n-1}}(u)e^{-i\omega u}du.
\end{aligned}
$$

By repetition of this rule, (6.7.4) is held, for more details see [42, 43].

□

To find the the inverse Fourier transform of aerodynamic potential flow, the following key formula (table 3.7.2.3 page 278 [44]) which is the Fourier sine transform F_s of $f(t) = t^{-1}\ln t$, in this chapter has been used,

$$
F_s\left(f,\omega\right) = \int_0^{\infty}\frac{\ln t}{t}\sin\left(\omega t\right)dt = -\frac{\pi}{2}\left(\gamma + \ln\omega\right). \tag{6.7.5}
$$

To prove (6.7.5) we follow three below steps:

1. Euler constant γ

The Euler constant γ is defined as the limit of the decreasing sequence "$\sum_{m=1}^{n} \frac{1}{m} - \ln n$ "as $n \to \infty$ [45] and numerically it is estimated $\gamma \approx 0.5772$. An equivalent value for Euler number is related to *Gamma* function [46]

$$\Gamma(x) = \int_0^\infty e^{-t} t^{x-1} dt, \quad x > 0,$$

is

$$\gamma = -\frac{\Gamma'(1)}{\Gamma(1)}, \quad \Gamma'(x) = \frac{d}{dx}\Gamma(x),$$

so,

$$\gamma = -\int_0^\infty e^{-t} (\ln t)\, dt. \tag{6.7.6}$$

2. Fourier sine of $1/t$

There are different ways to prove

$$F_s\left(1/t, \omega\right) = \int_0^\infty (\frac{\sin t\omega}{t}) dt = \operatorname{sgn}(\omega)\,\frac{\pi}{2}. \tag{6.7.7}$$

Here we present two different proofs:

- Using residues theory for complex functions as suggested in [41]

 Lemma 6.7.4. *[41]Let the point $z = x_0$ be a real simple pole of a function f, and let B_0 denote the residue of f at the pole. Let C_ρ show the upper half circle with radius ρ centered at x_0 where the orientation is in the clockwise direction (Left: figure 6.1), let also ρ be small enough such that f is analytic on $0 < |z - x_0| \preceq \rho$ and it can be presented by*

$$f(z) = \frac{B_0}{z - x_0} + g(z), \tag{6.7.8}$$

where g is continuous on $|z - x_0| \preceq \rho$, *then,*

$$\lim_{\rho \to 0} \int_{C_\rho} f(z)dz = -B_0 \pi i. \tag{6.7.9}$$

Proof. Since $\int_{C_\rho} \frac{B_0}{z-x_0} dz = \int_\pi^0 \frac{B_0}{\rho e^{i\theta}} i\rho e^{i\theta} d\theta = -B_0 \pi i$, then,

$$\left| \int_{C_\rho} f(z)dz - (-B_0 \pi i) \right| = \left| \int_{C_\rho} g(z)dz \right| \leq \pi \rho M_g. \tag{6.7.10}$$

where $M_g = \max_{|z-x_0| \preceq \rho} |g(z)|$.

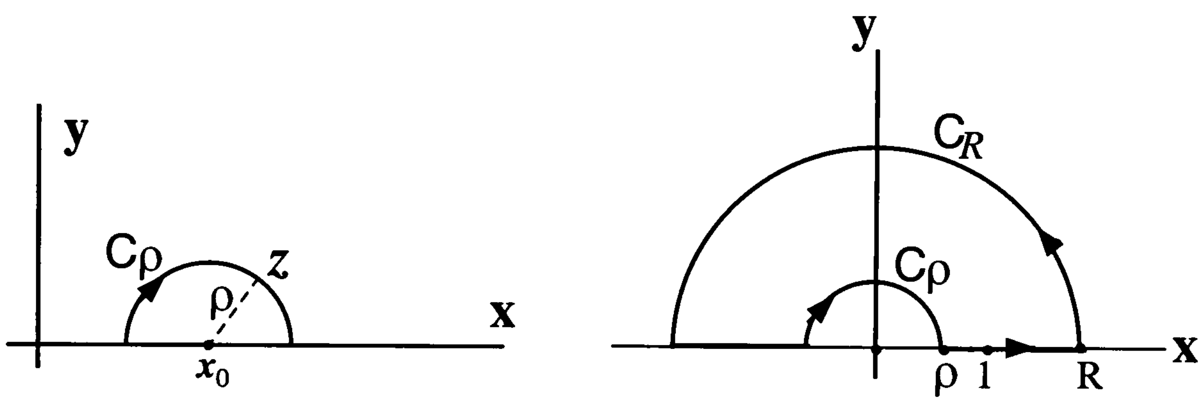

Figure 6.1: Left: Simple real pole, Right: $\rho < 1$, and $R > 1$.

□

Corollary 6.7.5.

$$\int_0^\infty \frac{\sin x}{x} dx = \frac{\pi}{2}, \tag{6.7.11}$$

Proof. The function $\frac{e^{iz}}{z}$ on and inside the closed contort C shown in figure 6.1 (Right) is holomorphic so, $\int_C \frac{e^{iz}}{z} dz = 0$. On the other hand,

$$\int_C \frac{e^{iz}}{z} dz = \int_{C_\rho} \frac{e^{iz}}{z} dz + \int_\rho^R \frac{e^{ix}}{x} dx + \int_{C_R} \frac{e^{iz}}{z} dz + \int_{-R}^{-\rho} \frac{e^{ix}}{x} dx. \tag{6.7.12}$$

According to lem.6.7.4

$$\lim_{\rho \to 0} \int_{C_\rho} \frac{e^{iz}}{z} dz = -\pi i. \tag{6.7.13}$$

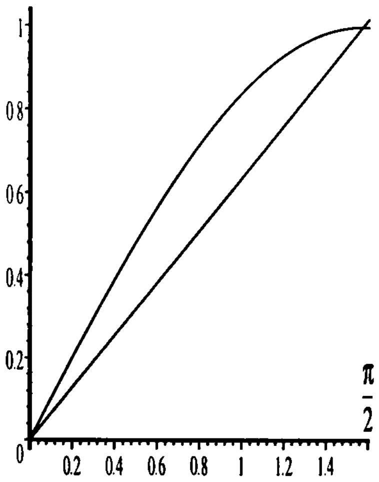

Figure 6.2: $\sin\theta$ and $\frac{2}{\pi}\theta$.

For $\sin\theta \geq \frac{2}{\pi}\theta$, for $0 \leq \theta \leq \frac{\pi}{2}$, (see figure 6.2), then

$$\left|\int_{C_R} \frac{e^{iz}}{z} dz\right| = \left|\int_0^{\pi} \frac{e^{Rie^{i\sin\theta}}}{Re^{i\sin\theta}} Rie^{i\sin\theta} d\theta\right| = \int_0^{\pi} e^{-R\sin\theta} d\theta =$$
$$\int_0^{\frac{\pi}{2}} e^{-R\sin\theta} d\theta + \int_{\frac{\pi}{2}}^{\pi} e^{-R\sin\theta} d\theta = 2\int_0^{\frac{\pi}{2}} e^{-R\sin\theta} d\theta \tag{6.7.14}$$
$$\preceq 2\int_0^{\frac{\pi}{2}} e^{-\frac{2R}{\pi}\theta} d\theta = \frac{\pi}{2R}(1 - e^{-R}),$$

and since

$$\int_{\rho}^{R} \frac{e^{ix}}{x} dx + \int_{-R}^{-\rho} \frac{e^{ix}}{x} dx = \int_{\rho}^{R} \frac{e^{ix} - e^{-ix}}{x} dx = 2i\int_{\rho}^{R} \frac{\sin x}{x} dx. \tag{6.7.15}$$

So, as $\rho \to 0$ and $R \to \infty$ from (6.7.13), (6.7.14) and (6.7.15), now (6.7.11) holds. □

Corollary 6.7.6. *From corollary (6.7.5) we have*

$$\int_0^{\infty} \frac{\sin(\omega t)}{t} dt = \mathrm{sgn}(\omega)\int_0^{\infty} \frac{\sin(x)}{x/\omega}\frac{1}{\omega} dx = \mathrm{sgn}(\omega)\int_0^{\infty} \frac{\sin(x)}{x} dx = \mathrm{sgn}(\omega)\frac{\pi}{2},$$

which proves (6.7.7).

- Using Laplace transforms as suggested in p.392 [47]

$$L\left[\int_0^{\infty} (\frac{\sin t\omega}{\omega}) d\omega\right] = \int_0^{\infty} \left[L(\frac{\sin t\omega}{\omega})\right] = \int_0^{\infty} \frac{1}{\omega}\left[L(\sin t\omega)\right] d\omega$$
$$= \int_0^{\infty} \frac{1}{\omega}\left[\frac{\omega}{s^2+\omega^2}\right] d\omega = \int_0^{\infty} \frac{1}{s^2+\omega^2} d\omega \tag{6.7.16}$$
$$= \frac{1}{s}\arctan(\frac{\omega}{s})|_0^{\infty} = \frac{\pi}{2}\frac{1}{s},$$

since $L^{-1}\left[\frac{1}{s}\right] = 1,$ then

$$\int_0^\infty \left(\frac{\sin t\omega}{t}\right) dt = \operatorname{sgn}(\omega)\,\frac{\pi}{2}.$$

3. Using differential equation

Let us define

$$F(\omega) = \int_0^\infty e^{-\omega t} (\ln t)\, dt \quad (\omega > 0), \tag{6.7.17}$$

then

$$\begin{aligned} F'(\omega) &= -\int_0^\infty (t \ln t)\, e^{-\omega t} dt = \frac{1}{\omega} e^{-\omega t} (t \ln t)]_0^\infty - \frac{1}{\omega}\int_0^\infty e^{-\omega t}\,((\ln t) + 1)\, dt \\ &= -\frac{1}{\omega}\int_0^\infty e^{-\omega t} (\ln t)\, dt - \frac{1}{\omega}\int_0^\infty e^{-\omega t} dt = -\frac{1}{\omega} F(\omega) - \frac{1}{\omega^2}, \end{aligned}$$

so we will have the first order differential equation

$$F'(\omega) + \frac{1}{\omega} F(\omega) = -\frac{1}{\omega^2}, \tag{6.7.18}$$

and the solution of (6.7.18) is

$$F(\omega) = e^{-\int \frac{1}{\omega} d\omega} \left[\int e^{\int \frac{1}{\omega} d\omega} \left(-\frac{1}{\omega^2}\right) d\omega + c\right] = \frac{1}{\omega}[-\ln \omega + c],$$

since from (6.7.6) we have $c = F(1) = -\gamma$, so,

$$F(\omega) = \frac{1}{\omega}[-\ln \omega - \gamma]. \tag{6.7.19}$$

Now let us again define

$$G(\omega) = \int_0^\infty e^{-\omega t} \left(\frac{\ln t}{t}\right) dt,$$

then according to (6.7.17)

$$G'(\omega) = -\int_0^\infty e^{-\omega t}(\ln t)\,dt = -F(\omega)$$

and therefore from (6.7.19) we shall have

$$G(\omega) = -\int F(\omega)d\omega = \int \frac{1}{\omega}(\ln\omega + \gamma)\,d\omega = \frac{1}{2}\ln^2\omega + \gamma\ln\omega. \tag{6.7.20}$$

Hence from (6.7.20) we should have

$$\begin{aligned} G(i\omega) &= \frac{1}{2}\ln^2 i\omega + \gamma \ln i\omega = \frac{1}{2}\left(\ln\omega + i\frac{\pi}{2}\right)^2 + \gamma\left(\ln\omega + i\frac{\pi}{2}\right) \\ &= \frac{1}{2}\left(\ln^2\omega - \frac{\pi^2}{4} + 2i\frac{\pi}{2}\ln\omega\right) + \gamma\left(\ln\omega + i\frac{\pi}{2}\right) \\ &= \left(\frac{1}{2}\ln^2\omega - \frac{\pi^2}{8} + \gamma\ln\omega\right) + i\frac{\pi}{2}(\ln\omega + \gamma). \end{aligned} \tag{6.7.21}$$

on the other hand

$$G(i\omega) = \int_0^\infty e^{-i\omega t}\left(\frac{\ln t}{t}\right)dt = \int_0^\infty \left(\frac{\ln t}{t}\right)(\cos\omega t - i\sin\omega t)dt. \tag{6.7.22}$$

Combining (6.7.21) and (6.7.22) together, formula (6.7.5) now is held.

6.7.1 Bessel function

The linear equation

$$x^2\frac{d^2y}{dx^2} + (1-2\alpha)x\frac{dy}{dx} + [\beta^2\gamma^2x^{2\gamma} + (\alpha^2 - p^2\gamma^2)]y = 0,$$

is the general Bessel equation. By series methods, this equation can be shown to have the solution [48]

$$\begin{aligned} y &= Ax^\alpha J_p(\beta x^\gamma) + Bx^\alpha J_{-p}(\beta x^\gamma), \quad p \text{ not an integer or zero} \\ y &= Ax^\alpha J_p(\beta x^\gamma) + Bx^\alpha Y_p(\beta x^\gamma), \quad p \text{ an integer} \end{aligned}$$

One important formulation of the two linearly independent solutions to Bessel's equation are the Hankel functions $H^1_\alpha(x)$ and $H^2_\alpha(x)$, defined by:

$$H^1_\alpha(x) = J_\alpha(x) + iY_\alpha(x).$$
$$H^2_\alpha(x) = J_\alpha(x) - iY_\alpha(x).$$

Modified Bessel functions

The Bessel functions are valid even for complex arguments x, and an important special case is that of a purely imaginary argument. In this case, the solutions to the Bessel equation are called the modified Bessel functions of the first and second kind, and are defined by:

$$I_\alpha(x) = i^{-\alpha} J_\alpha(ix).$$
$$K_\alpha(x) = \tfrac{\pi}{2} i^{\alpha+1} H^1_\alpha(ix).$$

These are chosen to be real-valued for real arguments x. They are the two linearly independent solutions to the modified Bessel's equation:

$$x^2 \frac{d^2y}{dx^2} + x\frac{dy}{dx} - (x^2 + \alpha^2)y = 0.$$

The following required formulas are forwarded from [38]:

$$I_\nu(z) = (\frac{1}{2}z)^\nu \sum_{m=0}^{\infty} \frac{(\frac{1}{4}z^2)^m}{m!\Gamma(\nu + m + 1)}. \tag{6.7.23}$$

$$I_{2k}(z) = (\frac{1}{2}z)^{2k} \sum_{m=0}^{\infty} \frac{(\frac{1}{4}z^2)^m}{m!\Gamma(2k + m + 1)} = (\frac{1}{2}z)^{2k} \sum_{m=0}^{\infty} \frac{(\frac{1}{4}z^2)^m}{m!(2k + m)!}. \tag{6.7.24}$$

$$I_0(z) = 1 + \frac{\frac{1}{4}z^2}{(1!)^2} + \frac{(\frac{1}{4}z^2)^2}{(2!)^2} + \frac{(\frac{1}{4}z^2)^3}{(3!)^2} + ... \tag{6.7.25}$$

$$K_0(z) = -\{\ln(\frac{z}{2}) + \gamma\}I_0(z) + \frac{\frac{1}{4}z^2}{(1!)^2} + (1+\frac{1}{2})\frac{(\frac{1}{4}z^2)^2}{(2!)^2} + (1+\frac{1}{2}+\frac{1}{3})\frac{(\frac{1}{4}z^2)^3}{(3!)^2} + ... \quad (6.7.26)$$

$$K_0(z) = -\{\ln(\frac{z}{2}) + \gamma\}I_0(z) + 2\sum_{k=1}^{\infty}\frac{I_{2k}(z)}{k}. \quad (6.7.27)$$

Eq.(6.7.27) is known as C. P. Singer's formula [49] Ex.1 no. 16.

Formulas (9.6.4, 9.6.21 [38], p.376) for $k > 0$ imply

$$\int_0^{\infty}\frac{\cos krt}{\sqrt{t^2+1}}\,dt = K_0(kr). \quad (6.7.28)$$

The asymptotic form for $K_0(\epsilon)$ 6.1[8] is

$$K_0(\epsilon) \approx [\ln(\frac{2}{\epsilon}) - \gamma][1 + \mathcal{O}(\epsilon^2)], \quad (6.7.29)$$

where it is a direct result from 6.7.26.

Chapter 7

Discussion and application

An investigation into inviscid potential flow theory, in particular in relation to the manoeuvring of bodies in fluid has been undertaken.

If the potential flow is assumed regular such that no singularities or discontinuities are allowed to exist in the fluid, then for a fixed body in a uniform flow field both lift and drag are zero from D'Alembert's paradox.

In aerodynamics, this assumption is relaxed so we may have a singular vortex wake, usually a wake sheet emanating from the trailing edge. For this model, it has always been assumed that the resulting lift evaluation is in good agreement with experiment. However, Chadwick [1] found a flaw in the theory which suggests the lift has been calculated inappropriately. In this thesis we have confirmed this result, and for a thin wing found the cause of the miscalculation: a jump in lift across the trailing edge. Further, the drag force is shown to be infinite for this model.

It is therefore concluded that the inviscid flow model with a trailing wake is flawed.

Slender body theory is also researched for solutions with a shed wake, and a complete near field expansion is given for a distribution of sources over a finite line. Again, it is seen there are anomalies with the inviscid flow model because the matching is non-unique, and the application of the Kutta condition is proposed to restore a unique matching. The validity of the Kutta condition is only by experimental verification and so is an external constraint.

To recap, it is suggested that the inviscid flow model is inappropriate for problems which model a shed vortex wake, and will give incorrect evaluation for the forces. Instead, it is suggested that the viscous terms in the Navier-Stokes equation are retained through the analysis.

Bibliography

[1] E. Chadwick, "A slender wing theory in potential flow," *Proceeding of the Royal Society A*, vol. 461, pp. 415–432, 2005.

[2] F. W. Lanchester, *Aerodynamics*, vol. 2. London: Archibald Constable and Co., 1907.

[3] F. W. Lanchester, *Aerodynamics*, vol. 2. London: Archibald Constable and Co., 1908.

[4] L. Prandtl, "Theorie ds flugzeugtragflugels im zusammendruckbaren medium," *Luftfahrtforsch*, vol. 13, p. 313, 1936.

[5] S. Goldstein, *Lectures on Fluid Mechanics*, vol. 2. New York: Interscience publishers, Inc., 1960.

[6] G. K. Batchelor, "On steady laminar flow with closed streamlines at large Reynolds number," *Fluid mech.*, pp. 177–190, 1956.

[7] G. K. Batchelor, "Axial flow in trailing line vortices," *Fluid mech.*, no. 20, pp. 645–658, 1964.

[8] B. Thwaites, *Incompressible Aerodynamics*. New York: Dover, 1960.

[9] M. M. Munk, "The aerodynamic forces on an airship hull," Tech. Rep. 184, Nat. Adu Comm. Aero., Washington, 1924.

[10] R. Jones, "Properties of low-aspect-ratio pointed wings at speed below and above the speed of sound," Tech. Rep. 835, Nat. Adv. Comm. Aero., Washington, 1945.

[11] M. Lighthill, "Note on the swimming of slender fish," *Journal of Fluid Mechanics*, no. 9, pp. 305–317, 1960.

[12] F. Ursell, "Slender oscilating ships at zero forward speed," *Journal of Fluid Mechanics*, no. 14, pp. 496–516, 1962.

[13] J. N. Nielsen, *Missile Aerodynamics.* New York: McGraw-Hill, 1960.

[14] A. Sellier, "Stokes flow past a slender particle," *Proceedings of the Royal Society A*, no. 455, pp. 2975–3002, 1999.

[15] E. Chadwick, "A slender-body theory in oseen flow," *Proceding of the Royal Society A*, pp. 2007–2016, April 2002.

[16] E. Tuck, *Wave Asymptotics*, ch. 10 Analytic aspects of Slender Body Theory, pp. 184–201. Cambridge University, 1992.

[17] R. W. Fox and A. T. McDonald, *Introduction to Fluid Mechanics.* USA: John Wily & Sons, 4 ed., 1994.

[18] J. B. Evett and C. Liu, *Fundamentals of Fluid Mechanics.* Singapore: McGraw-Hill, 1987.

[19] Y. Nakayama, *Introduction to Fluid Mechanics.* Elsevier, 2000.

[20] C. Pozrikidis, *Fluid Dynamics - Theory, Computation, and Numerical Simulation.* USA: Kluwer Academic Publishers, 2001.

[21] G. K. Batchelor, *An Introduction to Fluid Dynamics.* Cambridge: Cambridge University Press, 1967.

[22] D. Bernoulli, *Hydrodynamics.* New York: Dover Publications, 1968.

[23] C. Oseen, *Neure Methoden Und Ergebnisse In Der Hydrodynamik.* 1927.

[24] G. E. Mase, *Contiuum mechanics.* USA: McGraw-Hill, Inc., 1970.

[25] E. G. H. R. H. Sabersky, A. J. Acosta and E. M. Gates, *Fluid Flow.* Upper Saddle River, Newjersy 07458: Macmillan publising company, 4 ed., 1999.

[26] O. Reynold, *Osborne Reynold and his work in hydraulics and hydrodynamics.* Science in Britain, London: Longmans, Green and Co, 1946.

[27] H. Lamb, *Hydrodynamics*, vol. 6. Bentley House, 200 Euston Road, London, N.W.1: The Syndics of the Cambridge University Press, 1932.

[28] L. Prandtl, *Essentials of Fluid Dynamics.* London: Blackie and Son, 1949.

[29] W. Kutta, *Auftriebskräfte in Strömenden Flüssigkeiten.* Illustrierte Aeronaut, July 1902.

[30] N. Joukowski, *De la chute dans l'aire de corps légers de forme allongée, animés d'un mouvement rotatoir*, vol. I of *Aeronaut.* Koutchino, Fasc.I, St. Petersbourg: Bull. de l'Inst, 1906.

[31] J. Lighthill, *An Infomal Introduction to Theoritical Fluid Mechanics.* Waltn Street,Oxfored Ox2 6DP: Oxford University Press, 1986.

[32] Lagerstrom, *High Speed Aerodynamics and Jet Propulsion*, vol. 6. 1964.

[33] B. *et al*, *Maple V Language Reference Manual.* New York: Springer, 1st ed., 1991.

[34] E. Chadwick, "The far field oseen velocity expansion," *Proceding of the Royal Society A*, pp. 2059–2082, August 1998.

[35] J. Lighthill, *An informal introduction to theoritical fluid mechanics.* IMA monograph series, Oxford, U.K.: Oxford University Press, 1989.

[36] J. Katz and A. Plotkin, *Low-speed aerodynamics.* Cambridge: Cambridge University press, 2nd ed., 2001.

[37] J. Newman, *Marine Hydrodynamics.* Cambridge, Massachussets: M.I.T Press, 1977.

[38] M. A. . I. A. Stegun, *Handbook of Mathematical Functions with Formulas, Graphs, and Mathematical Tables.* New York ; Chicester: John Wiley and Sons, tenth printing with corrections ed., December 1972. Issued June 1964.

[39] G. N. Ward, *Linearized theory.* Cambridge University Press, 1955.

[40] P. A. Martin and G. R. Wickham, *Wave Asymptotics.* Cambdidge university Press, 1992.

[41] R. V. Churchill and J. W. Browm, *Complex Variables and Applications.* McGraw-hill book company, 4 ed., 1984.

[42] I. N. Sneddon, *Fourie Transforms.* London: McGraw-Hill, 1951.

[43] M. D. Greenberg, *Advanced Engineering Mathematics.* Upper Saddle River, New Jersey 07458: Printice-Hall, Inc, 2 ed., 1998.

[44] A. D. Poularikas, ed., *The Transforms and Applications handbook.* 2000 Corporate Blvd., N. W. Boca Raton, Florida 33431: CRC Press, Inc., 1995.

[45] E. M. Stein and R. Shakarchi, *Fourier Analysis.* Princeton University Press, UK, 2002.

[46] M. R. Spiegel, *Theory and problems of Fourier Analysis.* Schaum's outline series, McGraw-hill book company, 1947.

[47] R. G. Rice and D. D. Do, *Applied Mathematics and Modeling for Chemical Engineers.* John Wiley & Sons, 1995.

[48] R. P. . D. Green, *Perry's Chemical Engineers Handbook.* McGraw-Hill, 7 ed., 1997.

[49] C. J. Tranter, *Bessel Functions With Some Applications*, vol. 1. St Paul's house, Warwick Lane, London EC4: English Universities Press LTD, 1968.